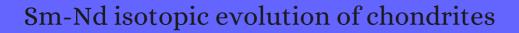
CITATION REPORT List of articles citing



DOI: 10.1016/0012-821x(80)90125-9 Earth and Planetary Science Letters, 1980, 50, 139-155.

Source: https://exaly.com/paper-pdf/14884690/citation-report.pdf

Version: 2024-04-28

This report has been generated based on the citations recorded by exaly.com for the above article. For the latest version of this publication list, visit the link given above.

The third column is the impact factor (IF) of the journal, and the fourth column is the number of citations of the article.

#	Paper	IF	Citations
1625	A two-reservoir recycling model for mantle-crust evolution. 1980 , 77, 6298-302		33
1624	The Shabogamo Intrusive Suite, Labrador: Sr and Nd isotopic evidence for contaminated mafic magmas in the Proterozoic. <i>Earth and Planetary Science Letters</i> , 1981 , 54, 217-235	5.3	47
1623	Sm-Nd age of lherzolite 67667: implications for the processes involved in lunar crustal formation. <i>Earth and Planetary Science Letters</i> , 1981 , 56, 1-8	5.3	34
1622	An estimate of the Nd isotopic composition of Iapetus seawater from ca. 490 Ma metalliferous sediments. <i>Earth and Planetary Science Letters</i> , 1981 , 56, 180-188	5.3	53
1621	Neodymium-strontium isotopic evidence for extreme contamination in a layered basic intrusion. <i>Earth and Planetary Science Letters</i> , 1981 , 56, 189-198	5.3	27
1620	Isotopic and REE studies of lunar basalt 12038: implications for petrogenesis of aluminous mare basalts. <i>Earth and Planetary Science Letters</i> , 1981 , 55, 335-355	5.3	42
1619	Precise determination of SmNd ratios, Sm and Nd isotopic abundances in standard solutions. 1981 , 45, 2311-2323		751
1618	Columbia River volcanism: the question of mantle heterogeneity or crustal contamination. 1981 , 45, 2483-2499		206
1617	Crustal growth and mantle evolution: inferences from models of element transport and Nd and Sr isotopes: (reply to a comment by R. L. Armstrong). 1981 , 45, 1253-1254		12
1616	Transport models for crust and mantle evolution. 1981, 75, 163-179		34
1615	Earth's neodymium budget and structure and evolution of the mantle. 1981 , 290, 208-213		85
1614	Early Archaean gneisses from the Yilgarn Block, Western Australia. 1981, 292, 322-324		44
1613	SmNd age of Kambalda and Kanowna greenstones and heterogeneity in the Archaean mantle. 1981, 294, 322-327		116
1612	Isotopic composition of neodymium in waters from the drake passage. 1982 , 217, 207-14		191
1611	The geochemical coherence of Pu and Nd and the ratio of the early solar system. 1982 , 46, 1793-1804		24
1610	Precise determination of initial ?Nd from Sm-Nd isochron data. 1982 , 46, 1983-1987		98
1609	Origin and evolution of the Nakhla meteorite inferred from the Sm-Nd and U-Pb systematics and REE, Ba, Sr, Rb and K abundances. 1982 , 46, 1555-1573		123

1608	Age and provenance of the target materials for tektites and possible impactites as inferred from Sm-Nd and Rb-Sr systematics. <i>Earth and Planetary Science Letters</i> , 1982 , 60, 155-177	5.3	134
1607	Nd isotopic characteristics of S- and I-type granites. <i>Earth and Planetary Science Letters</i> , 1982 , 58, 51-64	5.3	411
1606	Correlated Nd, Sr and Pb isotope variation in Walvis Ridge basalts and implications for the evolution of their mantle source. <i>Earth and Planetary Science Letters</i> , 1982 , 59, 327-342	5.3	221
1605	Isotopic analyses of inorganic and organic substances by mass spectrometry. 1982 , 45, 87-110		29
1604	Isotopic analysis related to some nuclear and geological applications. 1982 , 45, 259-274		2
1603	Evolution of continental crust and mantle heterogeneity: Evidence from Hf isotopes. 1982 , 78, 279-297		422
1602	Age and origin of the Cortlandt Complex, New York: Implications from Sm-Nd data. 1982 , 79, 290-294		8
1601	Nd, Sr and Pb isotopic systematics in a three-component mantle: a new perspective. 1982 , 298, 519-523		246
1600	SmNd, RbBr and UIIhPb systematics of granulite facies rocks from Fyfe Hills, Enderby Land, Antarctica. 1982 , 298, 614-618		129
1599	Mantle reservoirs and ocean island basalts. 1983 , 301, 229-231		365
1598	Origin of Hawaiian tholeiite and alkalic basalt. 1983 , 302, 785-789		208
1597	Pb, Sr, Nd and Hf isotopic evidence of multiple sources for Oahu, Hawaii basalts. 1983 , 304, 25-29		192
1596	SmNd age and isotopic systematics of the bimodal suite, ancient gneiss complex, Swaziland. 1983 , 305, 701-704		62
1595	Neodymium isotopic evidence for Galapagos hotspot\(\mathbb{B}\)preading centre system evolution. 1983 , 306, 654-657		66
1594	Sm-Nd model ages across the margins of the Archaean Yilgarn Block, Western Australiall; southwest transect into the Proterozoic Albany-Fraser Province. 1983 , 30, 333-340		37
1593	Importance of the Lu-Hf isotopic system in studies of planetary chronology and chemical evolution. 1983 , 47, 81-91		236
1592	Sr and Nd isotope geochronology, geologic history, and origin of the Adirondack Anorthosite. 1983 , 47, 1875-1885		71
1591	Influence of the Mediterranean Outflow on the isotopic composition of neodymium in waters of the North Atlantic. 1983 , 88, 5997		90

1590	Geochemical evolution of the crust and mantle. 1983 , 21, 1347		8
1589	A Nd isotope investigation of sediments related to crustal development in the British Isles. <i>Earth and Planetary Science Letters</i> , 1983 , 63, 229-240	5.3	236
1588	Sm-Nd studies of Archaean metasediments and metavolcanics from West Greenland and their implications for the Earth's early history. <i>Earth and Planetary Science Letters</i> , 1983 , 62, 263-272	5.3	284
1587	Nd-Sr systematics of the Setouchi volcanic rocks, southwest Japan: a clue to the origin of orogenic andesite. <i>Earth and Planetary Science Letters</i> , 1983 , 64, 327-340	5.3	56
1586	Chemical structure and evolution of the mantle and continents determined by inversion of Nd and Sr isotopic data, I. Theoretical methods. <i>Earth and Planetary Science Letters</i> , 1983 , 66, 177-190	5.3	106
1585	Chemical structure and evolution of the mantle and continents determined by inversion of Nd and Sr isotopic data, II. Numerical experiments and discussion. <i>Earth and Planetary Science Letters</i> , 1983 , 66, 191-213	5.3	146
1584	Origin of Mesozoic and Tertiary granite in the western United States and implications for Pre-Mesozoic crustal structure: 1. Nd and Sr isotopic studies in the geocline of the Northern Great Basin. 1983 , 88, 3379		252
1583	Sm-Nd model ages across the margins of the Archaean Yilgarn Block, Western Australia; northwest transect into the proterozoic gascoyne province. 1983 , 30, 167-174		23
1582	Analysis of Terrestrial and Extraterrestrial Materials. 1984 , 15, 119-161		1
1581	Revised SmNd systematics of Kambalda greenstones, Western Australia. 1984, 307, 697-701		50
1580	Origin of diamonds in old enriched mantle. 1984 , 310, 198-202		552
1579	Sm-Nd, K-Ar and petrologic study of some kimberlites from eastern United States and their implication for mantle evolution. 1984 , 86, 35-44		18
1578	Age and origin of anorthosites, charnockites, and granulites in the Central Virginia Blue Ridge: Nd and Sr isotopic evidence. 1984 , 85, 279-291		54
1577	Nd and Sr isotopic variations in acidic rocks from Japan: significance of upper-mantle heterogeneity. 1984 , 87, 407-417		31
1576	Sm-Nd and Rb-Sr systematics in volcanics and ultramafic xenoliths from Malaita, Solomon Islands, and the nature of the Ontong Java Plateau. 1984 , 89, 2415-2424		20
1575	Lu-Hf and Sm-Nd evolution in lunar mare basalts. 1984 , 89, B459		44
1574	Sm?Nd geochronology of greenstone belts in the Yilgarn Block, Western Australia. 1984 , 26, 333-361		60
1573	Sm-Nd ages of the Arunta, Tennant creek, and Georgetown inliers of Northern Australia. 1984 , 31, 49-6	60	32

1572	Nd and Pb isotope evidence from the Seychelles granites and their xenoliths: Mantle origin with slight upper-crust interaction for alkaline anorogenic complexes. 1984 , 46, 13-35		5
1571	A Sm-Nd isotopic study of atmospheric dusts and particulates from major river systems. <i>Earth and Planetary Science Letters</i> , 1984 , 70, 221-236	5.3	1374
1570	Hydrothermal Mn-deposits of the Franciscan Assemblage, II. Isotope and trace element geochemistry, and implications for hydrothermal convection at spreading centers. <i>Earth and Planetary Science Letters</i> , 1984 , 71, 31-45	5.3	32
1569	Geochemistry of tholeiitic and alkalic lavas from the Koolau Range, Oahu, Hawaii: Implications for Hawaiian volcanism. <i>Earth and Planetary Science Letters</i> , 1984 , 69, 141-158	5.3	129
1568	Sm-Nd isotopic evolution of chondrites and achondrites, II. <i>Earth and Planetary Science Letters</i> , 1984 , 67, 137-150	5.3	569
1567	A Nd and Sr isotopic study of the Trinity peridotite; implications for mantle evolution. <i>Earth and Planetary Science Letters</i> , 1984 , 68, 361-378	5.3	88
1566	Recycling processes in granite-granodiorite complex genesis: the Querigut case studied by NdSr isotope systematics. <i>Earth and Planetary Science Letters</i> , 1984 , 69, 290-300	5.3	93
1565	SmNd study of Archean alkalic rocks from the Superior Province of the Canadian Shield. <i>Earth and Planetary Science Letters</i> , 1984 , 70, 40-46	5.3	50
1564	Isotopic constraints on Columbia River flood basalt genesis and the nature of the subcontinental mantle. 1984 , 48, 2357-2372		182
1563	Nd and Sr isotopic crustal contamination patterns in an Archaean meta-basic dyke from northern Labrador. 1984 , 48, 71-83		15
1562	Radiogenic Isotopes (Some Geological Applications. 1984 , 2, 375-421		20
1561	SmNd ages from the Ballantrae complex, SW Scotland. 1984 , 75, 183-187		36
1560	Geophysical and isotopic constraints on mantle convection: An interim synthesis. 1984 , 89, 6017-6040		144
1559	Classification of island arcs by Nd-Sr isotopic data 1984 , 18, 1-9		15
1558	Sm-Nd model ages across the margins of the Archaean Yilgarn Block, Western Australia III. The western margin. 1985 , 32, 73-82		34
1557	Rb-Sr, Sm-Nd and Pb-Pb geochronology of ancient gneisses from Mt Narryer, Western Australia. 1985 , 32, 349-358		20
1556	Precambrian geochronology and the geological record. 1985 , 10, 10-28		2
1555	Isotopenzusammensetzungen von Strontium und Neodym als Kennzeichen von Erdmantelmaterial. 1985 , 21, 165-169		

1554	Resetting of Nd and Sr whole-rock isochrons from polymetamorphic granulites, northeastern Alberta. 1985 , 22, 992-1000		8
1553	Isotope analysis of crystalline impact melt rocks from Apollo 16 stations 11 and 13, North Ray Crater. 1985 , 90, C431		16
1552	Smlld and Rbllr isotope systematics of an Archean anorthosite and related rocks from the Superior Province of the Canadian Shield. <i>Earth and Planetary Science Letters</i> , 1985 , 74, 338-346	5.3	26
1551	Mantle dynamics and basalt petrogenesis. 1985 , 112, 17-34		16
1550	Sm-Nd in marine carbonates and phosphates: Implications for Nd isotopes in seawater and crustal ages. 1985 , 49, 503-518		260
1549	ratio and composition of the Earth's upper mantle. 1985 , 49, 2123-2132		117
1548	Upper crustal recycling in southern Britain: evidence from Nd and Sr isotopes. <i>Earth and Planetary Science Letters</i> , 1985 , 75, 1-12	5.3	100
1547	Strontium and neodymium isotopes in hot springs on the East Pacific Rise and Guaymas Basin. <i>Earth and Planetary Science Letters</i> , 1985 , 72, 341-356	5.3	103
1546	The age and emplacement of obducted oceanic crust in the Urals from SmNd and RbSr systematics. Earth and Planetary Science Letters, 1985 , 72, 389-404	5.3	75
1545	A depleted mantle source for kimberlites from Zaire: Nd, Sr and Pb isotopic evidence. <i>Earth and Planetary Science Letters</i> , 1985 , 73, 269-277	5.3	24
1544	Variations in the Nd isotopic composition of foraminifera from Atlantic Ocean sediments. <i>Earth and Planetary Science Letters</i> , 1985 , 73, 299-305	5.3	78
1543	Age of the Mulcahy Lake intrusion, northwest Ontario, and implications for the evolution of greenstone-granite terrains. <i>Earth and Planetary Science Letters</i> , 1985 , 73, 306-316	5.3	31
1542	Kimberlite-borne garnet peridotite xenoliths from old enriched subcontinental lithosphere. <i>Earth and Planetary Science Letters</i> , 1985 , 75, 116-128	5.3	131
1541	Strontium, neodymium and lead isotopic compositions of deep crustal xenoliths from the Snake River Plain: evidence for Archean basement. <i>Earth and Planetary Science Letters</i> , 1985 , 75, 354-368	5.3	115
1540	Petrogenesis of layered gabbros and ultramafic rocks from Val Sesia, the Ivrea Zone, NW Italy: trace element and isotope geochemistry. 1986 , 24, 231-249		30
1539	In search of a bulk-Earth composition. 1986 , 57, 247-267		523
1538	Dating the oldest terrestrial rocks (Fact and fiction. 1986 , 57, 63-86		147
1537	Morphology versus UPb systematics in zircon: a high-resolution isotopic study of a zircon population from a Variscan dike in the Central Alps. <i>Earth and Planetary Science Letters</i> , 1986 , 78, 339-35	5 :3	56

1536	Geochronology and petrogenesis of Apollo 14 very high potassium mare basalts. 1986 , 91, 214-228	10
1535	Rb-Sr and Sm-Nd internal isochron ages of a subophitic basalt clast and a matrix sample from the Y75011 eucrite. 1986 , 91, 8137	71
1534	Isotopic modeling of the evolution of the mantle and crust. 1986 , 24, 311	24
1533	Nd and Pb isotopic studies of an Archaean layered mafic-ultramafic complex, Western Australia, and implications for mantle heterogeneity. 1986 , 50, 1-10	53
1532	Geochronology and isotopic variation of the early Archaean Amitsoq gneisses of the Isukasia area, southern West Greenland. 1986 , 50, 2173-2183	86
1531	Sm-Nd isotope study of early Archean rocks, Qianan, Hebei Province, China. 1986 , 50, 625-631	104
1530	Rare earth elements and neodymium isotopes in ferromanganese oxide coatings of Cenozoic foraminifera from the Atlantic Ocean. 1986 , 50, 409-417	116
1529	Sr, Nd and Pb isotopes in Proterozoic intrusives astride the Grenville Front in Labrador: Implications for crustal contamination and basement mapping. 1986 , 50, 2571-2585	69
1528	Mantle heterogeneity and crustal recycling in Archean granite-greenstone belts: Evidence from Nd isotopes and trace elements in the Rainy Lake area, Superior Province, Ontario, Canada. 1986 , 50, 2631-2651	237
1527	The Pb-Sr-Nd isotope geochemistry of some recent circum-Mediterranean granites. 1986 , 92, 331-340	89
1526	Nd and Sr isotopic systematics of central Australian granulites: chronology of crustal development and constraints on the evolution of lower continental crust. 1986 , 94, 289-303	52
1525	Geochronology of the Big Spruce Lake alkaline intrusion. 1986 , 23, 1-10	15
1524	Isotopic analysis of basaltic fragments from lunar breccia 14321: Chronology and petrogenesis of pre-Imbrium mare volcanism. 1987 , 51, 3241-3254	52
1523	Geochronology of high-K aluminous mare basalt clasts from Apollo 14 breccia 14304. 1987 , 51, 3255-3271	15
1522	Archean depleted mantle: Evidence from Nd and Sr initial isotopic ratios of carbonatites. 1987 , 51, 291-298	106
1521	Observations and controls on the occurrence of inherited zircon in Concord-type granitoids, New Hampshire. 1987 , 51, 2549-2558	80
1520	Age of the Archean Talga-Talga Subgroup, Pilbara Block, Western Australia, and early evolution of the mantle: new SmNd isotopic evidence. <i>Earth and Planetary Science Letters</i> , 1987 , 85, 105-116	89
1519	The Sm/Nd secular evolution of the continental crust and the depleted mantle. <i>Earth and Planetary Science Letters</i> , 1987 , 82, 25-35	58

1518	Isotopic abundances: inferences on solar system and planetary evolution. <i>Earth and Planetary Science Letters</i> , 1987 , 86, 129-173	5.3	48
1517	Metals and isotopes in Juan de Fuca Ridge hydrothermal fluids and their associated solid materials. 1987 , 92, 11400-11410		42
1516	Nd-Sr-Pb systematics and age of the Kings River ophiolite, California: implications for depleted mantle evolution. 1987 , 96, 281-290		23
1515	A Sm-Nd isotopic study of 500 Ma old oceanic crust in the Variscan belt of Western Europe: the Chamrousse ophiolite complex, Western Alps (France). 1987 , 96, 406-413		51
1514	A Nd and Sr isotopic study of the Ivrea zone, Southern Alps, N-Italy. 1987 , 97, 31-42		79
1513	The western border of the Archaean province of the Baltic shield: evidence from northern Sweden. 1987 , 95, 437-450		55
1512	The petrogenesis of massif anorthosites: a Nd and Sr isotopic investigation of the Proterozoic of Rogaland/Vest-Agder, SW Norway. 1988 , 98, 363-373		62
1511	Nd and Sr isotopic variations in acidic rocks formed under a peculiar tectonic environment in Miocene Southwest Japan. 1988 , 99, 1-10		54
1510	Decoupled evolution of Nd and Sr isotopes in the continental crust and the mantle. 1988 , 336, 733-738		76
1509	Neodymium isotopes as tracers in marine sediments and aerosols: North Atlantic. <i>Earth and Planetary Science Letters</i> , 1988 , 87, 367-378	5.3	198
1508	Nd and Sr isotopic systematics of river water suspended material: implications for crustal evolution. Earth and Planetary Science Letters, 1988 , 87, 249-265	5.3	751
1507	The age of ferroan anorthosite 60025: oldest crust on a young Moon?. <i>Earth and Planetary Science Letters</i> , 1988 , 90, 119-130	5.3	158
1506	Lower crustal evolution under central Arizona: Sr, Nd and Pb isotopic and geochemical evidence from the mafic xenoliths of Camp Creek. <i>Earth and Planetary Science Letters</i> , 1988 , 90, 26-40	5.3	58
1505	Isotopic constraints on crustal growth and recycling. Earth and Planetary Science Letters, 1988, 90, 315-32	;9 <u>,</u>	125
1504	Nd isotopic variations of Phanerozoic paleoceans. Earth and Planetary Science Letters, 1988, 90, 395-410 g	5.3	75
1503	Stored mafic/ultramafic crust and early Archean mantle depletion. <i>Earth and Planetary Science Letters</i> , 1988 , 91, 66-72	5.3	138
1502	Isotopic and chemical constraints on mantle-crust evolution. 1988 , 52, 1341-1350		83
1501	Laser probe 40Ar-39Ar studies of the Peace River shocked L6 chondrite. 1988 , 52, 2487-2499		74

1500	Nd and Sr isotope systematics of clastic metasediments from Isua, West Greenland: Identification of pre-3.8 Ga Differentiated Crustal Components. 1988 , 93, 338-354		98
1499	Comparison of Isotopic and Petrographic Provenance Indicators in Sediments from Tertiary Continental Basins of New Mexico. 1988 , Vol. 58,		8
1498	Abstracts of the 51st Meeting of the Meteoritical Society Fayetteville, Arkansas, 18½2 July 1988. 1988 , 23, 255-315		4
1497	Chapter 2. RADIOGENIC ISOTOPE GEOCHEMISTRY OF RARE EARTH ELEMENTS. 1989 , 25-44		3
1496	Isotopic and trace element constraints on the origin and evolution of saline groundwaters from central Missouri. 1989 , 53, 383-398		178
1495	SmNd age of the Fisken?sset Anorthosite Complex, West Greenland. <i>Earth and Planetary Science Letters</i> , 1989 , 91, 261-270	5.3	29
1494	UITh Pb systematics of morphologically characterized zircon and allanite: a high-resolution isotopic study of the Alpine Rensen pluton (northern Italy). <i>Earth and Planetary Science Letters</i> , 1989 , 95, 235-254	5.3	78
1493	Limits on chemical and convective isolation in the Earth's interior. 1989 , 75, 257-290		95
1492	Evolution and composition of the lithospheric mantle underneath the western Arabian peninsula: constraints from SrNd isotope systematics of mantle xenoliths. 1990 , 105, 460-472		81
1491	Non-monotonic chemical and O, Sr, Nd, and Pb isotope zonations and heterogeneity in the maficto silicic-composition magma chamber of the Grizzly Peak Tuff, Colorado. 1990 , 105, 677-690		24
1490	Anomalous SmNd ages for the early Archean Onverwacht Group Volcanics. 1990, 104, 27-34		31
1489	H, O, Sr, Nd, and Pb isotope geochemistry of the Latir volcanic field and cogenetic intrusions, New Mexico, and relations between evolution of a continental magmatic center and modifications of the lithosphere. 1990 , 104, 99-124		82
1488	Nd isotopes as tracers in water column particles: the western Mediterranean Sea. 1990 , 30, 389-407		21
1487	Literature. 1990 , 381-444		
1486	Chemical geodynamics in the back-arc region of Japan based on the trace element and Sr?Nd isotopic compositions. 1990 , 174, 207-233		74
1485	Actinide abundances in ordinary chondrites. 1990 , 54, 2847-2858		44
1484	Age of a eucrite clast from the Bholghati howardite. 1990 , 54, 2195-2206		43
1483	The theoretical effect of metasomatism on Sm-Nd isotopic systems. 1990 , 54, 1337-1341		43

1482	Origin of microgranular enclaves in granitoids: Equivocal Sr-Nd Evidence From Hercynian Rocks in the Massif Central (France). 1990 , 95, 17821	72
1481	Development of continental lithospheric mantle as reflected in the chemistry of the Mesozoic Appalachian Tholeiites, U.S.A <i>Earth and Planetary Science Letters</i> , 1990 , 97, 316-331	65
1480	Volcanism in the Sumisu Rift, II. Subduction and non-subduction related components. <i>Earth and Planetary Science Letters</i> , 1990 , 100, 195-209	133
1479	Sources of Hercynian granitoids from the French Massif Central: Inferences from Nd isotopes and consequences for crustal evolution. 1990 , 83, 281-296	91
1478	Isotopic evidence for crust-mantle evolution with emphasis on the Canadian Shield. 1990 , 83, 149-163	36
1477	Precise measurement of cerium isotope composition in rock samples. 1991 , 94, 1-11	39
1476	Early Proterozoic continental tholeiites from western Bergslagen, Central Sweden, II. Nd and Sr isotopic variations and implications from Sm?Nd systematics for the Svecofennian sub-continental mantle. 1991 , 52, 215-230	20
1475	Nd isotopic evidence for crustal recycling in the ca. 2.0 Ga subsurface of western Canada. 1991 , 28, 1140-114	7 34
1474	U P b ages and Sm N d signature of two subsurface granites from the Fort Simpson magnetic high, northwest Canada. 1991 , 28, 1003-1008	55
1473	Nd and Pb isotopic constraints on the origin of the Purtuniq ophiolite and Early Proterozoic Cape Smith Belt, northern Qubec, Canada. 1991 , 91, 357-371	20
1472	The continental crustal age distribution: Methods of determining mantle separation ages from Sm-Nd isotopic data and application to the southwestern United States. 1991 , 96, 2071	318
1471	Isotopic composition of Oligocene mafic volcanic rocks in the Northern Rio Grande Rift: Evidence for contributions of ancient intraplate and subduction magmatism to evolution of the lithosphere. 1991 , 96, 13593-13608	32
1470	The provenance of Archean clastic metasediments in the Narryer Gneiss Complex, Western Australia: Trace element geochemistry, Nd isotopes, and U-Pb ages for detrital zircons. 1991 , 55, 1915-1932	131
1469	Sm-Nd and Rb-Sr isotopic systematics of ureilites. 1991 , 55, 829-848	32
1468	Early mantle differentiation and its thermal consequences. 1991 , 55, 227-239	131
1467	Geochemical evidence for Triassic rifting in southwestern Florida. 1991 , 188, 291-302	27
1466	Precise measurement of cerium isotope composition in rock samples. 1991 , 94, 1-11	15
1465	Neodymium isotope evidence for ultra-depleted mantle in the early Proterozoic. 1991 , 354, 384-387	24

1464	Physical and chemical evidence on the cause and source characteristics of flood basalt volcanism. 1991 , 38, 525-544		110
1463	Character and U-Pb zircon age of the Proterozoic Ale granite, northern Sweden. 1991 , 113, 105-112		11
1462	Constraints on Archean Trondhjemite Genesis from Hydrous Crystallization Experiments on N ^o k Gneiss at 10-17 Kbar. 1992 , 100, 57-68		35
1461	Field relations, geochemistry, origin and emplacement of the Baltoro granite, Central Karakoram. 1992 , 83, 519-538		55
1460	Nd isotopic compositions of felsic igneous rocks in Cape Breton Island, Nova Scotia. 1992 , 29, 650-657		52
1459	Samarium-neodymium evolution of meteorites. 1992 , 56, 797-815		122
1458	Early magmatic phase in the Oslo Rift and its related stress regime. 1992 , 208, 37-54		29
1457	Rb-Sr and Sm-Nd chronology of an Apollo 17 KREEP basalt. <i>Earth and Planetary Science Letters</i> , 1992 , 108, 203-215	5.3	37
1456	Loss of isotopic (Nd, O) and chemical (REE) memory during metamorphism of komatiites: new evidence from eastern Finland. 1992 , 112, 66-82		59
1455	Petrogenesis of Variscan high-temperature Group A eclogites from the Moldanubian Zone of the Bohemian Massif, Czechoslovakia. 1992 , 111, 468-483		84
1454	Evidence from coupled 147SmII43Nd and 146SmII42Nd systematics for very early (4.5-Gyr) differentiation of the Earth's mantle. 1992 , 360, 728-732		138
1453	Conventional and ion-microprobe U-Pb dating of detrital zircons of the Tentudâ Group (Serie Negra, SW Spain): implications for zircon systematics, stratigraphy, tectonics and the Precambrian/Cambrian boundary. 1993 , 113, 289-299		49
1452	On the relationship between mantle metasomatism and partial melting Evidence from mantle-derived lherzolite xenoliths from Nahan, China. 1993 , 12, 289-307		5
1451	Primordial Ce isotopic composition of the solar system. 1993 , 106, 197-205		31
1450	Concentration and isotopic composition of Nd in the South Atlantic Ocean. <i>Earth and Planetary Science Letters</i> , 1993 , 117, 581-591	5.3	195
1449	Collision-related granitoid magmatism and crustal structure of the Hunza Karakoram, North Pakistan. 1993 , 74, 53-68		12
1448	Geochemistry and tectonic discrimination of Late Proterozoic arc-related volcaniclastic turbidite sequences, Antigonish Highlands, Nova Scotia. 1993 , 30, 2273-2282		21
1447	Sm?Nd, U?Pb, and Rb?Sr geochronology and lithostructural relationships in the southwestern Rae province: constraints on crustal assembly in the western Canadian shield. 1993 , 61, 27-50		39

1446	The geochemical balance of the rare earth elements and neodymium isotopes in the oceans. 1993 , 57, 1957-1986	314
1445	Antarctic polymict eucrite Yamato 792769 and the cratering record on the HED parent body. 1993 , 57, 2111-2121	8
1444	Ages of pristine noritic clasts from lunar breccias 15445 and 15455. 1993 , 57, 915-931	58
1443	An extremely low source in the Moon: U?Th?Pb, Sm?Nd, Rb?Sr, and isotopic systematics and age of lunar meteorite Asuka 881757. 1993 , 57, 4687-4702	53
1442	The evolution of a calc-alkaline basic to silicic magma system: Geochemical and Rb-Sr, Sm-Nd, and isotopic evidence from the Late Hercynian Atesina-Cima d'Asta volcano-plutonic complex, northern Italy. 1993 , 57, 4285-4300	39
1441	Lower Palaeozoic and Precambrian igneous rocks from eastern England, and their bearing on late Ordovician closure of the Tornquist Sea: constraints from U-Pb and Nd isotopes. 1993 , 130, 835-846	92
1440	Zircon ages and the distribution of Archaean and Proterozoic rocks in the Rauer Islands. 1993 , 5, 193-206	112
1439	References. 231-244	
1438	. 1993,	46
1437	Particulate and dissolved Nd in the western Mediterranean Sea: Sources, fate and budget. 1994 , 45, 283-305	63
	Particulate and dissolved Nd in the western Mediterranean Sea: Sources, fate and budget. 1994 , 45, 283-305 Archaean crustal development in the Lewisian complex of northwest Scotland. 1994 , 370, 552-555	63 25
1436	Archaean crustal development in the Lewisian complex of northwest Scotland. 1994 , 370, 552-555 The origin of fluids and the effects of metamorphism on the primary chemical compositions of Barberton komatiites: New evidence from geochemical (REE) and isotopic (Nd, O, H,) data. 1994 ,	25
1436 1435	Archaean crustal development in the Lewisian complex of northwest Scotland. 1994 , 370, 552-555 The origin of fluids and the effects of metamorphism on the primary chemical compositions of Barberton komatiites: New evidence from geochemical (REE) and isotopic (Nd, O, H,) data. 1994 , 58, 969-984 The size-isotopic evolution connection among layered mafic intrusions: Clues from a Sr-Nd isotopic	25 53
1436 1435 1434	Archaean crustal development in the Lewisian complex of northwest Scotland. 1994, 370, 552-555 The origin of fluids and the effects of metamorphism on the primary chemical compositions of Barberton komatiites: New evidence from geochemical (REE) and isotopic (Nd, O, H,) data. 1994, 58, 969-984 The size-isotopic evolution connection among layered mafic intrusions: Clues from a Sr-Nd isotopic study of a small complex. 1994, 99, 9441-9451 Aluminous subsolvus anorogenic granite genesis in the light of Nd isotopic heterogeneity. 1994,	25537
1436 1435 1434 1433	Archaean crustal development in the Lewisian complex of northwest Scotland. 1994, 370, 552-555 The origin of fluids and the effects of metamorphism on the primary chemical compositions of Barberton komatiites: New evidence from geochemical (REE) and isotopic (Nd, O, H,) data. 1994, 58, 969-984 The size-isotopic evolution connection among layered mafic intrusions: Clues from a Sr-Nd isotopic study of a small complex. 1994, 99, 9441-9451 Aluminous subsolvus anorogenic granite genesis in the light of Nd isotopic heterogeneity. 1994, 112, 199-219 Sm-Nd isotope systematics of 1.9-1.8-Ga granites from western Bergslagen, Sweden: inferences on	2553748
1436 1435 1434 1433	Archaean crustal development in the Lewisian complex of northwest Scotland. 1994, 370, 552-555 The origin of fluids and the effects of metamorphism on the primary chemical compositions of Barberton komatiites: New evidence from geochemical (REE) and isotopic (Nd, O, H,) data. 1994, 58, 969-984 The size-isotopic evolution connection among layered mafic intrusions: Clues from a Sr-Nd isotopic study of a small complex. 1994, 99, 9441-9451 Aluminous subsolvus anorogenic granite genesis in the light of Nd isotopic heterogeneity. 1994, 112, 199-219 Sm-Nd isotope systematics of 1.9-1.8-Ga granites from western Bergslagen, Sweden: inferences on a 2.1-2.0-Ga crustal precursor. 1994, 112, 21-37 Structural relationships and Sr?Nd isotope systematics of polymetamorphic granitic gneisses and granitic rocks from central Rajasthan, India: implications for the evolution of the Aravalli craton.	25 53 7 48 18

(1995-1994)

1428	U-Pb, Single Zircon Pb-Evaporation, and Sm-Nd Isotopic Study of a Granulite Domain in SE Madagascar. 1994 , 102, 523-538	194
1427	Silurian turbidites used to reconstruct a volcanic terrain and its Mesoproterozoic basement in the Irish Caledonides. 1995 , 152, 269-278	13
1426	Extreme Nd isotopic variation in the Trinity Ophiolite Complex and the role of melt/rock reactions in the oceanic lithosphere. 1995 , 121, 337-350	26
1425	Geochemical and isotopic characteristics of lower crustal xenoliths, San Francisco Volcanic Field, Arizona, U.S.A. 1995 , 36, 203-225	37
1424	REE and Nd isotope geochemistry, petrogenesis and volcanic evolution of contaminated komatiites at Kambalda, Western Australia. 1995 , 34, 127-157	139
1423	Sr-Nd isotopic constraints on the petrogenesis of the Central Bohemian Pluton, Czech Republic. 1995 , 84, 520-534	72
1422	Rapid accretion and early differentiation of Mars indicated by 142Nd/144Nd in SNC meteorites. 1995 , 267, 213-7	137
1421	Mylonitic mafic granulite in fault megabreccia at Clarke Head, Nova Scotia: a sample of Avalonian lower crust?. 1995 , 132, 81-90	7
1420	Sm?Nd evidence for late Archaean crust formation in the Lapland-Kola Mobile Belt, Kola Peninsula, Russia and Norway. 1995 , 72, 97-107	57
1419	Evolution of the Western European continental crust: implications from Nd and Pb isotopes in Iberian sediments. 1995 , 121, 345-357	48
1418	Origin of late Variscan granitoids from NE Bavaria, Germany, exemplified by REE and Nd isotope systematics. 1995 , 125, 249-270	46
1417	Exchange of neodymium and its isotopes between seawater and small and large particles in the Sargasso Sea. 1995 , 59, 535-547	149
1416	The age of the Earth. 1995 , 59, 1445-1456	248
1415	Geochemical and isotopic study of a norite-eclogite transition in the European Variscan belt: Implications for U?Pb zircon systematics in metabasic rocks. 1995 , 59, 1611-1622	63
1414	A lead isotopic study of circum-antarctic manganese nodules. 1995 , 59, 1809-1820	87
1413	The 4.56 Ga U?Pb age of the MET 780058 ureilite. 1995 , 59, 2319-2329	23
1412	Further evidence for a low U/Pb source in the moon: U?Th?Pb, Sm?Nd, and Ar?Ar isotopic systematics of lunar meteorite Yamato-793169. 1995 , 59, 2621-2632	22
1411	U?Th?Pb and Sm?Nd isotopic systematics of the Goalpara ureilite: Resolution of terrestrial contamination. 1995 , 59, 381-390	25

1410	Reply to the comment by C. A. Goodrich, G. W. Lugmair, M. J. Drake, and P. J. Patchett on U ThPb and SmNd isotopic systematics of the Goalpara ureilite: Resolution of terrestrial contamination 1995 , 59, 4087-4091	11
1409	The Relationship between Petrology and Nd Isotopes as Evidence for Contrasting Anorogenic Granite Genesis: Example of the Corsican Province (SE France). 1995 , 36, 1251-1274	98
1408	SmINd isotopic evidence for crustal contamination in the ca. 1750 Ma Wanapitei Complex, western Grenville Province, Ontario. 1995 , 32, 486-495	10
1407	Sm?Nd systematics of a silicate inclusion in the Caddo IAB iron meteorite. <i>Earth and Planetary Science Letters</i> , 1996 , 143, 1-12	25
1406	Enriched Nd?Sr?Pb isotopic signatures in the Dovyren layered intrusion (eastern Siberia, Russia): evidence for source contamination by ancient upper-crustal material. 1996 , 129, 39-69	36
1405	The neodymium isotopic compositions and rare earth patterns in highly depleted ultramafic rocks. 1996 , 60, 4537-4550	68
1404	Geochemistry of garnet peridotite massifs from lower Austria and the composition of deep lithosphere beneath a Palaeozoic convergent plate margin. 1996 , 134, 49-65	46
1403	Resetting of Sm?Nd systematics during metamorphism of > 3.7-Ga rocks: implications for isotopic models of early Earth differentiation. 1996 , 133, 225-240	105
1402	UPb, PbPb and SmNd dating of authigenic monazite: implications for the diagenetic evolution of the Welsh Basin. <i>Earth and Planetary Science Letters</i> , 1996 , 144, 421-433	65
1401	Geochemical and isotopic characteristics of Early Silurian clastic sequences in Antigonish Highlands, Nova Scotia, Canada: constraints on the accretion of Avalonia in the Appalachian ICaledonlde Orogen. 1996 , 33, 379-388	39
1400	An Archean oceanic felsic dyke swarm in a nascent arc: the Hunter Mine Group, Abitibi Greenstone Belt, Canada. 1996 , 72, 37-57	16
1399	Neodymium and strontium isotope study of the Blue Tier Batholith, NE Tasmania, and its bearing on the origin of tin-bearing alkali feldspar granites. 1996 , 10, 339-365	25
1398	Petrology of a 2.41 Ga remarkably fresh komatiitic basalt lava lake in Lion Hills, central Vetreny Belt, Baltic Shield. 1996 , 124, 273-290	54
1397	Age, origin and geodynamic significance of a polymetamorphic felsic intrusion in the E ztal Crystalline Basement, Tirol, Austria. 1996 , 58, 171-196	16
1396	Characterization and Origin of Aluminous A-type Granites from the Lachlan Fold Belt, Southeastern Australia. 1997 , 38, 371-391	778
1395	Continental Lithospheric Contribution to Alkaline Magmatism: Isotopic (Nd, Sr, Pb) and Geochemical (REE) Evidence from Serra de Monchique and Mount Ormonde Complexes. 1997 , 38, 115-132	36
1394	Cryptic trace-element variation as an indicator of reverse zoning in a granitic pluton: the Ricany granite, Czech Republic. 1997 , 154, 807-815	18
1393	Granitoid pluton formation by spreading of continental crust: the Wiley Glacier complex, northwest Palmer Land, Antarctica. 1997 , 283, 35-60	17

1392	Petrology and geochemistry of crustally contaminated komatiitic basalts from the Vetreny Belt, southeastern Baltic Shield: Evidence for an early Proterozoic mantle plume beneath rifted Archean continental lithosphere. 1997 , 61, 1205-1222		170	
1391	Crystallization, recrystallization, and impact-metamorphic ages of eucrites Y792510 and Y791186. 1997 , 61, 2119-2138		31	
1390	Secular changes of lead and neodymium in central Pacific seawater recorded by a Fe?Mn crust. 1997 , 61, 3957-3974		93	
1389	True K-feldspar granites in oceanic crust (Masirah ophiolite, Sultanate of Oman): A U?Pb and Sm?Nd isotope study. 1997 , 138, 119-126		11	
1388	Depleted-mantle source for the Ulungur River A-type granites from North Xinjiang, China: geochemistry and NdBr isotopic evidence, and implications for Phanerozoic crustal growth. 1997 , 138, 135-159		398	
1387	Sm?Nd signature of modern and late Quaternary sediments from the northwest North Atlantic: Implications for deep current changes since the Last Glacial Maximum. <i>Earth and Planetary Science Letters</i> , 1997 , 146, 607-625	5.3	49	
1386	Patagonian origin of glacial dust deposited in East Antarctica (Vostok and Dome C) during glacial stages 2, 4 and 6. <i>Earth and Planetary Science Letters</i> , 1997 , 146, 573-589	5.3	304	
1385	The Lu-Hf isotope geochemistry of chondrites and the evolution of the mantle-crust system. <i>Earth and Planetary Science Letters</i> , 1997 , 148, 243-258	5.3	2491	
1384	Effects of interaction between ultramafic tectonite and mafic magma on Nd-Pb-Sr isotopic systems in the Neoproterozoic Chaya Massif, Baikal-Muya ophiolite belt. <i>Earth and Planetary Science Letters</i> , 1997 , 148, 299-316	5.3	31	
1383	A comparison of the Skiddaw and Manx groups (English Lake District and Isle of Man) using neodymium isotopes. 1997 , 51, 343-347		13	
1382	Closure of the Central American Isthmus and its effect on deep-water formation in the North Atlantic. 1997 , 386, 382-385		182	
1381	Nd and Sr isotopic constraints on the origin of igneous rocks resulting from the opening of the Japan Sea, southwestern Japan. 1997 , 129, 75-86		8	
1380	A mantle-derived bimodal suite in the Hercynian Belt: Nd isotope and trace element evidence for a subduction-related rift origin of the Late Devonian Brvenne metavolcanics, Massif Central (France). 1997 , 129, 222-238		156	
1379	Petrology and geochemistry of syn- to post-collisional metaluminous A-type granites major and trace element and NdBrPbD-isotope study from the Proterozoic Damara Belt, Namibia. 1998 , 45, 147-175		106	
1378	Post-collisional Variscan lamprophyres (Black Forest, Germany): 40Ar/39Ar phlogopite dating, Nd, Pb, Sr isotope, and trace element characteristics. 1998 , 45, 395-411		45	
1377	Petrology of mafic lavas within the Onega plateau, central Karelia: evidence for 2.0 Ga plume-related continental crustal growth in the Baltic Shield. 1998 , 130, 134-153		91	
1376	Extreme Nd isotope homogeneity in a large rhyolitic province: the Estfel massif, southeast France. 1998 , 60, 213-223		11	
1375	The Sr, Nd isotopic composition of lamprophyres in Laowangzhai gold orefield, Yunnan Province. 1998 , 43, 950-954		3	

1374	Nd isotopic evolution of the upper mantle during the Precambrian: models, data and the uncertainty of both. 1998 , 91, 233-252		116
1373	Oxygen, strontium, and neodymium isotope composition of fossil shark teeth as a proxy for the palaeoceanography and palaeoclimatology of the Miocene northern Alpine Paratethys. 1998 , 142, 107-	121	49
1372	Concentrations and isotopic compositions of neodymium in the eastern Indian Ocean and Indonesian straits. 1998 , 62, 2597-2607		108
1371	Metamorphic overprinting of Sm?Nd isotopic systems in volcanic rocks: the Telemark supergroup, southern Norway. 1998 , 145, 1-16		29
1370	Hf isotope constraints on mantle evolution. 1998 , 145, 447-460		250
1369	Importance of late-magmatic and hydrothermal fluids on the SmNd isotope mineral systematics of hypersolvus granites. 1998 , 146, 187-203		40
1368	The origin of U-shaped rare earth patterns in ophiolite peridotites: assessing the role of secondary alteration and melt/rock reaction. 1998 , 62, 3545-3560		82
1367	Geochronology and geochemistry of a Mesozoic magmatic arc system, Fiordland, New Zealand. 1998 , 155, 1037-1053		146
1366	Pre-lamprophyre mafic dykes of the Cape Meredith Complex, West Falkland. 1998 , 135, 495-500		10
1365	European contribution of ice-rafted sand to Heinrich layers H3 and H4. 1999 , 158, 197-208		69
1364	Lithospheric sources of North Florida, USA tholeiites and implications for the origin of the Suwannee terrane. 1999 , 46, 215-233		34
1363	Geochemistry of Glimmerite Veins in Peridotites from Lower AustriaImplications for the Origin of K-rich Magmas in Collision Zones. 1999 , 40, 315-338		52
1362	Relationships between Lull and Smld isotopic systems in the global sedimentary system. <i>Earth and Planetary Science Letters</i> , 1999 , 168, 79-99	5.3	804
1361	Precise ReDs mineral isochron and PbNdDs isotope systematics of a maficultramafic sill in the 2.0 Ga Onega plateau (Baltic Shield). <i>Earth and Planetary Science Letters</i> , 1999 , 170, 447-461	5.3	73
1360	Actual timing of neodymium isotopic variations recorded by FeMn crusts in the western North Atlantic. <i>Earth and Planetary Science Letters</i> , 1999 , 171, 149-156	5.3	68
1359	Erosional history of the Himalayan and Burman ranges during the last two glacialInterglacial cycles. <i>Earth and Planetary Science Letters</i> , 1999 , 171, 647-660	5.3	211
1358	Combined mantle plume-island arc model for the formation of the 2.9 ga sumozero-kenozero greenstone belt, se baltic shield: isotope and trace element constraints. 1999 , 63, 3579-3595		123
1357	Deep circulation changes in the Labrador Sea since the Last Glacial Maximum: New constraints from Sm-Nd data on sediments. 1999 , 14, 777-788		33

(2000-2000)

1356	Sr and Nd isotope ratios and REE abundances of moraines in the mountain areas surrounding the Taklimakan Desert, NW China 2000 , 34, 407-427	52
1355	Taking the roof off a suture zone: basin setting and provenance of conglomerates in the ORS Dingle Basin of SW Ireland. 2000 , 180, 185-222	9
1354	Proto-Avalonia: A 1.2🛮.0 Ga tectonothermal event and constraints for the evolution of Rodinia. 2000 , 28, 1071	111
1353	Evolution of the Pan-African Wadi Haimur metamorphic sole, Eastern Desert, Egypt. 2000 , 18, 639-651	55
1352	Hf-Nd isotope evidence for a transient dynamic regime in the early terrestrial mantle. 2000 , 404, 488-90	51
1351	Evolution of the sublayer of the Sudbury Igneous Complex: geochemical, SmNd isotopic and petrologic evidence. 2000 , 51, 271-292	34
1350	The Isotope and Trace Element Budget of the Cambrian Devil River Arc System, New Zealand: Identification of Four Source Components. 2000 , 41, 759-788	72
1349	Petrogenesis of Mafic to Felsic Plutonic Rock Associations: the Calc-alkaline Qufigut Complex, French Pyrenees. 2000 , 41, 809-844	140
1348	Silurian provenance variation in the Southern Uplands terrane, Scotland, assessed using neodymium isotopes and linked with regional tectonic evolution. 2000 , 91, 447-455	12
1347	Tectonic influence on sedimentation along the southern flank of the late Paleozoic Magdalen basin in the Canadian Appalachians: Geochemical and isotopic constraints on the Horton Group in the St. Marys basin, Nova Scotia. 2000 , 112, 997-1011	39
1346	Gòchronologie U P b et gòchimie isotopique Sr N Id des granitodes nòprotfozoques des suites Galilîa et Urucum, vallè du Rio Doce, Sud-Est du Brŝil. 2000 , 331, 459-466	
1345	Resolving crystallisation ages of Archean maficultramafic rocks using the ReDs isotope system. Earth and Planetary Science Letters, 2000, 179, 453-467 5-3	23
1344	HfNd isotopic evolution of the lower crust. <i>Earth and Planetary Science Letters</i> , 2000 , 181, 115-129 5.3	149
1343	Provenance and transport of terrigenous sediment in the south Atlantic Ocean and their relations to glacial and interglacial cycles: Nd and Sr isotopic evidence. 2000 , 64, 3813-3827	110
1342	Change of Sm-Nd isotope composition during weathering of till. 2000 , 64, 813-820	57
1341	Fossil fish teeth as proxies for seawater Sr and Nd isotopes. 2000 , 64, 835-847	115
1340	Reassessment of the origin of the Dun Mountain Ophiolite, New Zealand: Nd-isotopic and geochemical evolution of magma suites. 2000 , 43, 133-146	29
1339	Taltson basement gneissic rocks: U?Pb and Nd isotopic constraints on the basement to the Paleoproterozoic Taltson magmatic zone, northeastern Alberta. 2000 , 37, 1575-1596	64

1338	Volcanic layers in Antarctic (Vostok) ice cores: Source identification and atmospheric implications. 2001 , 106, 31915-31931	62
1337	Zooming in on Heinrich layers. 2001 , 16, 240-259	115
1336	Nd isotopic and geochemical signature of the Paleoproterozoic Trans-Hudson Orogen, southern Baffin Island, Canada: implications for the evolution of eastern Laurentia. 2001 , 108, 113-138	31
1335	Trace element and isotopic (Sr, Nd, Pb, O) arguments for a mid-crustal origin of Pan-African garnet-bearing S-type granites from the Damara orogen (Namibia). 2001 , 110, 325-355	77
1334	Tracing Papua New Guinea imprint on the central Equatorial Pacific Ocean using neodymium isotopic compositions and Rare Earth Element patterns. <i>Earth and Planetary Science Letters</i> , 2001 , 5.3 186, 497-512	185
1333	Geochemical and Nd-isotopic systematics of the Permo-Triassic Gympie Group, southeast Queensland. 2001 , 48, 377-393	29
1332	On the Lu-Hf Isotope Geochemistry of Silicate Rocks. 2001 , 25, 41-56	99
1331	The Aguablanca CuNi ore deposit (Extremadura, Spain), a case of synorogenic orthomagmatic mineralization: age and isotope composition of magmas (Sr, Nd) and ore (S). 2001 , 18, 237-250	57
1330	Hf isotope evidence for a hidden mantle reservoir. 2002 , 30, 771	78
1329	Hf Isotope Evidence for a Miocene Change in the Kerguelen Mantle Plume Composition. 2002 , 43, 1327-1339	25
1329 1328	Hf Isotope Evidence for a Miocene Change in the Kerguelen Mantle Plume Composition. 2002 , 43, 1327-1339 Andesite petrogenesis in the Ordovician Borrowdale Volcanic Group of the English Lake District by fractionation, assimilation and mixing. 2002 , 159, 417-424	259
	Andesite petrogenesis in the Ordovician Borrowdale Volcanic Group of the English Lake District by	
1328	Andesite petrogenesis in the Ordovician Borrowdale Volcanic Group of the English Lake District by fractionation, assimilation and mixing. 2002 , 159, 417-424 Basement Geochemistry and Geochronology of Central Malaita, Solomon Islands, with Implications	9
1328 1327	Andesite petrogenesis in the Ordovician Borrowdale Volcanic Group of the English Lake District by fractionation, assimilation and mixing. 2002, 159, 417-424 Basement Geochemistry and Geochronology of Central Malaita, Solomon Islands, with Implications for the Origin and Evolution of the Ontong Java Plateau. 2002, 43, 449-484 The geochemistry of lamprophyres in the Laowangzhai gold deposits, Yunnan Province, China:	9
1328 1327 1326	Andesite petrogenesis in the Ordovician Borrowdale Volcanic Group of the English Lake District by fractionation, assimilation and mixing. 2002, 159, 417-424 Basement Geochemistry and Geochronology of Central Malaita, Solomon Islands, with Implications for the Origin and Evolution of the Ontong Java Plateau. 2002, 43, 449-484 The geochemistry of lamprophyres in the Laowangzhai gold deposits, Yunnan Province, China: Implications for its characteristics of source region 2002, 36, 91-112 Geochemistry of the Neoproterozoic Metasedimentary Gamble Brook Formation, Avalon Terrane, Nova Scotia: Evidence for a Rifted-Arc Environment along the West Gondwanan Margin of Rodinia.	9 157 18
1328 1327 1326 1325	Andesite petrogenesis in the Ordovician Borrowdale Volcanic Group of the English Lake District by fractionation, assimilation and mixing. 2002, 159, 417-424 Basement Geochemistry and Geochronology of Central Malaita, Solomon Islands, with Implications for the Origin and Evolution of the Ontong Java Plateau. 2002, 43, 449-484 The geochemistry of lamprophyres in the Laowangzhai gold deposits, Yunnan Province, China: Implications for its characteristics of source region 2002, 36, 91-112 Geochemistry of the Neoproterozoic Metasedimentary Gamble Brook Formation, Avalon Terrane, Nova Scotia: Evidence for a Rifted-Arc Environment along the West Gondwanan Margin of Rodinia. 2002, 110, 407-419 Geochemistry and Nd-isotope systematics of chemical and terrigenous sediments from the Dun	9 157 18
1328 1327 1326 1325	Andesite petrogenesis in the Ordovician Borrowdale Volcanic Group of the English Lake District by fractionation, assimilation and mixing. 2002, 159, 417-424 Basement Geochemistry and Geochronology of Central Malaita, Solomon Islands, with Implications for the Origin and Evolution of the Ontong Java Plateau. 2002, 43, 449-484 The geochemistry of lamprophyres in the Laowangzhai gold deposits, Yunnan Province, China: Implications for its characteristics of source region 2002, 36, 91-112 Geochemistry of the Neoproterozoic Metasedimentary Gamble Brook Formation, Avalon Terrane, Nova Scotia: Evidence for a Rifted-Arc Environment along the West Gondwanan Margin of Rodinia. 2002, 110, 407-419 Geochemistry and Nd-isotope systematics of chemical and terrigenous sediments from the Dun Mountain Ophiolite, New Zealand. 2002, 45, 427-451	9 157 18 33

1320	147SmIl43Nd and 176LuIl76Hf in eucrites and the differentiation of the HED parent body. <i>Earth and Planetary Science Letters</i> , 2002 , 204, 167-181	147
1319	Late Neoproterozoic crustal growth in the European Variscides: Nd isotope and geochemical evidence from the Sierra de Cfdoba Andesites (Ossa-Morena Zone, Southern Spain). 2002 , 352, 133-151	32
1318	Glacial[hterglacial cycles in Sr and Nd isotopic composition of Arctic marine sediments triggered by the Svalbard/Barents Sea ice sheet. 2002 , 182, 351-372	103
1317	Neodymium isotopic composition of Ordovician conodonts as a seawater proxy: Testing paleogeography. 2002 , 3, n/a-n/a	17
1316	Petrogenesis of metaluminous A-type rhyolites from the St Francois Mountains, Missouri and the Mesoproterozoic evolution of the southern Laurentian margin. 2002 , 113, 269-291	58
1315	Pb- and Nd-isotope systematics of stromatolitic limestones from the 2.7 Ga Ngezi Group of the Belingwe Greenstone Belt: constraints on timing of deposition and provenance. 2002 , 114, 277-294	46
1314	Neodymium isotope characteristics of Ordovician sediment provenance on the Avalonian margin of the Iapetus Ocean. 2002 , 38, 143-153	4
1313	SmINd isotopic systematics as tectonic tracers: an example from West Avalonia in the Canadian Appalachians. 2002 , 59, 77-100	103
1312	Mantle and Crustal Sources in the Genesis of Late-Hercynian Granitoids (NW Portugal): Geochemical and Sr-Nd Isotopic Constraints. 2002 , 5, 287-305	50
1311	Trace element and isotope (Sr, Nd) geochemistry of porphyry- and skarn-mineralising Late Cretaceous intrusions from Banat, western South Carpathians, Romania. 2002 , 37, 568-586	20
1310	Synorogenic melting of mafic lower crust: constraints from geochronology, petrology and Sr, Nd, Pb and O isotope geochemistry of quartz diorites (Damara orogen, Namibia). 2002 , 143, 551-566	95
1309	In situ investigations of allanite hydrothermal alteration: examples from calc-alkaline and anorogenic granites of Corsica (southeast France). 2002 , 142, 485-500	61
1308	Geochemistry of carbonatites in Maoniuping REE deposit, Sichuan province, China. 2003 , 46, 246-256	34
1307	Geochemistry and mineralogy of Platinum-group elements in the Ransko gabbroperidotite massif, Bohemian Massif (Czech Republic). 2003 , 38, 298-311	5
1306	The «Venice Granodiorite»: constraints on the «Caledonian» and Variscan events in the Alpine domain. 2003 , 14, 179-204	2
1305	Lower crustal melting and the role of open-system processes in the genesis of syn-orogenic quartz dioritegraniteleucogranite associations: constraints from SrNdD isotopes from the Bandombaai Complex, Namibia. 2003 , 67, 205-226	69
1304	Patterns and processes in reef fish diversity. 2003 , 421, 933-6	258
1303	Early history of Earth's crust-mantle system inferred from hafnium isotopes in chondrites. 2003 , 421, 931-3	157

1302	Geochemistry: Lost terrains of early Earth. 2003 , 421, 901-3	3
1301	A New Digestion and Chemical Separation Technique for Rapid and Highly Reproducible Determination of Lu/Hf and Hf Isotope Ratios in Geological Materials by MC-ICP-MS. 2003 , 27, 133-145	80
1300	Late Pleistocene sedimentation in the Western Mediterranean Sea: implications for productivity changes and climatic conditions in the catchment areas. 2003 , 190, 121-137	40
1299	Petrology of basement-dominated terranes. 2003 , 199, 1-28	55
1298	Nb/Ta, Zr/Hf and REE in the depleted mantle: implications for the differentiation history of the crustfhantle system. <i>Earth and Planetary Science Letters</i> , 2003 , 205, 309-324	141
1297	Isotopic evidence for the magmatic and tectonic histories of the Carolina terrane: implications for stratigraphy and terrane affiliation. 2003 , 371, 187-211	24
1296	Low-pressure metamorphism and leucogranite magmatism, northeastern Yeongnam Massif, Korea: implication for Paleoproterozoic crustal evolution. 2003 , 122, 235-251	59
1295	Petrology and geochemistry of the Lyngdal granodiorite (Southern Norway) and the role of fractional crystallisation in the genesis of Proterozoic ferro-potassic A-type granites. 2003 , 124, 149-184	60
1294	A geochronological and geochemical study of rocks from Gjelsvikfjella, Dronning Maud Land, Antarctical Implications for Mesoproterozoic correlations and assembly of Gondwana. 2003 , 125, 113-138	67
1293	Quantification of Magmatic and Hydrothermal Processes in a Peralkaline Syenite-Alkali Granite Complex Based on Textures, Phase Equilibria, and Stable and Radiogenic Isotopes. 2003 , 44, 1247-1280	74
1292	A geochemical and Sr-Nd-O isotopic study of the Proterozoic Eriksfjord Basalts, Gardar Province, South Greenland: Reconstruction of an OIB signature in crustally contaminated rift-related basalts. 2003 , 67, 831-853	36
1291	Compositional Evolution of the Mantle. 2003 , 493-519	43
1290	Long-lived Isotopic Tracers in Oceanography, Paleoceanography, and Ice-sheet Dynamics. 2003, 453-489	127
1289	First Characterization and Dating of East Antarctic Bedrock Inclusions from Subglacial Lake Vostok Accreted Ice. 2004 , 1, 90	10
1288	Protolith ages of eclogites, Marun-Keu Complex, Polar Urals, Russia: implications for the pre- and early Uralian evolution of the northeastern European continental margin. 2004 , 30, 87-105	21
1287	Deciphering the petrogenesis of deeply buried granites: whole-rock geochemical constraints on the origin of largely undepleted felsic granulites from the Moldanubian Zone of the Bohemian Massif. 2004 , 95, 141-159	85
1286	Deciphering the petrogenesis of deeply buried granites: whole-rock geochemical constraints on the origin of largely undepleted felsic granulites from the Moldanubian Zone of the Bohemian Massif. 2004 ,	2
1285	Pin-pricking the elephant: evidence on the origin of the Ontong Java Plateau from Pb-Sr-Hf-Nd isotopic characteristics of ODP Leg 192 basalts. 2004 , 229, 133-150	35

1284	Geochemical and isotopic studies of aeolian sediments in China. 2004 , 51, 211-230	121
1283	Ion microprobe and ID-TIMS U P b dating on zircon grains from leg 173 amphibolites: evidence for Permian magmatism on the West Iberian margin. 2004 , 16, 226-231	9
1282	Petrology of an intrusion-related high-grade migmatite: implications for partial melting of metasedimentary rocks and leucosome-forming processes. 2004 , 16, 425-445	37
1281	Trace element and CDBrNd isotope evidence for subduction-related carbonateBilicate melts in mantle xenoliths (Pannonian Basin, Hungary). 2004 , 75, 89-113	47
1280	Crustal contamination of mafic magmas: evidence from a petrological, geochemical and Sr?Nd?Os?O isotopic study of the Proterozoic Isortoq dike swarm, South Greenland. 2004 , 74, 199-232	54
1279	Comparing the Epica and Vostok dust records during the last 220,000 years: stratigraphical correlation and provenance in glacial periods. 2004 , 66, 63-87	212
1278	Zircon ages, geochemistry, and Nd isotopic systematics of pre-Variscan orthogneisses from the Erzgebirge, Saxony (Germany), and geodynamic interpretation. 2004 , 93, 706-727	40
1277	Dust size evidence for opposite regional atmospheric circulation changes over east Antarctica during the last climatic transition. 2004 , 23, 427-438	112
1276	Shear zone-related syenites in the Damara belt (Namibia): the role of crustal contamination and source composition. 2004 , 148, 104-121	17
1275	Geochemical constraints on the petrogenesis of arc picrites and basalts, New Georgia Group, Solomon Islands. 2004 , 148, 288-304	83
1274	The giant Vergenoeg fluorite deposit in a magnetitefluoriteflayalite REE pipe: a hydrothermally-altered carbonatite-related pegmatoid?. 2004 , 80, 173-199	19
1273	TTG magmatism in the Congo craton; a view from major and trace element geochemistry, RbBr and SmBd systematics: case of the Sangmelima region, Ntem complex, southern Cameroon. 2004 , 40, 61-79	80
1272	The Early Cretaceous San Juan Plutonic Suite, Ecuador: a magma chamber in an oceanic plateau?. 2004 , 41, 1237-1258	22
1271	Neodymium isotopic composition and rare earth element concentrations in the deep and intermediate Nordic Seas: Constraints on the Iceland Scotland Overflow Water signature. 2004 , 5, n/a-n/a	81
1270	Subpolar Mode Water formation traced by neodymium isotopic composition. 2004, 31,	57
1269	An Overview of Isotopic Anomalies in Extraterrestrial Materials and Their Nucleosynthetic Heritage. 2004 , 55, 25-64	37
1268	H, O, Sr, Nd, and Pb isotopic evidence for recycled oceanic crust in the Transitional Volcanic Group of Fuerteventura, Canary Islands, Spain. 2004 , 205, 37-54	24
1267	Petrogenesis of the Gross Spitzkoppe topaz granite, central western Namibia: a geochemical and NdBrBb isotope study. 2004 , 206, 43-71	30

1266	U P b zircon ages and Nd, Sr, and Pb isotopes of lower crustal xenoliths from North China Craton: insights on evolution of lower continental crust. 2004 , 211, 87-109		198
1265	SmNd systematics of zircon. 2004 , 211, 375-387		25
1264	Sm-Nd, Lu-Hf and Pb-Pb signatures of gneisses and granitoids from the La Grande belt: extent of late Archean crustal recycling in the northeastern Superior Province, Canada. 2004 , 68, 1099-1113		15
1263	Nd-, O-, and H-isotopic evidence for complex, closed-system fluid evolution of the peralkaline Il^2 maussaq intrusion, south Greenland. 2004 , 68, 3379-3395		71
1262	Lullf and SmNd isotopic systematics in chondrites and their constraints on the Lullf properties of the Earth. <i>Earth and Planetary Science Letters</i> , 2004 , 222, 29-41	5.3	117
1261	SmNd systematics of chondrites. <i>Earth and Planetary Science Letters</i> , 2004 , 223, 267-282	5.3	42
1260	Behaviour of high field strength elements in subduction zones: constraints from KamchatkaAleutian arc lavas. <i>Earth and Planetary Science Letters</i> , 2004 , 224, 275-293	5.3	259
1259	Nature of the depleted upper mantle beneath the Atlantic: evidence from Hf isotopes in normal mid-ocean ridge basalts from 79°N to 55°S. <i>Earth and Planetary Science Letters</i> , 2004 , 225, 89-103	5.3	48
1258	Franciscan subduction off to a slow start: evidence from high-precision Lull garnet ages on high grade-blocks. <i>Earth and Planetary Science Letters</i> , 2004 , 225, 147-161	5.3	160
1257	Trace element fractionation during fluid-induced eclogitization in a subducting slab: trace element and LulfBmId isotope systematics. <i>Earth and Planetary Science Letters</i> , 2004 , 227, 441-456	5.3	186
1256	Basement tracing using Mid-Proterozoic anorthosites straddling a palaeoterrane boundary, Ontario, Canada. 2004 , 129, 169-184		4
1255	Geochemical evidence for a Neoproterozoic magmatic continental margin in Sri Lankalelevance for the Rodinial ondwana supercontinent cycle. 2004 , 130, 185-198		26
1254	Basement terrane correlations and crustal recycling in the western Superior Province: Nd isotopic character of granitoid and felsic volcanic rocks in the Wabigoon subprovince, N. Ontario, Canada. 2004 , 132, 245-274		56
1253	Evolution of the continental crust in the Kerala Khondalite Belt, southernmost India: evidence from Nd isotope mapping, UBb and RbBr geochronology. 2004 , 134, 275-292		56
1252	Deciphering the petrogenesis of deeply buried granites: whole-rock geochemical constraints on the origin of largely undepleted felsic granulites from the Moldanubian Zone of the Bohemian Massif. 2004 , 95, 141		47
1251	Petrogenesis of Cogenetic Nepheline and Quartz Syenites and Granites (Northern Damara Orogen, Namibia): Enriched Mantle versus Crustal Contamination. 2005 , 113, 651-672		26
1250	Nd and Sr isotopic signatures of fine-grained clastic sediments: A case study of western Pacific marginal basins. 2005 , 182, 183-199		39
1249	REE and [Nd of clay fractions in sediments from the eastern Pacific Ocean: Evidence for clay sources. 2005 , 48, 701-712		1

(2005-2005)

1248	Late Oligocene post-obduction granitoids of New Caledonia: A case for reactivated subduction and slab break-off. 2005 , 14, 254-271	48
1247	Late Archean high-Mg granitoids (sanukitoids) in the southern Karelian domain, eastern Finland: Pb and Nd isotopic constraints on crustthantle interactions. 2005 , 79, 161-178	118
1246	Major and trace element and isotopic (Sr, Nd, O) constraints for Pan-African crustally contaminated grey granite gneisses from the southern Kaoko belt, Namibia. 2005 , 84, 25-50	30
1245	Isotopic equilibrium/disequilibrium in granites, metasedimentary rocks and migmatites (Damara orogen, Namibia) consequence of polymetamorphism and melting. 2005 , 84, 168-184	24
1244	Late Quaternary climatic control on erosion and weathering in the eastern Tibetan Plateau and the Mekong Basin. 2005 , 63, 316-328	78
1243	U P b baddeleyite ages and Hf, Nd isotope chemistry constraining repeated mafic magmatism in the Fennoscandian Shield from 1.6 to 0.9 Ga. 2005 , 150, 174-194	167
1242	Post-collisional plutonism with adakite-like signatures: the Eocene Sarayc—k granodiorite (Eastern Pontides, Turkey). 2005 , 150, 441-455	156
1241	Nd, Sr and Pb isotopic and REE geochemical study of some Miocene submarine hydrothermal deposits (Kuroko deposits) in Japan. 2005 , 149, 388-399	3
1240	The Sm B ld method. 2005 , 70-100	
1239	Petrogenesis of a Late Jurassic Peraluminous Volcanic Complex and its High-Mg, Potassic, Quenched Enclaves at Xiangshan, Southeast China. 2005 , 46, 1121-1154	126
1238	Petrogenesis of alkali pyroxenite and ijolite xenoliths from the Tertiary LoucnaOberwiesenthal Volcanic Centre, Bohemian Massif in the light of new mineralogical, geochemical, and isotopic data. 2005 , 182, 57-79	8
1237	Temporal relationships of carbon cycling and ocean circulation at glacial boundaries. 2005, 307, 1933-8	237
1236	Potassic Magmatism in Western Sichuan and Yunnan Provinces, SE Tibet, China: Petrological and Geochemical Constraints on Petrogenesis. 2005 , 46, 33-78	186
1235	Geochemistry of the Tremadocian Ti-u Formation (Southern Mexico): Provenance in the Underlying ~1 Ga Oaxacan Complex on the Southern Margin of the Rheic Ocean. 2005 , 47, 887-900	12
1234	A new estimate for the composition of weathered young upper continental crust from alluvial sediments, Queensland, Australia. 2005 , 69, 1041-1058	276
1234		276 7
	sediments, Queensland, Australia. 2005 , 69, 1041-1058 Evolution of Palaeoproterozoic mafic intrusions located within the thermal aureole of the Sudbury	

1230	Neodymium isotopes as a new tool for quantifying exchange fluxes at the continentDcean interface. <i>Earth and Planetary Science Letters</i> , 2005 , 232, 245-257	5.3	296
1229	Grand Comore Island: A well-constrained Ibw 3He/4HeImantle plume. <i>Earth and Planetary Science Letters</i> , 2005 , 233, 391-409	5.3	44
1228	Sediment provenances and drainage evolution of the Neogene Amazonian foreland basin. <i>Earth and Planetary Science Letters</i> , 2005 , 239, 57-78	5.3	86
1227	Sediment sources and East Asian monsoon intensity over the last 450 ky. Mineralogical and geochemical investigations on South China Sea sediments. 2005 , 228, 260-277		100
1226	Isotopic composition (O, C, Sr, and Nd) and trace element ratios (Sr/Ca, Mg/Ca) of Miocene marine and brackish ostracods from North Alpine Foreland deposits (Germany and Austria) as indicators for palaeoclimate. 2005 , 225, 216-247		44
1225	The Shishkhid ophiolite, northern Mongolia: A key to the reconstruction of a Neoproterozoic island-arc system in central Asia. 2005 , 138, 125-150		108
1224	142Nd evidence for early (>4.53 Ga) global differentiation of the silicate Earth. 2005 , 309, 576-81		474
1223	Acquisition of the neodymium isotopic composition of the North Atlantic Deep Water. 2005 , 6, n/a-n/a		105
1222	Sm-Nd isotope and trace element evidence for heterogeneous igneous protoliths of Variscan mafic blueschists in the East Krkono B Complex (West Sudetes, NE Bohemian Massif, Czech Republic). 2005 , 18, 363-374		9
1221	IGNEOUS ALBITITE DIKES IN OROGENIC LHERZOLITES, WESTERN PYRENEES, FRANCE: A POSSIBLE SOURCE FOR CORUNDUM AND ALKALI FELDSPAR XENOCRYSTS IN BASALTIC TERRANES. II. GEOCHEMICAL AND PETROGENETIC CONSIDERATIONS. 2006 , 44, 843-856		32
1220	Evolution of weathering patterns in the Indo-Burman Ranges over the last 280 kyr: Effects of sediment provenance on 87Sr/86Sr ratios tracer. 2006 , 7, n/a-n/a		100
1219	Temporal stability of the neodymium isotope signature of the Holocene to glacial North Atlantic. 2006 , 21,		59
1218	Eastern Australia: A possible source of dust in East Antarctica interglacial ice. <i>Earth and Planetary Science Letters</i> , 2006 , 249, 1-13	5.3	163
1217	Reduced Agulhas Leakage during the Last Glacial Maximum inferred from an integrated provenance and flux study. <i>Earth and Planetary Science Letters</i> , 2006 , 250, 72-88	5.3	61
1216	A new geochemical model for the Earth's mantle inferred from 146Sma 42Nd systematics. <i>Earth and Planetary Science Letters</i> , 2006 , 250, 254-268	5.3	173
1215	A chemical Earth model with whole mantle convection: The importance of a corefhantle boundary layer (D?) and its early formation. 2006 , 226, 79-99		64
1214	Geochemical characteristics of the Neoarchean (2800\(\mathbb{Q}\)700 Ma) Taishan greenstone belt, North China Craton: Evidence for plumedraton interaction. 2006 , 230, 60-87		140
1213	Provenance of the Triassic Songpantanzi flysch, west China. 2006 , 231, 159-175		91

1212	Astoria Fan sediments, DSDP site 174, Cascadia Basin: HfNdPb constraints on provenance and outburst flooding. 2006 , 233, 276-292	40
1211	Contrasting conditions preceding MIS3 and MIS2 Heinrich events. 2006 , 54, 225-238	33
121 0	Geochemical decoupling of water masses in the Variscan oceanic system during Late Devonian times. 2006 , 240, 108-119	32
1209	Petrogenesis of Neoarchaean volcanic rocks of the MacQuoid supracrustal belt: A back-arc setting for the northwestern Hearne subdomain, western Churchill Province, Canada. 2006 , 144, 140-165	55
1208	Age and geochemical constraints for partial melting of granulites in Estonia. 2006 , 86, 277-300	8
1207	Evolution of Tethyan phosphogenesis along the northern edges of the Arabian African shield during the Cretaceous Eocene as deduced from temporal variations of Ca and Nd isotopes and rates of P accumulation. 2006 , 78, 27-57	102
1206	A hybrid origin for the Qianshan A-type granite, northeast China: Geochemical and SrNdHf isotopic evidence. 2006 , 89, 89-106	401
1205	Petrology and geochemistry and KAr ages for Cenozoic tinguaites from the Ohre/Eger Rift (NW Bohemia). 2006 , 183, 41-61	5
1204	Low-pressure Granulites of the Lidv Massif, Southern Bohemia: Visan Metamorphism of Late Devonian Plutonic Arc Rocks. 2006 , 47, 705-744	89
1203	Exhumation History of a Garnet Pyroxenite-bearing Mantle Section from a Continent Dcean Transition (Northern Apennine Ophiolites, Italy). 2006 , 47, 1943-1971	68
1202	Solar nebula heterogeneity in p-process samarium and neodymium isotopes. 2006 , 314, 806-9	130
1201	Post-collisional, Potassic and Ultrapotassic Magmatism of the Northern Tibetan Plateau: Constraints on Characteristics of the Mantle Source, Geodynamic Setting and Uplift Mechanisms. 2006 , 47, 1177-1220	212
1200	Geochemistry, zircon ages and whole-rock Nd isotopic systematics for Palaeoproterozoic A-type granitoids in the northern part of the Delhi belt, Rajasthan, NW India: implications for late Palaeoproterozoic crustal evolution of the Aravalli craton. 2007 , 144, 361-378	62
1199	Nd and Sr isotope systematics and geochemistry of a plume-related Early Cretaceous alkaline-mafic-ultramafic igneous complex from Jasra, Shillong plateau, northeastern India. 2007 , 815-830	4
1198	Sm-Nd isotope and trace element study of Late Proterozoic metabasalts (Epilites) from the Central Barrandian domain (Bohemian Massif, Czech Republic). 2007 ,	3
1197	Calc-Alkaline Magmatism at the Archean B roterozoic Transition: the CaiclComplex Basement (NE Brazil). 2007 , 48, 2149-2185	96
1196	6. Late quaternary interglacials in East Antarctica from ice-core dust records. 2007 , 53-73	25
1195	No change in the neodymium isotope composition of deep water exported from the North Atlantic on glacial-interglacial time scales. 2007 , 35, 37	50

1194	Geochemistry and tectonic setting of mafic rocks in western Dronning Maud Land, East Antarctica: implications for the geodynamic evolution of the Proterozoic Maud Belt. 2007 , 164, 465-475	36
1193	Clay minerals in late glacial and Holocene sediments of the northern and southern Aegean Sea. 2007 , 249, 36-57	87
1192	The 1.75🛮.68Ga anorthosite-mangerite-alkali granitoid-rapakivi granite suite from the northern North China Craton: Magmatism related to a Paleoproterozoic orogen. 2007 , 155, 287-312	166
1191	Os P b N d isotope and highly siderophile and lithophile trace element systematics of komatiitic rocks from the Volotsk suite, SE Baltic Shield. 2007 , 158, 119-137	53
1190	Nd⊞fBr P b isotopes and trace element geochemistry of Proterozoic lamproites from southern India: Subducted komatiite in the source. 2007 , 236, 291-302	35
1189	A uniform isotopic and chemical signature of dust exported from Patagonia: Rock sources and occurrence in southern environments. 2007 , 238, 107-120	88
1188	Isotopic Nd compositions and concentrations of the lithogenic inputs into the ocean: A compilation, with an emphasis on the margins. 2007 , 239, 156-164	169
1187	Modeling the neodymium isotopic composition with a global ocean circulation model. 2007 , 239, 165-177	95
1186	Initial Hf isotope compositions in magmatic zircon from early Proterozoic rocks from the Gawler Craton, Australia: A test for zircon model ages. 2007 , 241, 23-37	97
1185	Reliable extraction of a deepwater trace metal isotope signal from FeIMn oxyhydroxide coatings of marine sediments. 2007 , 242, 351-370	180
1184	40Ar/39Ar ages of hornblende grains and bulk Sm/Nd isotopes of circum-Antarctic glacio-marine sediments: Implications for sediment provenance in the southern ocean. 2007 , 244, 507-519	82
1183	The origin of enriched mantle beneath Sâ Miguel, Azores. 2007 , 71, 219-240	88
1182	Derivation of Mesozoic adakitic magmas from ancient lower crust in the North China craton. 2007 , 71, 2591-2608	136
1181	Chemical composition of Earth's primitive mantle and its variance: 2. Implications for global geodynamics. 2007 , 112,	34
1180	Geochemistry and petrogenesis of spinel lherzolite xenoliths from Boeun, Korea. 2007 , 29, 29-40	13
1179	A highly depleted moon or a non-magma ocean origin for the lunar crust?. <i>Earth and Planetary Science Letters</i> , 2007 , 262, 505-516	81
1178	Abstracts. 2007 , 42, A11-A171	3
1177	Archaean crustal accretion at the northern border of the Congo Craton (South Cameroon). The charnockite-TTG link. 2007 , 178, 331-342	49

(2008-2007)

1176	climatic and tectoric controls on weathering in south China and Indochina Peninsula: Clay mineralogical and geochemical investigations from the Pearl, Red, and Mekong drainage basins. 2007, 8, n/a-n/a	159
1175	Lullf geochronology and trace element distribution in garnet: Implications for uplift and exhumation of ultra-high pressure granulites in the Sudetes, SW Poland. 2007 , 95, 363-380	102
1174	Post-collisional adakites in south Tibet: Products of partial melting of subduction-modified lower crust. 2007 , 96, 205-224	281
1173	Neo-Proterozoic rift-related syenites (Northern Damara Belt, Namibia): Geochemical and NdBrBbD isotope constraints for mantle sources and petrogenesis. 2007 , 96, 415-435	42
1172	KAr age, whole-rock and isotope geochemistry of A-type granitoids in the DivriBivas region, eastern-central Anatolia, Turkey. 2007 , 97, 193-218	80
1171	Magmatic history of granite-derived mylonites from the southern DesnĴUnit (Silesicum, Czech Republic). 2007 , 89, 45-75	10
1170	Archaean high-K granitoids produced by remelting of earlier Tonalitell rondhjemitel ranodiorite (TTG) in the Sangmelima region of the Ntem complex of the Congo craton, southern Cameroon. 2007 , 96, 817-841	69
1169	The role of slab melting in the petrogenesis of high-Mg andesites: evidence from Simbo Volcano, Solomon Islands. 2007 , 153, 85-103	46
1168	Intraplate volcanism in New Zealand: the role of fossil plume material and variable lithospheric properties. 2007 , 153, 669-687	61
1167	~3,850 Ma tonalites in the Nuuk region, Greenland: geochemistry and their reworking within an Eoarchaean gneiss complex. 2007 , 154, 385-408	55
1166	Zircon 207Pb/206Pb evaporation ages of Panafrican metasedimentary rocks in the Komb ^a ll area (Bafia Group, Cameroon): Constraints on protolith age and provenance. 2008 , 51, 77-88	30
1165	Composition of the Earth's interior: the importance of early events. 2008 , 366, 4077-103	59
1164	Influence of brine formation on Arctic Ocean circulation over the past 15 million years. 2008, 1, 68-72	71
1163	Geochronology of high-pressure mafic granulite dykes in SW Sweden: tracking the PIII path of metamorphism using Hf isotopes in zircon and baddeleyite. 2008 , 26, 539-560	45
1162	REE and Nd-isotope evidence for the origin of siderite from the Jebel Awam deposit (Central Morocco). 2008 , 34, 337-342	10
1161	Petrology, geochemistry and geodynamic implications of Jurassic island arc magmatism as revealed by mafic volcanic rocks in the Mesozoic low-grade sequence, eastern Rhodope, Bulgaria. 2008 , 100, 210-233	54
1160	From orthogneiss to migmatite: Geochemical assessment of the melt infiltration model in the Gfbl Unit (Moldanubian Zone, Bohemian Massif). 2008 , 102, 508-537	37
1159	Geochemistry, isotope systematics and petrogenesis of the volcanic rocks in the Zhongtiao Mountain: An alternative interpretation for the evolution of the southern margin of the North China Craton. 2008 , 102, 158-178	82

1158	Petrogenesis of basalts and gabbros from an ancient continentBcean transition (External Liguride ophiolites, Northern Italy). 2008 , 101, 453-479		61
1157	Geochemical and SrNdPb isotopic characteristics of Paleocene plagioleucitites from the Eastern Pontides (NE Turkey). 2008 , 105, 149-161		82
1156	An investigation of dissolution methods for Lu-Hf and Sm-Nd isotope studies in zircon- and garnet-bearing whole-rock samples. 2008 , 9, n/a-n/a		15
1155	Radiogenic isotope record of Arctic Ocean circulation and weathering inputs of the past 15 million years. 2008 , 23, n/a-n/a		55
1154	Oceanographic and climatic evolution of the Miocene Mediterranean deduced from Nd, Sr, C, and O isotope compositions of marine fossils and sediments. 2008 , 23, n/a-n/a		32
1153	Miocene phosphorites from the Murray Ridge, northwestern Arabian Sea. 2008 , 260, 347-358		17
1152	Provenance of Proterozoic Basal Aravalli mafic volcanic rocks from Rajasthan, Northwestern India: Nd isotopes evidence for enriched mantle reservoirs. 2008 , 162, 150-159		38
1151	Age, geochemistry and SmNd isotopic signature of the 0.76 Ga Burin Group: Compositional equivalent of Avalonian basement?. 2008 , 165, 37-48		33
1150	Cambrian ensialic rift-related magmatism in the Ossa-Morena Zone (VoraAracena metamorphic belt, SW Iberian Massif): SmNd isotopes and SHRIMP zircon UThPb geochronology. 2008 , 461, 91-113		85
1149	Neoproterozoic E arly Devonian magmatism in the Antigonish Highlands, Avalon terrane, Nova Scotia: Tracking the evolution of the mantle and crustal sources during the evolution of the Rheic Ocean. 2008 , 461, 181-201		41
1148	Genesis and evolution of a syn-orogenic basin in transpression: Insights from petrography, geochemistry and SmNd systematics in the Variscan Pedroches basin (Mississippian, SW Iberia). 2008 , 461, 395-413		22
1147	The ca. 350´Ma Beja Igneous Complex: A record of transcurrent slab break-off in the Southern Iberia Variscan Belt?. 2008 , 461, 356-377		73
1146	Where on Earth is the enriched Hadean reservoir?. Earth and Planetary Science Letters, 2008, 266, 14-28	5.3	46
1145	Tracing the Nd isotope evolution of North Atlantic Deep and Intermediate Waters in the western North Atlantic since the Last Glacial Maximum from Blake Ridge sediments. <i>Earth and Planetary Science Letters</i> , 2008 , 266, 61-77	5.3	107
1144	Sources and evolution of arc magmas inferred from coupled O and Hf isotope systematics of plutonic zircons from the Cretaceous Separation Point Suite (New Zealand). <i>Earth and Planetary Science Letters</i> , 2008 , 268, 312-324	5.3	111
1143	Seawater carbonate ion-II3C systematics and application to glacialInterglacial North Atlantic ocean circulation. <i>Earth and Planetary Science Letters</i> , 2008 , 271, 209-220	5.3	87
1142	Oscillating glacial northern and southern deep water formation from combined neodymium and carbon isotopes. <i>Earth and Planetary Science Letters</i> , 2008 , 272, 394-405	5.3	84
1141	Modeling the distribution of Nd isotopes in the oceans using an ocean general circulation model. <i>Earth and Planetary Science Letters</i> , 2008 , 272, 610-619	5.3	61

(2009-2008)

1140	The Lull and Smld isotopic composition of CHUR: Constraints from unequilibrated chondrites and implications for the bulk composition of terrestrial planets. <i>Earth and Planetary Science Letters</i> , 2008 , 273, 48-57	5.3	1968
1139	Mobility of tungsten in subduction zones. Earth and Planetary Science Letters, 2008, 274, 82-92	5.3	87
1138	Towards explaining the Nd paradox using reversible scavenging in an ocean general circulation model. <i>Earth and Planetary Science Letters</i> , 2008 , 274, 448-461	5.3	135
1137	Seasonal and provenance controls on NdBr isotopic compositions of Amazon rivers suspended sediments and implications for Nd and Sr fluxes exported to the Atlantic Ocean. <i>Earth and Planetary Science Letters</i> , 2008 , 274, 511-523	5.3	64
1136	Helar and NdBr isotopic compositions of late Pleistocene felsic plutonic back arc basin rocks from Ulleungdo volcanic island, South Korea: Implications for the genesis of young plutonic rocks in a back arc basin. 2008 , 253, 180-195		15
1135	Sr- and Nd-isotope geochemistry of the Atlantis Massif (30°N, MAR): Implications for fluid fluxes and lithospheric heterogeneity. 2008 , 254, 19-35		67
1134	Rhenium-Osmium Isotope and Platinum-Group Element Constraints on the Origin and Evolution of the 1{middle dot}27 Ga Muskox Layered Intrusion. 2008 , 49, 1255-1295		52
1133	The Spi Lake Formation of the central Hearne domain, western Churchill Province, Canada: an axial intracratonic continental tholeiite trough above the cogenetic Kaminak dyke swarmGeological Survey of Canada Contribution 20070462 2008 , 45, 745-767		18
1132	Two Distinctive Granite Suites in the SW Bohemian Massif and their Record of Emplacement: Constraints from Geochemistry and Zircon 207Pb/206Pb Chronology. 2008 , 49, 1853-1872		35
1131	The Magmatic and Fluid Evolution of the Motzfeldt Intrusion in South Greenland: Insights into the Formation of Agpaitic and Miaskitic Rocks. 2008 , 49, 1549-1577		37
1130	References. 473-489		
1129	A modeling sensitivity study of the influence of the Atlantic meridional overturning circulation on neodymium isotopic composition at the Last Glacial Maximum. 2008 , 4, 191-203		27
1128	Detrital-zircon ages and geochemistry of sedimentary rocks in basement Mesozoic terranes and their cover rocks in New Caledonia, and provenances at the Eastern Gondwanaland margin*View all notes. 2009 , 56, 1023-1047		51
1127	Petrogenesis of the 1.9 Ga mafic hanging wall sequence to the Flin Flon, Callinan, and Triple 7 massive sulphide deposits, Flin Flon, Manitoba, CanadaThis is a companion paper to DeWolfe, Y.M., Gibson, H.L., Lafrance, B., and Bailes, A.H. 2009. Volcanic reconstruction of Paleoproterozoic arc		13
1126	Improving constraints on apatite provenance: Nd measurement on fission-track-dated grains. 2009 , 324, 57-72		7
1125	Partial Melting of Mantle and Crustal Sources beneath South Karakorum, Pakistan: Implications for the Miocene Geodynamic Evolution of the India-Asia Convergence Zone. 2009 , 50, 427-449		73
1124	Partial melting of diverse crustal sources © constraints from SrNdD isotope compositions of quartz dioritegranodiorite eucogranite associations (Kaoko Belt, Namibia). 2009 , 111, 236-251		46
1123	Late Paleozoic to Early Mesozoic maficultramafic complexes from the northern North China Block: Constraints on the composition and evolution of the lithospheric mantle. 2009 , 110, 229-246		166

1122	Layered granitoids: Interaction between continental crust recycling processes and mantle-derived magmatism. 2009 , 111, 125-141	31
1121	Formation and temporal evolution of the Kalahari sub-cratonic lithospheric mantle: Constraints from Venetia xenoliths, South Africa. 2009 , 112, 1069-1082	12
1120	Record of 1.82 Ga Andean-type continental arc magmatism in NE Rajasthan, India: Insights from zircon and SmNd ages, combined with NdBr isotope geochemistry. 2009 , 16, 56-71	86
1119	Textural, chemical, and isotopic effects of late-magmatic carbonatitic fluids in the carbonatiteByenite Tamazeght complex, High Atlas Mountains, Morocco. 2009 , 97, 23-42	19
1118	Early Permian plutons from the northern North China Block: constraints on continental arc evolution and convergent margin magmatism related to the Central Asian Orogenic Belt. 2009 , 98, 1441-1467	, 187
1117	Origin of a Mesozoic granite with A-type characteristics from the North China craton: highly fractionated from I-type magmas?. 2009 , 158, 113-130	71
1116	Facies effects on the behaviour of Nd and Sr isotope systems in turbidite mudrocks during diagenesis. 2009 , 56, 863-872	2
1115	Southern Ocean evidence for reduced export of North Atlantic Deep Water during Heinrich event 1. 2009 , 37, 195-198	55
1114	Hf and Nd isotopes in marine sediments: Constraints on global silicate weathering. <i>Earth and Planetary Science Letters</i> , 2009 , 277, 318-326	92
1113	Contrasting compositions of Saharan dust in the eastern Atlantic Ocean during the last deglaciation and African Humid Period. <i>Earth and Planetary Science Letters</i> , 2009 , 278, 257-266	93
1112	The hafnium Beodymium isotopic composition of Atlantic seawater. Earth and Planetary Science Letters, 2009, 280, 118-127	122
1111	Geochemistry of Fe-rich peridotites and associated pyroxenites from HornîBory, Bohemian Massif: Insights into subduction-related meltBock reactions. 2009 , 259, 152-167	61
1110	Age, lithology and structural evolution of the c. 3.53 Ga Theespruit Formation in the Tjakastad area, southwestern Barberton Greenstone Belt, South Africa, with implications for Archaean tectonics. 2009 , 261, 115-139	71
1109	Determining melt productivity of mantle sources from 238UØ30Th and 235UØ31Pa disequilibria; an example from Pico Island, Azores. 2009 , 73, 2103-2122	46
1108	PtReDs and SmNd isotope and HSE and REE systematics of the 2.7Ga Belingwe and Abitibi komatiites. 2009 , 73, 6367-6389	63
1107	A method to estimate the composition of the bulk silicate Earth in the presence of a hidden geochemical reservoir. 2009 , 73, 6952-6964	17
1106	Constraints on Miocene oceanography and climate in the Western and Central Paratethys: O-, Sr-, and Nd-isotope compositions of marine fish and mammal remains. 2009 , 271, 117-129	47
1105	The geochemistry of Neoarchean (ca. 2700 Ma) tholeiitic basalts, transitional to alkaline basalts, and gabbros, Wawa Subprovince, Canada: Implications for petrogenetic and geodynamic processes.	69

(2010-2009)

1104	Upper Carboniferous retroarc volcanism with submarine and subaerial facies at the western Gondwana margin of Argentina. 2009 , 27, 299-308	8
1103	Reconstructing seawater circulation on the Moroccan shelf of Gondwana during the Late Devonian: Evidence from Nd isotope composition of conodonts. 2009 , 10, n/a-n/a	23
1102	Orogenic Processes in the Alpine Collision Zone. 2009,	
1101	Grain size effect on Sr and Nd isotopic compositions in eolian dust: Implications for tracing dust provenance and Nd model age. 2009 , 43, 123-131	58
1100	Constraints on the origin of gabbroic rocks from the Moldanubian-Moravian units boundary (Bohemian Massif, Czech Republic and Austria). 2010 , 61, 175-191	3
1099	Radioisotopes as chronometers. 230-307	
1098	Magmatic evolution of the ultramafichafic Kharaelakh intrusion (Siberian Craton, Russia): insights from trace-element, UPb and Hf-isotope data on zircon. 2010 , 159, 753-768	49
1097	Paleocene alkaline volcanism in the Nares Strait region: evidence from volcanic pebbles. 2010 , 99, 863-890	21
1096	Zircon U-Pb geochronology, Hf isotopic composition and geological implications of the rhyodacite and rhyodacitic porphyry in the Xiangshan uranium ore field, Jiangxi Province, China. 2010 , 53, 1411-1426	41
1095	Geochemistry and SmNd isotopic systematics of EdiacaranDrdovician, sedimentary and bimodal igneous rocks in the western Acatln Complex, southern Mexico: Evidence for rifting on the southern margin of the Rheic Ocean. 2010 , 114, 155-167	18
1094	Geochemical systematics of basalts of the Lower Basalt Unit, 2.7Ga Kambalda Sequence, Yilgarn craton, Australia: Plume impingement at a rifted craton margin. 2010 , 115, 82-100	48
1093	Carboniferous high-potassium I-type granitoid magmatism in the Eastern Pontides: The Gfhflane pluton (NE Turkey). 2010 , 116, 92-110	198
1092	Neoproterozoic continental growth prior to Gondwana assembly: Constraints from zirconlitanite geochronology, geochemistry and petrography of ring complex granitoids, Sudan. 2010 , 118, 61-81	18
1091	Provenances of atmospheric dust over Korea from SrNd isotopes and rare earth elements in early 2006. 2010 , 44, 2401-2414	38
1090	Geochemical characterization and isotopic age of Caradocian magmatism in the northeastern Iberian Peninsula: Insights into the Late Ordovician evolution of the northern Gondwana margin. 2010 , 17, 325-337	38
1089	Late Archaean high-K granite geochronology of the northern metacratonic margin of the Archaean Congo craton, Southern Cameroon: Evidence for Pb-loss due to non-metamorphic causes. 2010 , 18, 337-355	58
1088	Geochemical character and petrogenesis of Pan-African Amspoort suite of the Boundary Igneous Complex in the Kaoko Belt (NW Namibia). 2010 , 18, 688-707	34
1087	Zircon and titanite age evidence for coeval granitization and migmatization of the early Middle and early Late Proterozoic Saharan Metacraton; example from the central North Sudan basement. 2010 57, 492-524	19

1086	Footwall dip of a core complex detachment fault: thermobarometric constraints from the northern Snake Range (Basin and Range, USA). 2010 , 28, 997-1020		32
1085	Modeling the Nd isotopic composition in the North Atlantic basin using an eddy-permitting model. 2010 , 6, 789-797		10
1084	Intermediate water formation in the Bering Sea during glacial periods: Evidence from neodymium isotope ratios. 2010 , 38, 435-438		58
1083	Sahwave Batholith, NW Nevada: Cretaceous arc flare-up in a basinal terrane. 2010 , 2, 423-446		19
1082	Hafnium and neodymium isotopes in surface waters of the eastern Atlantic Ocean: Implications for sources and inputs of trace metals to the ocean. 2010 , 74, 540-557		87
1081	Boninites as windows into trace element mobility in subduction zones. 2010 , 74, 684-704		107
1080	Tungsten isotopes as tracers of corelhantle interactions: The influence of subducted sediments. 2010 , 74, 751-762		17
1079	Tracing the metasomatic and magmatic evolution of continental mantle roots with Sr, Nd, Hf and and Pb isotopes: A case study of Middle Atlas (Morocco) peridotite xenoliths. 2010 , 74, 1417-1435		36
1078	Deep mantle storage of the Earth missing niobium in late-stage residual melts from a magma ocean. 2010 , 74, 4392-4404		34
1077	Deep-sea coral aragonite as a recorder for the neodymium isotopic composition of seawater. 2010 , 74, 6014-6032		55
1076	SrNdDs evidence for a stable erosion regime in the Himalaya during the past 12 Myr. <i>Earth and Planetary Science Letters</i> , 2010 , 290, 474-480	5.3	66
1075	The influence of small-scale mantle heterogeneities on Mid-Ocean Ridge volcanism: Evidence from the southern Mid-Atlantic Ridge (7°30?S to 11°30?S) and Ascension Island. <i>Earth and Planetary Science Letters</i> , 2010 , 296, 299-310	5.3	38
1074	Testing the application of in situ SmNd isotopic analysis on detrital apatites: A provenance tool for constraining the timing of India Eurasia collision. <i>Earth and Planetary Science Letters</i> , 2010 , 297, 42-49	5.3	26
1073	Depleted mantle sources through time: Evidence from Lull and Smld isotope systematics of Archean komatiites. <i>Earth and Planetary Science Letters</i> , 2010 , 297, 598-606	5.3	136
1072	Geochemical characteristics of the high- and low-Ti basaltic rocks from the uplifted shoulder of the OhB (Eger) Rift, Western Bohemia. 2010 , 70, 319-333		6
1071	Elemental and Nd-isotope systematics of the Upper Basalt Unit, 2.7 Ga Kambalda Sequence: Quantitative modeling of progressive crustal contamination of plume asthenosphere. 2010 , 273, 193-2	11	30
1070	Fingerprinting sources of orogenic plutonic rocks from Variscan belt with lithium isotopes and possible link to subduction-related origin of some A-type granites. 2010 , 274, 94-107		52
1069	~2.7Ga crust growth in the North China craton. 2010 , 179, 37-49		197

(2011-2010)

1068	Ca. 2.5 billion year old coeval ultramafichafic and syenitic dykes in Eastern Hebei: Implications for cratonization of the North China Craton. 2010 , 180, 143-155	98
1067	Magnesian dyke suites of the 2.7Ga Kambalda Sequence, Western Australia: Evidence for coeval melting of plume asthenosphere and metasomatised lithospheric mantle. 2010 , 180, 183-203	17
1066	100,000 Years of African monsoon variability recorded in sediments of the Nile margin. 2010 , 29, 1342-1362	197
1065	Changes in North Atlantic Deep Water strength and bottom water masses during Marine Isotope Stage 3 (45B5kaBP). 2010 , 29, 2451-2461	30
1064	Neodymium isotopic composition of deep-sea corals from the NE Atlantic: implications for past hydrological changes during the Holocene. 2010 , 29, 2509-2517	65
1063	Nd isotopes in deep-sea corals in the North-eastern Atlantic. 2010 , 29, 2499-2508	54
1062	Late Quaternary variability of Mediterranean Outflow Water from radiogenic Nd and Pb isotopes. 2010 , 29, 2462-2472	48
1061	THE ORIGIN OF FERROAN-POTASSIC A-TYPE GRANITOIDS: THE CASE OF THE HORNBLENDE-BIOTITE GRANITE SUITE OF THE MESOPROTEROZOIC MAZURY COMPLEX, NORTHEASTERN POLAND. 2010 , 48, 947-968	23
1060	Nd isotope systematics of 1.8 Ga volcanic rocks within the Transscandinavian Igneous Belt, south-central Sweden. 2011 , 133, 89-100	2
1059	2.05-Ga Isotopic Ages for Transvaal Mississippi Valley¶ype Deposits: Evidence for Large-Scale Hydrothermal Circulation around the Bushveld Igneous Complex, South Africa. 2011 , 119, 69-80	24
1058	Grain size control on Sr-Nd isotope provenance studies and impact on paleoclimate reconstructions: An example from deep-sea sediments offshore NW Africa. 2011 , 12, n/a-n/a	104
1057	Zircon effect alone insufficient to generate seawater Nd-Hf isotope relationships. 2011 , 12, n/a-n/a	17
1056	Nonchondritic 142Nd in suboceanic mantle peridotites. 2011 , 12, n/a-n/a	21
1055	The provenance of sediments in the Gulf of Lions, western Mediterranean Sea. 2011 , 12, n/a-n/a	32
1054	Nd isotopic composition of water masses and dilution of the Mediterranean outflow along the southwest European margin. 2011 , 12, n/a-n/a	27
1053	Testing the extraction of past seawater Nd isotopic composition from North Atlantic deep sea sediments and foraminifera. 2011 , 12, n/a-n/a	62
1052	Spatio-temporal evolution of the West African monsoon during the last deglaciation. 2011 , 38, n/a-n/a	18
1051	The climate influence on the mid-depth Northeast Atlantic gyres viewed by cold-water corals. 2011 , 38, n/a-n/a	19

1050	Early Mesozoic Plutonism of the Cordillera de la Costa (34°B7°S), Chile: Constraints on the Onset of the Andean Orogeny. 2011 , 119, 159-184		32
1049	Calc-alkaline I-type plutons in the eastern Pontides, NE Turkey: UPb zircon ages, geochemical and SrNd isotopic compositions. 2011 , 71, 59-75		27
1048	Precise and accurate determination of 147Sm/144Nd and 143Nd/144Nd in monazite using laser ablation-MC-ICPMS. 2011 , 282, 45-57		45
1047	CO2 degassing and trapping during hydrothermal cycles related to Gondwana rifting in eastern Australia. 2011 , 75, 5444-5466		34
1046	Nd and Sr isotope compositions in modern and fossil bones Proxies for vertebrate provenance and taphonomy. 2011 , 75, 5951-5970		43
1045	Modelling Nd-isotopes with a coarse resolution ocean circulation model: Sensitivities to model parameters and source/sink distributions. 2011 , 75, 5927-5950		112
1044	Uranium-bearing and barren granites from the Taoshan Complex, Jiangxi Province, South China: Geochemical and petrogenetic discrimination and exploration significance. 2011 , 110, 126-135		33
1043	A fresh isotopic look at Greenland kimberlites: Cratonic mantle lithosphere imprint on deep source signal. <i>Earth and Planetary Science Letters</i> , 2011 , 305, 235-248	5.3	117
1042	Limits on conservative behavior of Nd isotopes in seawater assessed from analysis of fish teeth from Pacific core tops. <i>Earth and Planetary Science Letters</i> , 2011 , 310, 119-130	5.3	35
1041	Climatically driven changes in sediment supply on the SW Iberian shelf since the Last Glacial Maximum. <i>Earth and Planetary Science Letters</i> , 2011 , 312, 80-90	5.3	23
1040	Nature and origin of the Wenquan granite: Implications for the provenance of Proterozoic A-type granites in the North China craton. 2011 , 42, 76-82		46
1039	Isotopic dating of the Khoy metamorphic complex (KMC), northwestern Iran: A significant revision of the formation age and magma source. 2011 , 185, 87-94		71
1038	Geochemistry of Ore-bearing Lamprophyre from the Cu-Ni Deposit in Dhi Samir, Yemen. 2011 , 85, 200-2	210	5
1037	Persistent Nordic deep-water overflow to the glacial North Atlantic. 2011 , 39, 515-518		36
1036	40Ar/39Ar ages and SrNdPbDs geochemistry of CAMP tholeiites from Western Maranh® basin (NE Brazil). 2011 , 122, 137-151		87
1035	Petrogenesis of late Mesozoic granitoids in southern Jilin province, northeastern China: Geochronological, geochemical, and SrNdPb isotopic evidence. 2011 , 125, 27-39		36
1034	Post-collisional adakite-like magmatism in the Allanis Massif and implications for the evolution of the Eocene magmatism in the Eastern Pontides (NE Turkey). 2011 , 125, 131-150		108
1033	Early Cretaceous volcanism of the Coastal Ranges, NW Syria: Magma genesis and regional dynamics. 2011 , 126, 290-306		14

1032	Constraints to the timing of India Eurasia collision; a re-evaluation of evidence from the Indus Basin sedimentary rocks of the Indus Esangpo Suture Zone, Ladakh, India. 2011 , 106, 265-292	59
1031	Mississippian volcanism in the south-central Andes: New UPb SHRIMP zircon geochronology and whole-rock geochemistry. 2011 , 19, 524-534	20
1030	Zircon ages of late Palaeoproterozoic (ca. 1.72¶.70 Ga) extension-related granitoids in NE Rajasthan, India: Regional and tectonic significance. 2011 , 19, 1040-1053	62
1029	Precambrian sources of Early Paleozoic SE Gondwana sediments as deduced from combined Lu⊞f and UBb systematics of detrital zircons, Takaka and Buller terrane, South Island, New Zealand. 2011 , 20, 427-442	17
1028	U P b dating of baddeleyite and zircon from the Shizhaigou diorite in the southern margin of North China Craton: Constrains on the timing and tectonic setting of the Paleoproterozoic Xiong'er group. 2011 , 20, 184-193	82
1027	146Sm-142Nd systematics measured in enstatite chondrites reveals a heterogeneous distribution of 142Nd in the solar nebula. 2011 , 108, 7693-7	73
1026	Structural-morphological and REE geochemical control of the correctness of Sm-Nd dating for fluorite formation in the garsonui deposit, eastern Transbaikalia. 2011 , 19, 297-302	4
1025	Metasomatized lithospheric mantle beneath Turkana depression in southern Ethiopia (the East Africa Rift): geochemical and SrNdPb isotopic characteristics. 2011 , 162, 889-907	19
1024	Geochemical, zircon UPb dating and SrNdHf isotopic constraints on the age and petrogenesis of an Early Cretaceous volcanic-intrusive complex at Xiangshan, Southeast China. 2011 , 101, 21-48	79
1023	1420 Ma diabasic intrusives from the Mesoproterozoic Singhora Group, Chhattisgarh Supergroup, India: Implications towards non-plume intrusive activity. 2011 , 120, 223-236	37
1022	Character and origin of variably deformed granitoids in central southern Sweden: implications from geochemistry and Nd isotopes. 2011 , 46, 597-618	13
1021	The importance of the terrigenous fraction within a cold-water coral mound: A case study. 2011 , 282, 13-25	11
1020	New SHRIMP, Rb/Sr and Sm/Nd isotope and whole rock chemical data from central Mozambique and western Dronning Maud Land, Antarctica: Implications for the nature of the eastern margin of the Kalahari Craton and the amalgamation of Gondwana. 2011 , 59, 74-100	44
1019	Strontium and neodymium isotopic signatures indicate the provenance and depositional process of loams intercalated in coastal dune sand, western Japan. 2011 , 236, 272-278	6
1018	Geochemistry and UPb dating of felsic volcanic rocks in the RiotintoNerva unit, Iberian Pyrite Belt, Spain: crustal thinning, progressive crustal melting and massive sulphide genesis. 2011, 168, 717-732	28
1017	Petrogenesis of a Late Cretaceous composite pluton from the eastern Pontides: the Daßall pluton, NE Turkey. 2011 , 188, 211-233	32
1016	Provenance of Cenozoic sedimentary rocks from the Sulaiman fold and thrust belt, Pakistan: implications for the palaeogeography of the Indus drainage system. 2011 , 168, 499-516	24
1015	Tectonic significance of Late Ordovician silicic magmatism, Avalon terrane, northern Antigonish Highlands, Nova Scotia 1 This article is one of a series of papers published in CJES Special Issue: In honour of Ward Neale on the theme of Appalachian and Grenvillian geology.2 Contribution to	22

1014	Permian-Carboniferous arc magmatism and basin evolution along the western margin of Pangea: Geochemical and geochronological evidence from the eastern Acatlan Complex, southern Mexico. 2012 , 124, 1607-1628	50
1013	Characterization of Modern and Fossil Mineral Dust Transported to High Altitude in the Western Alps: Saharan Sources and Transport Patterns. 2012 , 2012, 1-14	6
1012	Tectonomagmatic Constraints on the Sources of Eastern Mediterranean K-rich Lavas. 2012 , 53, 27-65	51
1011	Geochronological evidence and tectonic significance of Carboniferous magmatism in the southwest Trabzon area, eastern Pontides, Turkey. 2012 , 54, 1776-1800	74
1010	Devonian magmatism in the western Sakarya Zone, Karacabey region, NW Turkey. 2012 , 25, 183-201	33
1009	GEOTRACES intercalibration of neodymium isotopes and rare earth element concentrations in seawater and suspended particles. Part 1: reproducibility of results for the international intercomparison. 2012 , 10, 234-251	93
1008	Zircon response to high-grade metamorphism as revealed by UPb and cathodoluminescence studies. 2012 , 101, 2105-2123	16
1007	Petrogenesis of the Early Cretaceous adakite-like porphyries and associated basaltic andesites in the eastern Jiangnan orogen, southern China. 2012 , 61, 243-256	23
1006	Triassic high-Mg adakitic andesites from Linxi, Inner Mongolia: Insights into the fate of the Paleo-Asian ocean crust and fossil slab-derived meltperidotite interaction. 2012 , 328, 89-108	64
1005	Intensifying weathering and land use in Iron Age Central Africa. 2012 , 335, 1219-22	139
1005	Characterizing source reservoirs of igneous rocks: A new perspective Fractionation of radiogenic	139
	Characterizing source reservoirs of igneous rocks: A new perspective. Fractionation of radiogenic	
1004	Characterizing source reservoirs of igneous rocks: A new perspective. Fractionation of radiogenic isotopes: A new tool for petrogenesis. 2012 , 72, 323-332 Provenance and climate change inferred from SrNdPb isotopes of late Quaternary sediments in	1
1004	Characterizing source reservoirs of igneous rocks: A new perspective. Fractionation of radiogenic isotopes: A new tool for petrogenesis. 2012, 72, 323-332 Provenance and climate change inferred from SrNdPb isotopes of late Quaternary sediments in the Huanghe (Yellow River) Delta, China. 2012, 78, 561-571 SrNd isotopic constraints on terrigenous sediment provenances and Kuroshio Current variability in	1 47
1004	Characterizing source reservoirs of igneous rocks: A new perspective. Fractionation of radiogenic isotopes: A new tool for petrogenesis. 2012, 72, 323-332 Provenance and climate change inferred from SrNdPb isotopes of late Quaternary sediments in the Huanghe (Yellow River) Delta, China. 2012, 78, 561-571 SrNd isotopic constraints on terrigenous sediment provenances and Kuroshio Current variability in the Okinawa Trough during the late Quaternary. 2012, 365-366, 38-47 Two-Stage, Extreme Albitization of A-type Granites from Rajasthan, NW India. 2012, 53, 919-948 Ice-rafting from the BritishItish ice sheet since the earliest Pleistocene (2.6 million years ago):	1 47 66
1004 1003 1002	Characterizing source reservoirs of igneous rocks: A new perspective. Fractionation of radiogenic isotopes: A new tool for petrogenesis. 2012, 72, 323-332 Provenance and climate change inferred from Sr®ld®b isotopes of late Quaternary sediments in the Huanghe (Yellow River) Delta, China. 2012, 78, 561-571 Sr®ld isotopic constraints on terrigenous sediment provenances and Kuroshio Current variability in the Okinawa Trough during the late Quaternary. 2012, 365-366, 38-47 Two-Stage, Extreme Albitization of A-type Granites from Rajasthan, NW India. 2012, 53, 919-948 Ice-rafting from the BritishlFish ice sheet since the earliest Pleistocene (2.6 million years ago):	1 47 66 64
1004 1003 1002 1001	Characterizing source reservoirs of igneous rocks: A new perspective. Fractionation of radiogenic isotopes: A new tool for petrogenesis. 2012, 72, 323-332 Provenance and climate change inferred from SrNdPb isotopes of late Quaternary sediments in the Huanghe (Yellow River) Delta, China. 2012, 78, 561-571 SrNd isotopic constraints on terrigenous sediment provenances and Kuroshio Current variability in the Okinawa Trough during the late Quaternary. 2012, 365-366, 38-47 Two-Stage, Extreme Albitization of A-type Granites from Rajasthan, NW India. 2012, 53, 919-948 Ice-rafting from the Britishlish ice sheet since the earliest Pleistocene (2.6 million years ago): implications for long-term mid-latitudinal ice-sheet growth in the North Atlantic region. 2012, 44, 229-240 Preboreal onset of cold-water coral growth beyond the Arctic Circle revealed by coupled	1 47 66 64 54

996	UPb geochronology and geochemistry of the bedrocks and moraine sediments from the Windmill Islands: Implications for Proterozoic evolution of East Antarctica. 2012 , 206-207, 52-71		30
995	High-precision and accurate determinations of neodymium isotopic compositions at nanogram levels in natural materials by MC-ICP-MS. 2012 , 27, 1560		25
994	Sr and Nd Isotopes as Tracers of Chemical and Physical Erosion. 2012 , 521-552		11
993	Provenance of late Oligocene to quaternary sediments of the Ecuadorian Amazonian foreland basin as inferred from major and trace element geochemistry and NdBr isotopic composition. 2012 , 37, 136-153		10
992	Late Holocene intermediate water variability in the northeastern Atlantic as recorded by deep-sea corals. <i>Earth and Planetary Science Letters</i> , 2012 , 313-314, 34-44	5.3	31
991	Greater supply of Patagonian-sourced detritus and transport by the ACC to the Atlantic sector of the Southern Ocean during the last glacial period. <i>Earth and Planetary Science Letters</i> , 2012 , 317-318, 374-385	5.3	28
990	The hafnium and neodymium isotope composition of seawater in the Atlantic sector of the Southern Ocean. <i>Earth and Planetary Science Letters</i> , 2012 , 317-318, 282-294	5.3	141
989	A boundary exchange influence on deglacial neodymium isotope records from the deep western Indian Ocean. <i>Earth and Planetary Science Letters</i> , 2012 , 341-344, 35-47	5.3	55
988	Geochemistry, geochronology and Sr⊠d⊞f isotopes of two Mesozoic granitoids in the Xiaoqinling gold district: Implication for large-scale lithospheric thinning in the North China Craton. 2012 , 294-295, 173-189		80
987	Neodymium isotopic composition of the oceans: A compilation of seawater data. 2012 , 300-301, 177-18	4	93
986	Combined UPb geochronology and SrNd isotope analysis of the Ice River perovskite standard, with implications for kimberlite and alkaline rock petrogenesis. 2012 , 304-305, 10-17		30
985	Diffusional homogenization of light REE in garnet from the Day Nui Con Voi Massif in N-Vietnam: Implications for SmNd geochronology and timing of metamorphism in the Red River shear zone. 2012 , 318-319, 16-30		25
984	Asthenospheric source of Neoproterozoic and Mesozoic kimberlites from the North Atlantic craton, West Greenland: New high-precision UPb and SrNd isotope data on perovskite. 2012 , 320-321, 113-127		49
983	The neodymium isotopic composition of waters masses in the eastern Pacific sector of the Southern Ocean. 2012 , 79, 41-59		71
982	Sources and input mechanisms of hafnium and neodymium in surface waters of the Atlantic sector of the Southern Ocean. 2012 , 94, 22-37		39
981	Homogeneous superchondritic 142Nd/144Nd in the mid-ocean ridge basalt and ocean island basalt mantle. 2012 , 13, n/a-n/a		37
980	Sensitivity of Nd isotopic composition in seawater to changes in Nd sources and paleoceanographic implications. 2012 , 117, n/a-n/a		21
979	On the relationship between Nd isotopic composition and ocean overturning circulation in idealized freshwater discharge events. 2012 , 27, n/a-n/a		16

978	The distribution of neodymium isotopes and concentrations in the Eastern Equatorial Pacific: Water mass advection versus particle exchange. <i>Earth and Planetary Science Letters</i> , 2012 , 353-354, 198-207	63
977	Variations of North Atlantic inflow to the central Arctic Ocean over the last 14 million years inferred from hafnium and neodymium isotopes. <i>Earth and Planetary Science Letters</i> , 2012 , 353-354, 82-92 ³	27
976	Reconstruction of the Nd isotope composition of seawater on epicontinental seas: Testing the potential of FeMn oxyhydroxide coatings on foraminifera tests for deep-time investigations. 2012 , 99, 39-56	19
975	Nd isotopic composition of Late Devonian seawater in western Thailand: Geotectonic implications for the origin of the Sibumasu terrane. 2012 , 22, 1102-1109	27
974	Mid-Mesoproterozoic bimodal magmatic rocks in the northern North China Craton: Implications for magmatism related to breakup of the Columbia supercontinent. 2012 , 222-223, 339-367	132
973	Geochronology, geochemistry and tectonic significance of two Early Cretaceous A-type granites in the Gan-Hang Belt, Southeast China. 2012 , 150, 155-170	112
972	The Himalayan leucogranites: Constraints on the nature of their crustal source region and geodynamic setting. 2012 , 22, 360-376	180
971	Permo-Triassic granitoids in the northern part of the Truong Son belt, NW Vietnam: Geochronology, geochemistry and tectonic implications. 2012 , 22, 628-644	137
970	Petrochemistry, geochronology and SrNd isotopic systematics of the Tertiary collisional and post-collisional volcanic rocks from the Ulubey (Ordu) area, eastern Pontide, NE Turkey: Implications for extension-related origin and mantle source characteristics. 2012 , 128-131, 126-147	76
969	Petrology of the Coyaguayma ignimbrite, northern Puna of Argentina: Origin and evolution of a peraluminous high-SiO2 rhyolite magma. 2012 , 134-135, 179-200	17
968	SrNd isotopic and geochemical constraints on provenance of late Paleozoic to early cretaceous sedimentary rocks in the Western Hills of Beijing, North China: Implications for the uplift of the northern North China Craton. 2012 , 245-246, 17-28	14
967	PbBrBId isotope constraints on the fluid source of the Dahu AuMo deposit in Qinling Orogen, central China, and implication for Triassic tectonic setting. 2012 , 46, 60-67	102
966	Origin of Meso-Proterozoic post-collisional leucogranite suites (Kaokoveld, Namibia): constraints from geochronology and Nd, Sr, Hf, and Pb isotopes. 2012 , 163, 1-17	21
965	Mesoproterozoic (Grenville-age) terranes in the Kyrgyz North Tianshan: Zircon ages and Nd⊞f isotopic constraints on the origin and evolution of basement blocks in the southern Central Asian Orogen. 2013 , 23, 272-295	174
964	Assessment of seawater Nd isotope signatures extracted from foraminiferal shells and authigenic phases of Gulf of Guinea sediments. 2013 , 121, 414-435	33
963	Geochemistry and petrogenesis of Proterozoic mafic rocks from East Khasi Hills, Shillong Plateau, Northeastern India. 2013 , 230, 119-137	23
962	Analytical results for the material of the Chelyabinsk meteorite. 2013 , 51, 522-539	55
961	Major and trace element composition of the high 3He/4He mantle: Implications for the composition of a nonchonditic Earth. 2013 , 14, 2954-2976	47

(2013-2013)

960	40ArB9Ar dating, whole-rock and SrNdPb isotope geochemistry of post-collisional Eocene volcanic rocks in the southern part of the Eastern Pontides (NE Turkey): implications for magma evolution in extension-induced origin. 2013 , 166, 113-142	84
959	Post-collisional, K-rich mafic magmatism in south Tibet: constraints on Indian slab-to-wedge transport processes and plateau uplift. 2013 , 165, 1311-1340	94
958	Paleoenvironmental conditions and strontium isotope stratigraphy in the Paleogene Gafsa Basin (Tunisia) deduced from geochemical analyses of phosphatic fossils. 2013 , 102, 1111-1129	14
957	2.1¶.85Ga tectonic events in the Yangtze Block, South China: Petrological and geochronological evidence from the Kongling Complex and implications for the reconstruction of supercontinent Columbia. 2013, 182-183, 200-210	139
956	Isotopic evidence for chondritic Lu/Hf and Sm/Nd of the Moon. <i>Earth and Planetary Science Letters</i> , 2013 , 380, 77-87	60
955	Variable HfSrNd radiogenic isotopic compositions in a Saharan dust storm over the Atlantic: Implications for dust flux to oceans, ice sheets and the terrestrial biosphere. 2013 , 349-350, 18-26	51
954	Algorithms for estimating uncertainties in initial radiogenic isotope ratios and model ages. 2013 , 340, 131-138	37
953	Petrogenesis of the late Cretaceous Turnaglintrusion in the eastern Pontides: Implications for magma genesis in the arc setting. 2013 , 4, 423-438	38
952	Geochemistry and SmNd geochronology of the metasomatised mafic rocks in the Khetri complex, Rajasthan, NW India: Evidence of an Early Cryogenian metasomatic event in the northern Aravalli orogen. 2013 , 62, 401-413	18
951	Geochemical signatures of sediments documenting Arctic sea-ice and water mass export through Fram Strait since the Last Glacial Maximum. 2013 , 64, 136-151	28
950	Dust transport and synoptic conditions over the SaharaArabia deserts during the MIS6/5 and 2/1 transitions from grain-size, chemical and isotopic properties of Red Sea cores. <i>Earth and Planetary Science Letters</i> , 2013 , 382, 125-139	40
949	Geochemistry and tectonic implications of late Mesoproterozoic alkaline bimodal volcanic rocks from the Tieshajie Group in the southeastern Yangtze Block, South China. 2013 , 230, 179-192	84
948	Nucleosynthetic Nd isotope anomalies in primitive enstatite chondrites. 2013 , 121, 652-666	22
947	Subduction related tectonic evolution of the Neoarchean eastern Dharwar Craton, southern India: New geochemical and isotopic constraints. 2013 , 227, 204-226	67
946	Underplating generated A- and I-type granitoids of the East Junggar from the lower and the upper oceanic crust with mixing of mafic magma: Insights from integrated zircon UPb ages, petrography, geochemistry and NdBrHf isotopes. 2013 , 179, 293-319	47
945	Insights into early Earth from Barberton komatiites: Evidence from lithophile isotope and trace element systematics. 2013 , 108, 63-90	94
944	Contrasting geochemical cycling of hafnium and neodymium in the central Baltic Sea. 2013 , 123, 166-180	15
943	Sr-Nd-Hf-Pb isotope and trace element evidence for the origin of alkalic basalts in the Garibaldi Belt, northern Cascade arc. 2013 , 14, 3126-3155	26

942 Encyclopedia of Scientific Dating Methods. **2013**, 1-20

941	Concomitant measurement of 143Nd/144Nd and 147Sm/144Nd ratios without isotope dilution in		11
) T =	geological samples: An assessment of MC-ICP-MS capabilities. 2013 , 333, 34-43		
940	The effect of particulate dissolution on the neodymium (Nd) isotope and Rare Earth Element (REE) composition of seawater. <i>Earth and Planetary Science Letters</i> , 2013 , 369-370, 138-147	5.3	88
939	Plio-Pleistocene basanitic and melilititic series of the Bohemian Massif: K-Ar ages, major/trace element and SrNd isotopic data. 2013 , 73, 429-450		23
938	Neodymium isotopic composition of intermediate and deep waters in the glacial southwest Pacific. <i>Earth and Planetary Science Letters</i> , 2013 , 384, 27-36	5.3	22
937	Short length scale mantle heterogeneity beneath Iceland probed by glacial modulation of melting. <i>Earth and Planetary Science Letters</i> , 2013 , 379, 146-157	5.3	29
936	Zircon UPb chronology and elemental and SrNdHf isotope geochemistry of two Triassic A-type granites in South China: Implication for petrogenesis and Indosinian transtensional tectonism. 2013, 160-161, 292-306		73
935	Island arc-type bimodal magmatism in the eastern Tianshan Belt, Northwest China: Geochemistry, zircon UBb geochronology and implications for the Paleozoic crustal evolution in Central Asia. 2013 , 168-169, 48-66		70
934	High- and low-latitude forcing of the Nile River regime during the Holocene inferred from laminated sediments of the Nile deep-sea fan. <i>Earth and Planetary Science Letters</i> , 2013 , 364, 98-110	5.3	85
933	Hafnium-neodymium constraints on source heterogeneity of the economic ultramafic-mafic Noril'sk-1 intrusion (Russia). 2013 , 164-167, 36-46		15
932	First Nd isotope record of Mediterranean Atlantic water exchange through the Moroccan Rifian Corridor during the Messinian Salinity Crisis. <i>Earth and Planetary Science Letters</i> , 2013 , 368, 163-174	5.3	25
931	Tectonically restricted deep-ocean circulation at the end of the Cretaceous greenhouse. <i>Earth and Planetary Science Letters</i> , 2013 , 369-370, 169-177	5.3	40
930	Zircon UPb dating, trace element and SrNdHf isotope geochemistry of Paleozoic granites in the MiaoBrshanNuechengling batholith, South China: Implication for petrogenesis and tectonichagmatic evolution. 2013, 74, 244-264		44
929	Geochronology and geochemistry of volcanic rocks from the Shaojiwa Formation and Xingzi Group, Lushan area, SE China: Implications for Neoproterozoic back-arc basin in the Yangtze Block. 2013 , 238, 1-17		54
928	Decadal changes in the mid-depth water mass dynamic of the Northeastern Atlantic margin (Bay of Biscay). <i>Earth and Planetary Science Letters</i> , 2013 , 364, 134-144	5.3	20
927	Hf and Nd isotopes in Early Ordovician to Early Carboniferous granites as monitors of crustal growth in the Proto-Andean margin of Gondwana. 2013 , 23, 1617-1630		69
926	Initiation and Evolution of Plate Tectonics on Earth: Theories and Observations. 2013, 41, 117-151		298
925	Rapid changes in meridional advection of Southern Ocean intermediate waters to the tropical Pacific during the last 30kyr. <i>Earth and Planetary Science Letters</i> , 2013 , 368, 20-32	5.3	56

924	Nd and Sr isotope characteristics of Quaternary Indo-Gangetic plain sediments: Source distinctiveness in different geographic regions and its geological significance. 2013 , 344, 12-22	19
923	Changing rainfall patterns in NW Africa since the Younger Dryas. 2013 , 10, 111-123	22
922	Late Neoproterozoic arc-related magmatism in the Horse Cove Complex, eastern Avalon Zone, Newfoundland. 2013 , 50, 462-482	10
921	Evolving sources of eolian detritus on the Chinese Loess Plateau since early Miocene: Tectonic and climatic controls. <i>Earth and Planetary Science Letters</i> , 2013 , 371-372, 220-225	71
920	Glacial freshwater discharge events recorded by authigenic neodymium isotopes in sediments from the Mendeleev Ridge, western Arctic Ocean. <i>Earth and Planetary Science Letters</i> , 2013 , 369-370, 148-157 ^{5.3}	22
919	Changes in Pacific Ocean circulation following the Miocene onset of permanent Antarctic ice cover. Earth and Planetary Science Letters, 2013 , 365, 38-50 5.3	47
918	Mafic forearc cumulates and associated rocks in the central high-pressure belt of the Acatl n Complex of southern Mxico: geochemical constraints. 2013 , 55, 1401-1417	2
917	Geochemical and isotopic tracers of Arctic sea ice sources and export with special attention to the Younger Dryas interval. 2013 , 79, 184-190	22
916	Evidence of silicic acid leakage to the tropical Atlantic via Antarctic Intermediate Water during Marine Isotope Stage 4. 2013 , 28, 307-318	15
915	Petrogenesis and tectonic significance of Early Cretaceous high-Zr rhyolite in the Dazhou uranium district, Gan-Hang Belt, Southeast China. 2013 , 74, 303-315	25
914	Microscale neodymium distribution in sedimentary planktonic foraminiferal tests and associated mineral phases. 2013 , 100, 11-23	32
913	Controls on the incongruent release of hafnium during weathering of metamorphic and sedimentary catchments. 2013 , 101, 263-284	22
912	Mid-Silurian back-arc spreading at the northeastern margin of Gondwana: The Dapingzhang dacite-hosted massive sulfide deposit, Lancangjiang zone, southwestern Yunnan, China. 2013 , 24, 648-663	63
911	Metallogeny during continental outgrowth in the Columbia supercontinent: Isotopic characterization of the Zhaiwa Mollu system in the North China Craton. 2013 , 51, 43-56	60
910	Multiple sources for the origin of Late Jurassic Linglong adakitic granite in the Shandong Peninsula, eastern China: Zircon UPb geochronological, geochemical and SrNdHf isotopic evidence. 2013 , 162-163, 251-263	84
909	ISOTOPES ON THE BEACH, PART 2: NEODYMIUM ISOTOPIC ANALYSIS FOR THE PROVENANCING OF ROMAN GLASS-MAKING. 2013 , 55, 449-464	35
908	Geochemical, Sr-Nd-Pb, and Zircon Hf-O Isotopic Compositions of Eocene-Oligocene Shoshonitic and Potassic Adakite-like Felsic Intrusions in Western Yunnan, SW China: Petrogenesis and Tectonic Implications. 2013 , 54, 1309-1348	129
907	Geochemistry of 1.78 Ga A-type granites along the southern margin of the North China Craton: implications for Xiong'er magmatism during the break-up of the supercontinent Columbia. 2013 , 55, 496-509	29

906	Petrogenesis of the 🏻 ap˜l˜ Granitoid and its Mafic Enclaves in Elmal˜ Area (Nide, Central Anatolia, Turkey). 2013 , 87, 738-748	3
905	Abrupt drainage cycles of the Fennoscandian Ice Sheet. 2013 , 110, 6682-7	55
904	Meter-scale Nd isotopic heterogeneity in pyroxenite-bearing Ligurian peridotites encompasses global-scale upper mantle variability. 2013 , 41, 1055-1058	31
903	Neodymium isotopic composition and concentration in the Southwest Pacific Ocean. 2013 , 47, 409-422	18
902	Rare earth element concentrations and Nd isotopes in the Southeast Pacific Ocean. 2013 , 14, 328-341	47
901	An Isotopic Survey of Pacific Oceanic Plateaus: Implications for their Nature and Origin. 2013, 207-220	43
900	Campanian-Maastrichtian ocean circulation in the tropical Pacific. 2013 , 28, 562-573	27
899	Accretion and Early Differentiation History of the Earth Based on Extinct Radionuclides. 2013, 47-74	24
898	Holocene climate variability in the winter rainfall zone of South Africa. 2013, 9, 2347-2364	34
897	Ocean circulation reconstructions from 🏿 d: A model-based feasibility study. 2014 , 29, 1003-1023	12
896	A major change in North Atlantic deep water circulation 1.6 million years ago. 2014 , 10, 1441-1451	9
895	Petrology and SrNd Isotopic Disequilibrium of the Xiaohaizi Intrusion, NW China: Genesis of Layered Intrusions in the Tarim Large Igneous Province. 2014 , 55, 2567-2598	29
894	Encyclopedia of Scientific Dating Methods. 2014 , 1-20	8
893	Origin of two contrasting latest Permian Triassic volcanic rock suites in the northern North China Craton: implications for early Mesozoic lithosphere thinning. 2014 , 56, 1630-1657	12
892	Zircon UPb geochronology, geochemical and SrNdHf isotopic compositions of the Triassic granite and diorite dikes from the Wulonggou mining area in the Eastern Kunlun Orogen, NW China: Petrogenesis and tectonic implications. 2014 , 205, 266-283	76
891	Did a proto-ocean basin form along the southeastern Rae cratonic margin? Evidence from U-Pb geochronology, geochemistry (Sm-Nd and whole-rock), and stratigraphy of the Paleoproterozoic Piling Group, northern Canada. 2014 , 126, 1625-1653	21
890	Petrogenesis and geochronology of a post-orogenic calc-alkaline magmatic association: the Ūlovπ̀ Pluton, Bohemian Massif. 2014 , 415-440	25
889	Petrogenesis of the late Cretaceous K-rich volcanic rocks from the Central Pontide orogenic belt, North Turkey. 2014 , 23, 102-124	12

888	SmNd dating of hydrothermal carbonate formation: An example from the Breitenau magnesite deposit (Styria, Austria). 2014 , 387, 184-201	22
887	Evidences for a Paleocene marine incursion in southern Amazonia (Madre de Dios Sub-Andean Zone, Peru). 2014 , 414, 451-471	16
886	Devonian Permian magmatic pulses in the northern Vosges Mountains (NE France): result of continuous subduction of the Rhenohercynian Ocean and Avalonian passive margin. 2014 , 405, 197-223	11
885	Long-lived Isotopic Tracers in Oceanography, Paleoceanography, and Ice-sheet Dynamics. 2014 , 453-483	3
884	Sr, Nd, Pb and Os Isotope Systematics of CAMP Tholeiites from Eastern North America (ENA): Evidence of a Subduction-enriched Mantle Source. 2014 , 55, 133-180	58
883	SrNdPb isotope systematics of magnetite: Implications for the genesis of Makeng Fe deposit, southern China. 2014 , 57, 53-60	37
882	ReDs isotopic records in Pleistocene loesspaleosol sequences from the Yili Basin, northwestern China. 2014 , 373, 71-86	8
881	Geochronology, geochemistry and Nd, Sr and Pb isotopes of syn-orogenic granodiorites and granites (Damara orogen, Namibia) [Arc-related plutonism or melting of mafic crustal sources?. 2014 , 200-201, 386-401	21
880	Integrating 40ArB9Ar, 87RbB7Sr and 147SmI143Nd geochronology of authigenic illite to evaluate tectonic reactivation in an intraplate setting, central Australia. 2014 , 134, 155-174	14
879	Rare earth elements and Nd isotopes tracing water mass mixing and particle-seawater interactions in the SE Atlantic. 2014 , 125, 351-372	71
878	Biogeochemical implications from dissolved rare earth element and Nd isotope distributions in the Gulf of Alaska. 2014 , 126, 455-474	45
877	Hafnium isotope evidence for slab melt contributions in the Central Mexican Volcanic Belt and implications for slab melting in hot and cold slab arcs. 2014 , 377, 45-55	32
876	Implications for Rodinia reconstructions for the initiation of Neoproterozoic subduction at ~860Ma on the western margin of the Yangtze Block: Evidence from the Guandaoshan Pluton. 2014 , 196-197, 67-82	55
875	HafniumBeodymium isotope systematics of the 2.7Ga Gadwal greenstone terrane, Eastern Dharwar craton, India: Implications for the evolution of the Archean depleted mantle. 2014 , 127, 10-24	47
874	NdBr isotopic and REE geochemical compositions of Late Quaternary deposits in the desertIbess transition, north-central China: Implications for their provenance and past wind systems. 2014 , 334-335, 197-212	9
873	Phase Diagrams for Geoscientists. 2014 ,	6
872	K-Ar dating, whole-rock and Sr-Nd isotope geochemistry of calc-alkaline volcanic rocks around the Ginilane area: implications for post-collisional volcanism in the Eastern Pontides, Northeast Turkey. 2014 , 108, 245-267	42
871	The geochemistry of deep-sea coral skeletons: A review of vital effects and applications for palaeoceanography. 2014 , 99, 184-198	74

870	Geochronology, geochemistry, and mineralization of the granodiorite porphyry hosting the Matou CuMo (–W) deposit, Lower Yangtze River metallogenic belt, eastern China. 2014 , 79, 623-640	38
869	Geochronology, geochemistry and SrNdHf isotopes of the Haisugou porphyry Mo deposit, northeast China, and their geological significance. 2014 , 79, 777-791	51
868	The role of subduction channel mlanges and convergent subduction systems in the petrogenesis of post-collisional K-rich mafic magmatism in NW Tibet. 2014 , 198-199, 184-201	39
867	Temporal and spatial variations of Mesozoic magmatism and deformation in the North China Craton: Implications for lithospheric thinning and decratonization. 2014 , 131, 49-87	270
866	Constraining genesis and geotectonic setting of metavolcanic complexes: a multidisciplinary study of the Devonian Vrbno Group (HrubDesenk Mts., Czech Republic). 2014 , 103, 455-483	30
865	Petrochemical evidence of magma mingling and mixing in the Tertiary monzogabbroic stocks around the Bafra (Samsun) area in Turkey: implications of coeval mafic and felsic magma interactions. 2014 , 108, 353-370	20
864	A radiogenic isotope tracer study of transatlantic dust transport from Africa to the Caribbean. 2014 , 82, 130-143	51
863	Syn-orogenic high-temperature crustal melting: Geochronological and NdBr B b isotope constraints from basement-derived granites (Central Damara Orogen, Namibia). 2014 , 192-195, 21-38	24
862	LA-ICP MS zircon dating, whole-rock and SrNdPbD isotope geochemistry of the Camibo&z—pluton, Eastern Pontides, NE Turkey: Implications for lithospheric mantle and lower crustal sources in arc-related I-type magmatism. 2014 , 192-195, 271-290	57
861	Petrogenesis of synorogenic high-temperature leucogranites (Damara orogen, Namibia): Constraints from UBb monazite ages and Nd, Sr and Pb isotopes. 2014 , 25, 1614-1626	28
860	Mesoproterozoic crust in the San Lucas Range (Colombia): An insight into the crustal evolution of the northern Andes. 2014 , 245, 186-206	20
859	Petrology, geochronology and emplacement model of the giant 1.37 Ga arcuate Lake Victoria Dyke Swarm on the margin of a large igneous province in eastern Africa. 2014 , 97, 273-296	32
858	Geochemistry of primary-carbonate bearing K-rich igneous rocks in the Awulale Mountains, western Tianshan: Implications for carbon-recycling in subduction zone. 2014 , 143, 143-164	23
857	Petrology and geochemistry of the ultramafichafic Mawpyut complex, Meghalaya: a Sylhet trap differentiation centre in northeastern India. 2014 , 49, 111-128	4
856	Geochronology, petrogenesis and tectonic significance of the Jitang granitic pluton in eastern Tibet, SW China. 2014 , 184-187, 314-323	36
855	Geochronology and geochemistry of Early Mesoproterozoic meta-diabase sills from Quruqtagh in the northeastern Tarim Craton: Implications for breakup of the Columbia supercontinent. 2014 , 241, 29-43	58
854	ANATEXIS OF JUVENILE MAFIC TO INTERMEDIATE CRUST -CONSTRAINTS FROM MAJOR AND TRACE ELEMENT AND SR, ND, PB ISOTOPES OF DIORITES TO GRANITES (DAMARA OROGEN, NAMBIA). 2014 , 117, 149-171	8
853	Geochronology, geochemistry, and petrogenesis of the Maßa subvolcanic intrusions: implications for the Late Cretaceous magmatic and geodynamic evolution of the eastern part of the Sakarya Zone, northeastern Turkey. 2014 , 56, 1246-1275	42

852	Provenance of sedimentary kaolin deposits in Egypt: Evidences from the Pb, Sr and Nd isotopes. 2014 , 100, 532-540	9
851	The petrogenesis of Early Eocene non-adakitic volcanism in NE Turkey: Constraints on the geodynamic implications. 2014 , 208-209, 361-377	31
850	Late Pliocene variations of the Mediterranean outflow. 2014 , 357, 182-194	25
849	Evidence for the control of the geochemistry of Amazonian floodplain sediments by stratification of suspended sediments in the Amazon. 2014 , 387, 101-110	24
848	Peak Last Glacial weathering intensity on the North American continent recorded by the authigenic Hf isotope composition of North Atlantic deep-sea sediments. 2014 , 99, 97-111	17
847	Provenance of quaternary and modern alluvial deposits of the Amazonian floodplain (Brazil) inferred from major and trace elements and PbNdBr isotopes. 2014 , 411, 144-154	13
846	Source-derived heterogeneities in the composite (charnockite-granite) ferroan Farsund intrusion (SW Norway). 2014 , 251, 141-163	15
845	Lithospheric origin for NeogeneQuaternary Middle Atlas lavas (Morocco): Clues from trace elements and SrNdPbHf isotopes. 2014 , 205, 247-265	31
844	Geochronology and geochemistry of Cretaceous Nanshanping alkaline rocks from the Zijinshan district in Fujian Province, South China: Implications for crustthantle interaction and lithospheric extension. 2014 , 93, 253-274	27
843	Sediment provenance and paleoenvironmental change in the Ulleung Basin of the East (Japan) Sea during the last 21kyr. 2014 , 93, 146-157	11
842	Geochemistry of lamprophyres at the Daping gold deposit, Yunnan Province, China: Constraints on the timing of gold mineralization and evidence for mantle convection in the eastern Tibetan Plateau. 2014 , 93, 129-145	25
841	Geochronology, elemental and Nd⊞f isotopic geochemistry of Devonian A-type granites in central Jiangxi, South China: Constraints on petrogenesis and post-collisional extension of the Wuyi⊠unkai orogeny. 2014 , 206-207, 1-18	38
840	Sr and Nd isotopic compositions of apatite reference materials used in UIIhPb geochronology. 2014 , 385, 35-55	136
839	Geochronological (UPb, UIIhEotal Pb, SmNd) and geochemical (REE, 87Sr/86Sr, 180, 13C) tracing of intraplate tectonism and associated fluid flow in the Warburton Basin, Australia. 2014 , 168, 1	6
838	Neodymium isotopes and concentrations in Caribbean seawater: Tracing water mass mixing and continental input in a semi-enclosed ocean basin. <i>Earth and Planetary Science Letters</i> , 2014 , 406, 174-186 ^{5.3}	35
837	Geochronology and geochemistry of igneous rocks from the Kongling terrane: Implications for Mesoarchean to Paleoproterozoic crustal evolution of the Yangtze Block. 2014 , 255, 30-47	108
836	Tertiary alkaline Roztoky Intrusive Complex, <code>Bsk</code> 'st <code>BdohofMts.</code> , Czech Republic: petrogenetic characteristics. 2014 , 103, 1233-1262	9
835	Metasomatism of ferroan granites in the northern Aravalli orogen, NW India: geochemical and isotopic constraints, and its metallogenic significance. 2014 , 103, 1083-1112	15

834	Neodymium and hafnium boundary contributions to seawater along the West Antarctic continental margin. <i>Earth and Planetary Science Letters</i> , 2014 , 394, 99-110	5.3	35
833	Neodymium associated with foraminiferal carbonate as a recorder of seawater isotopic signatures. 2014 , 88, 1-13		56
832	Gorstian palaeoposition and geotectonic setting of Suchomasty Volcanic Centre (Silurian, Prague Basin, TeplæBarrandian Unit, Bohemian Massif). 2014 , 136, 262-265		8
831	SamariumEeodymium chronology and rubidiumEtrontium systematics of an Allende calciumEluminum-rich inclusion with implications for 146Sm half-life. <i>Earth and Planetary Science Letters</i> , 2014 , 405, 15-24	5.3	55
830	Thermohaline circulation crisis and impacts during the mid-Pleistocene transition. 2014 , 345, 318-22		81
829	Petrogenesis of Late Mesozoic granitoids and coeval mafic rocks from the Jiurui district in the Middlellower Yangtze metallogenic belt of Eastern China: Geochemical and SrNdPbHf isotopic evidence. 2014 , 190-191, 467-484		35
828	Timing and sources of pre-collisional Neoproterozoic sedimentation along the SW margin of the Congo Craton (Kaoko Belt, NW Namibia). 2014 , 26, 386-401		43
827	Distinct sources for syntectonic Variscan granitoids: Insights from the Aguiar da Beira region, Central Portugal. 2014 , 196-197, 83-98		11
826	Decreased influence of Antarctic intermediate water in the tropical Atlantic during North Atlantic cold events. <i>Earth and Planetary Science Letters</i> , 2014 , 389, 200-208	5.3	53
825	Measurement of fossil deep-sea coral Nd isotopic compositions and concentrations by TIMS as NdO+, with evaluation of cleaning protocols. 2014 , 374-375, 128-140		21
824	Mineralogy, geochemistry and ore genesis of the Dawan uranium deposit in southern Hunan Province, South China. 2014 , 138, 59-71		19
823	South Pacific dissolved Nd isotope compositions and rare earth element distributions: Water mass mixing versus biogeochemical cycling. 2014 , 127, 171-189		57
822	Lithospheric and asthenospheric sources of lamprophyres in the Jiaodong Peninsula: A consequence of rapid lithospheric thinning beneath the North China Craton?. 2014 , 124, 250-271		156
821	Tracing the Nd isotope evolution of North Pacific Intermediate and Deep Waters through the last deglaciation from South China Sea sediments. 2014 , 79, 564-573		14
820	Neoglacial change in deep water exchange and increase of sea-ice transport through eastern Fram Strait: evidence from radiogenic isotopes. 2014 , 92, 190-207		19
819	South Greenland ice-sheet collapse during Marine Isotope Stage 11. 2014 , 510, 525-8		70
818	Rare earth elements and neodymium isotopes in sedimentary organic matter. 2014 , 140, 177-198		88
817	Highly fractionated S-type granites from the giant Dahutang tungsten deposit in Jiangnan Orogen, Southeast China: geochronology, petrogenesis and their relationship with W-mineralization. 2014 , 202-203, 207-226		143

(2015-2014)

816	U/Pb SIMS age, trace elements and Sm/Nd isotopes: Case study from the Western Carpathians, Slovakia. 2014 , 205, 1-14	11
815	Geochemistry and petrogenesis of lava flows around Linga, Chhindwara area in the Eastern Deccan Volcanic Province (EDVP), India. 2014 , 91, 174-193	11
814	The transition on North America from the warm humid Pliocene to the glaciated Quaternary traced by eolian dust deposition at a benchmark North Atlantic Ocean drill site. 2014 , 93, 125-141	35
813	Source characteristics and tectonic setting of the Early and Middle Devonian volcanic rocks in the North Junggar, Northwest China: Insights from NdBr isotopes and geochemistry. 2014 , 184-187, 27-41	20
812	Geochemistry of Early Cretaceous calc-alkaline lamprophyres in the Jiaodong Peninsula: Implication for lithospheric evolution of the eastern North China Craton. 2014 , 25, 859-872	110
811	The seawater neodymium and lead isotope record of the final stages of Central American Seaway closure. 2014 , 29, 715-729	44
810	Dynamic intermediate ocean circulation in the North Atlantic during Heinrich Stadial 1: A radiocarbon and neodymium isotope perspective. 2014 , 29, 1072-1093	37
809	Nd and Sr isotope compositions of different phases of surface sediments in the South Pacific: Extraction of seawater signatures, boundary exchange, and detrital/dust provenance. 2014 , 15, 3502-3520	25
808	Influence of the Central American Seaway and Drake Passage on ocean circulation and neodymium isotopes: A model study. 2014 , 29, 1214-1237	7
807	Sr-Nd isotope composition and clay mineral assemblages in eolian dust from the central Philippine Sea over the last 600 kyr: Implications for the transport mechanism of Asian dust. 2014 , 119, 11,492-11,504	18
806	Permian back-arc extension in central Inner Mongolia, NE China: Elemental and SrNdPbHfD isotopic constraints from the Linxi high-MgO diabase dikes. 2015 , 24, 404-424	15
805	Neodymium isotopic composition in foraminifera and authigenic phases of the South China Sea sediments: Implications for the hydrology of the North Pacific Ocean over the past 25 kyr. 2015 , 16, 3883-390	4 ¹⁷
804	Movement of the Intertropical Convergence Zone during the mid-pleistocene transition and the response of atmospheric and surface ocean circulations in the central equatorial Pacific. 2015 , 16, 3973-3981	7
803	New insights into hydrological exchange between the South China Sea and the Western Pacific Ocean based on the Nd isotopic composition of seawater. 2015 , 122, 25-40	26
802	Tracking potential source areas of Central European loess:examples from Tokaj (HU), Nussloch (D) and Grub (AT). 2015 , 7,	16
801	Epigenetic silicification of the Upper Oxfordian limestones in the Sokole Hills (KrakŴ-Czstochowa Upland): relationship to facies development and tectonics. 2015 , 65, 192-214	4
800	Upper Cretaceous to Pleistocene melilitic volcanic rocks of the Bohemian Massif: petrology and mineral chemistry. 2015 , 66, 197-216	9
799	Millennial-scale fluctuations of the European Ice Sheet at the end of the last glacial, and their potential impact on global climate. 2015 , 123, 113-133	92

798	Interhemispheric controls on deep ocean circulation and carbon chemistry during the last two glacial cycles. 2015 , 30, 621-641	21
797	Provenance of the HP⊞T subducted margin in the Variscan belt (Cabo Ortegal Complex, NW Iberian Massif). 2015 , 33, 959-979	19
796	Quantitative estimates of Asian dust input to the western Philippine Sea in the mid-late Quaternary and its potential significance for paleoenvironment. 2015 , 16, 3182-3196	37
795	Mineralogy, petrology, chronology, and exposure history of the Chelyabinsk meteorite and parent body. 2015 , 50, 1790-1819	40
794	Shifting material source of Chinese Loess since ~2.7 Ma reflected by Sr isotopic composition. 2015 , 5, 10235	23
793	Composition of the Tarim mantle plume: Constraints from clinopyroxene antecrysts in the early Permian Xiaohaizi dykes, NW China. 2015 , 230, 69-81	22
792	Two distinct Late Mesoproterozoic/Early Neoproterozoic basement provinces in central/eastern Dronning Maud Land, East Antarctica: The missing link, 1521°E. 2015 , 265, 249-272	69
791	Petrogenesis of the Ultrapotassic Fanshan Intrusion in the North China Craton: Implications for Lithospheric Mantle Metasomatism and the Origin of Apatite Ores. 2015 , 56, 893-918	22
790	SrINd isotopic constraints on detrital sediment provenance and paleoenvironmental change in the northern Okinawa Trough during the late Quaternary. 2015 , 430, 74-84	34
789	Post-collisional high-K calc-alkaline volcanism in Tengchong volcanic field, SE Tibet: constraints on Indian eastward subduction and slab detachment. 2015 , 172, 624-640	29
788	Petrology and geochemistry of late Carboniferous hornblende gabbro from the Awulale Mountains, western Tianshan (NW China): Implication for an arclascent back-arc environment. 2015 , 113, 218-237	26
787	20,000 years of Nile River dynamics and environmental changes in the Nile catchment area as inferred from Nile upper continental slope sediments. 2015 , 130, 200-221	71
786	Geochemistry, Sr-Nd isotope data and petrogenesis of the Marziyan granitoid, SanandajBirjan Zone, western Iran. 2015 , 192, 195-210	
785	Geochemical evidence for intermediate water circulation in the westernmost Mediterranean over the last 20kyrBP and its impact on the Mediterranean Outflow. 2015 , 135, 38-46	23
7 ⁸ 4	A combined Y/Ho, high field strength element (HFSE) and Nd isotope perspective on basalt weathering, Deccan Traps, India. 2015 , 396, 25-41	57
783	Late Cretaceous granites from the giant Dulong Sn-polymetallic ore district in Yunnan Province, South China: Geochronology, geochemistry, mineral chemistry and Nd⊞f isotopic compositions. 2015 , 218-219, 54-72	73
782	Multi-stage metamorphism in the South Armenian Block during the Late Jurassic to Early Cretaceous: Tectonics over south-dipping subduction of Northern branch of Neotethys. 2015 , 102, 4-23	28
781	Late Cenozoic intraplate volcanism in Changbai volcanic field, on the border of China and North Korea: insights into deep subduction of the Pacific slab and intraplate volcanism. 2015 , 172, 648-663	34

(2015-2015)

7 ⁸ 0	The Late Triassic Dengfuxian A-type granite, Hunan Province: age, petrogenesis, and implications for understanding the late Indosinian tectonic transition in South China. 2015 , 57, 428-445		36	
779	Paleogene post-collisional lamprophyres in western Yunnan, western Yangtze Craton: Mantle source and tectonic implications. 2015 , 233, 139-161		69	
778	The Late Neoproterozoic magmatism in the Ediacaran series of the Eastern Pyrenees: new ages and isotope geochemistry. 2015 , 104, 909-925		25	
777	Persistently strong Indonesian Throughflow during marine isotope stage 3: evidence from radiogenic isotopes. 2015 , 112, 197-206		4	
776	Separating biogeochemical cycling of neodymium from water mass mixing in the Eastern North Atlantic. <i>Earth and Planetary Science Letters</i> , 2015 , 412, 245-260	5.3	51	
775	NdBr isotope geochemistry of fine-grained sands in the basin-type deserts, West China: Implications for the source mechanism and atmospheric transport. 2015 , 246, 458-471		19	
774	Encyclopedia of Scientific Dating Methods. 2015 , 739-740		1	
773	Lithological units at the boundary zone between the Jining and Huai'an Complexes (central-northern margin of the North China Craton): A Paleoproterozoic tectonic mlange?. 2015 , 227, 205-224		40	
772	Isotope (SBrNdPb) constraints on the genesis of the ca. 850 Ma Tumen MoE deposit in the Qinling Orogen, China. 2015 , 266, 108-118		21	
771	Mantle-derived sources of syenites from the A-type igneous suites INew approach to the provenance of alkaline silicic magmas. 2015 , 232, 242-265		45	
770	Mechanism of Continental Crustal Growth. 2015 , 173-199		1	
769	Age, nature, and origin of Ordovician Zhibenshan granite from the Baoshan terrane in the Sanjiang region and its significance for understanding Proto-Tethys evolution. 2015 , 57, 1922-1939		50	
768	Geochronology, geochemistry, and petrogenesis of the Eocene Bayburt intrusions, Eastern Pontides, NE Turkey: Evidence for lithospheric mantle and lower crustal sources in the high-K calc-alkaline magmatism. 2015 , 108, 97-116		37	
767	Geochemical characteristics and petrogenesis of phonolites and trachytic rocks from the #sk St#dohofVolcanic Complex, the Oh# Rift, Bohemian Massif. 2015 , 224-225, 256-271		24	
766	Deep circulation changes in the central South Atlantic during the past 145 kyrs reflected in a combined 231 Pa/ 230 Th, Neodymium isotope and benthic 13 record. <i>Earth and Planetary Science Letters</i> , 2015 , 419, 14-21	5.3	33	
765	Neodymium isotopic characterization of Ross Sea Bottom Water and its advection through the southern South Pacific. <i>Earth and Planetary Science Letters</i> , 2015 , 419, 211-221	5.3	36	
764	Provenance of the Variscan Upper Allochthon (Cabo Ortegal Complex, NW Iberian Massif). 2015 , 28, 1434-1448		42	
763	Age and origin of the Bulangshan and Mengsong granitoids and their significance for post-collisional tectonics in the ChangningMenglian Paleo-Tethys Orogen. 2015 , 113, 656-676		46	

762	Petrology of ferroan alkali-calcic granites: Synorogenic high-temperature melting of undepleted felsic lower crust (Damara orogen, Namibia). 2015 , 224-225, 114-125	19
761	Constraints on the role of tectonic and climate on erosion revealed by two time series analysis of marine cores around New Zealand. <i>Earth and Planetary Science Letters</i> , 2015 , 410, 174-185	20
760	Tracing the composition and origin of fluids at an ancient hydrocarbon seep (Hollard Mound, Middle Devonian, Morocco): A Nd, REE and stable isotope study. 2015 , 156, 50-74	30
759	A review of lunar chronology revealing a preponderance of 4.344.37 Ga ages. 2015 , 50, 715-732	89
758	New evidence for two sharp replacement fronts during albitization of granitoids from northern Aravalli orogen, northwest India. 2015 , 57, 1660-1685	23
757	The evolution of climatically driven weathering inputs into the western Arctic Ocean since the late Miocene: Radiogenic isotope evidence. <i>Earth and Planetary Science Letters</i> , 2015 , 419, 111-124	14
756	The Neoarchean ultramaficthafic complex in the Yinshan Block, North China Craton: Magmatic monitor of development of Archean lithospheric mantle. 2015 , 270, 80-99	23
755	Petrological and geochemical characteristics of Mesoproterozoic dyke swarms in the Gardar Province, South Greenland: Evidence for a major sub-continental lithospheric mantle component in the generation of the magmas. 2015 , 79, 909-939	24
754	Petrogenesis and tectonic implications of the iron-rich tholeiitic basalts in the Hutuo Group of the Wutai Mountains, Central Trans-North China Orogen. 2015 , 271, 225-242	14
753	Influence of atmospheric deposits and secondary minerals on Li isotopes budget in a highly weathered catchment, Guadeloupe (Lesser Antilles). 2015 , 414, 28-41	59
752	South Asian monsoon history over the past 60 kyr recorded by radiogenic isotopes and clay mineral assemblages in the Andaman Sea. 2015 , 16, 505-521	47
751	Cretaceous crustfhantle interaction and tectonic evolution of Cathaysia Block in South China: Evidence from pulsed mafic rocks and related magmatism. 2015 , 661, 136-155	22
75°	Bottoms up: Sedimentary control of the deep North Pacific Ocean® Ndsignature. 2015, 43, 1035-1035	61
749	Spatial variability of African dust in soils in a montane tropical landscape in Puerto Rico. 2015 , 412, 69-81	9
748	Evolution of the Late Miocene Mediterranean Atlantic gateways and their impact on regional and global environmental change. 2015 , 150, 365-392	136
747	Age, petrogenesis and tectonic implications of Early Devonian bimodal volcanic rocks in the South Altyn, NW China. 2015 , 111, 733-750	12
746	Early Paleozoic intracontinental felsic magmatism in the South China Block: Petrogenesis and geodynamics. 2015 , 234-235, 79-92	30
745	Post-collisional Ultrapotassic Mafic Magmatism in South Tibet: Products of Partial Melting of Pyroxenite in the Mantle Wedge Induced by Roll-back and Delamination of the Subducted Indian Continental Lithosphere Slab. 2015 , 56, 1365-1406	88

(2015-2015)

744	Obliquity pacing of the western Pacific Intertropical Convergence Zone over the past 282,000 years. 2015 , 6, 10018		65
743	UBb zircon geochronology, SrNd geochemistry, petrogenesis and tectonic setting of Mahoor granitoid rocks (Lut Block, Eastern Iran). 2015 , 111, 192-205		19
742	Origin of increased terrigenous supply to the NE South American continental margin during Heinrich Stadial 1 and the Younger Dryas. <i>Earth and Planetary Science Letters</i> , 2015 , 432, 493-500	5.3	48
741	Geochronology, geochemistry, and SrNdHf isotopes of the early Paleozoic igneous rocks in the Duobaoshan area, NE China, and their geological significance. 2015 , 97, 229-250		88
740	Late Triassic adakitic plutons within the Archean terrane of the North China Craton: Melting of the ancient lower crust at the onset of the lithospheric destruction. 2015 , 212-215, 353-367		23
739	Geochronology, geochemistry, and its geological significance of the Damaoqi Permian volcanic sequences on the northern margin of the North China Block. 2015 , 97, 307-319		27
738	A subduction-related metasomatically enriched mantle origin for the Luoboling and Zhongliao Cretaceous granitoids from South China: implications for magma evolution and Cu M o mineralization. 2015 , 57, 1239-1266		32
737	Constraints on the mantle mineralogy of an ultra-slow ridge: Hafnium isotopes in abyssal peridotites and basalts from the 9½5°E Southwest Indian Ridge. <i>Earth and Planetary Science Letters</i> , 2015 , 410, 42-53	5.3	29
736	Geochemical and SrNd isotope variations within Cretaceous continental flood-basalt suites of the Canadian High Arctic, with a focus on the Hassel Formation basalts of northeast Ellesmere Island. 2015 , 104, 1981-2005		21
735	New geochronological and SmNd constraints across the Pajala shear zone of northern Fennoscandia: Reactivation of a Paleoproterozoic suture. 2015 , 256, 102-119		28
734	Mineralogy of high-field-strength elements (Y, Nb, REE) in the world-class Vergenoeg fluorite deposit, South Africa. 2015 , 64, 583-601		26
733	Compositional polarity of Triassic granitoids in the Qinling Orogen, China: Implication for termination of the northernmost paleo-Tethys. 2015 , 27, 244-257		168
732	Nd isotope constraints on ocean circulation, paleoclimate, and continental drainage during the Jurassic breakup of Pangea. 2015 , 27, 1599-1615		46
731	Geochronology and geochemistry of the giant Qian'echong Mo deposit, Dabie Shan, eastern China: Implications for ore genesis and tectonic setting. 2015 , 27, 1217-1235		73
730	Geochronology, geochemistry and SrNdHf isotopes of mafic dikes in the Huicheng Basin: Constraints on intracontinental extension of the Qinling orogen. 2015 , 104, 115-126		8
729	Provenance of the Various Grain-Size Fractions in the Negev Loess and Potential changes in Major dust Sources to the Eastern Mediterranean. 2015 , 83, 105-115		36
728	Petrogenesis of synorogenic dioritegranodioritegranite complexes in the Damara Belt, Namibia: Constraints from UPb zircon ages and SrNdPb isotopes. 2015 , 101, 253-265		22
727	Zircon UBb dating, geochemistry and SrNdBb⊞f isotopes of the Wajilitag alkali mafic dikes, and associated diorite and syenitic rocks: Implications for magmatic evolution of the Tarim large igneous province. 2015 , 212-215, 428-442		21

726	The impact of sedimentary coatings on the diagenetic Nd flux. <i>Earth and Planetary Science Letters</i> , 2016 , 449, 217-227	36
725	Origin of Late Cenozoic AbagaDalinuoer basalts, eastern China: Implications for a mixed pyroxeniteDeridotite source related with deep subduction of the Pacific slab. 2016 , 37, 130-151	33
724	Neodymium in the oceans: a global database, a regional comparison and implications for palaeoceanographic research. 2016 , 374,	57
723	Anatexis of accretionary wedge, Pacific-type magmatism, and formation of vertically stratified continental crust in the Altai Orogenic Belt. 2016 , 35, 3095-3118	42
722	Reduced admixture of North Atlantic Deep Water to the deep central South Pacific during the last two glacial periods. 2016 , 31, 651-668	9
721	Response of the Pacific inter-tropical convergence zone to global cooling and initiation of Antarctic glaciation across the Eocene Oligocene Transition. 2016 , 6, 30647	11
720	Peridotitic Lithosphere Metasomatized by Volatile-bearing Melts, and its Association with Intraplate Alkaline HIMU-like Magmatism. 2016 , 57, 2053-2078	45
719	Variability of neodymium isotopes associated with planktonic foraminifera in the Pacific Ocean during the Holocene and Last Glacial Maximum. <i>Earth and Planetary Science Letters</i> , 2016 , 447, 130-138 ⁵⁻³	24
718	Rapid lithospheric thinning of the North China Craton: New evidence from cretaceous mafic dikes in the Jiaodong Peninsula. 2016 , 432, 1-15	76
717	Implications for post-comminution processes in subglacial suspended sediment using coupled radiogenic strontium and neodymium isotopes. 2016 , 259, 134-144	5
716	Zircon UPb dating, geochemical and SrNdHf isotopic characteristics of the Jintonghu monzonitic rocks in western Fujian Province, South China: Implication for Cretaceous crustInantle interactions and lithospheric extension. 2016, 260, 413-428	25
715	Linking the basement geology along the Africa-South America coasts in the South Atlantic. 2016 , 280, 221-230	34
714	A Sr-Nd-Hf isotope characterization of dust source areas in Victoria Land and the McMurdo Sound sector of Antarctica. 2016 , 141, 26-37	16
713	Geochemical constraints on petrogenesis of marble-hosted eclogites from the Sulu orogen in China. 2016 , 436, 35-53	16
712	Contribution of Asian dust and volcanic material to the western Philippine Sea over the last 220 kyr as inferred from grain size and Sr-Nd isotopes. 2016 , 121, 6911-6928	16
711	Elemental and isotopic composition of surface soils from key Saharan dust sources. 2016 , 442, 54-61	20
710	Evolving flux of Asian dust in the North Pacific Ocean since the late Oligocene. 2016 , 23, 11-20	35
709	Neodymium isotopes in authigenic phases, bottom waters and detrital sediments in the Gulf of Alaska and their implications for paleo-circulation reconstruction. 2016 , 193, 14-35	56

708	Stable and radiogenic isotope constraints on the magmatic and hydrothermal evolution of the Nechalacho Layered Suite, northwest Canada. 2016 , 440, 248-274	8
707	Geochemical response of the mid-depth Northeast Atlantic Ocean to freshwater input during Heinrich events 1 to 4. 2016 , 151, 236-254	12
706	Neodymium isotopic evidence for linked changes in Southeast Atlantic and Southwest Pacific circulation over the last 200 kyr. <i>Earth and Planetary Science Letters</i> , 2016 , 455, 106-114 5-3	23
705	The Ponto-Caspian basin as a final trap for southeastern Scandinavian Ice-Sheet meltwater. 2016 , 148, 29-43	38
704	Petrochronological Constraints on the Origin of the Mountain Pass Ultrapotassic and Carbonatite Intrusive Suite, California. 2016 , egw050	9
703	South Atlantic intermediate water advances into the North-east Atlantic with reduced Atlantic meridional overturning circulation during the last glacial period. 2016 , 17, 2336-2353	14
702	Extracting foraminiferal seawater Nd isotope signatures from bulk deep sea sediment by chemical leaching. 2016 , 439, 189-204	48
701	Neoproterozoic crustal growth at the margin of the East Gondwana continent lage and isotopic constraints from the easternmost inliers of Oman. 2016 , 58, 2046-2064	21
700	Robustness of fossil fish teeth for seawater neodymium isotope reconstructions under variable redox conditions in an ancient shallow marine setting. 2016 , 17, 679-698	14
699	Plio-Pleistocene evolution of water mass exchange and erosional input at the Atlantic-Arctic gateway. 2016 , 31, 582-599	5
698	Seawater Nd isotope variation in the Western Pacific Ocean since 80 Ma (ODP 807, Ontong Java Plateau). 2016 , 380, 138-147	8
697	Petrogenesis of MiddleIlate Triassic volcanic rocks from the Gangdese belt, southern Lhasa terrane: Implications for early subduction of Neo-Tethyan oceanic lithosphere. 2016 , 262, 320-333	138
696	Geochemical constraints on the source nature and melting conditions of Triassic granites from South Qinling in central China. 2016 , 264, 141-157	31
695	Abyssal origin for the early Holocene pulse of unradiogenic neodymium isotopes in Atlantic seawater. 2016 , 44, 831-834	27
694	A nucleosynthetic origin for the Earth's anomalous (142)Nd composition. 2016 , 537, 394-8	97
693	Antarctic intermediate water circulation in the South Atlantic over the past 25,000 years. 2016 , 31, 1302-131	4 22
692	SmNd and ArAr Isotopic Dating of the Nuri CuMMo Deposit in the Southern Gangdese, Tibet: Implications for the Porphyry-Skarn Metallogenic System and Metallogenetic Epochs of the Eastern Gangdese. 2016 , 66, 259-273	6
691	The coupled 182W-142Nd record of early terrestrial mantle differentiation. 2016 , 17, 2168-2193	62

690	Climatic control of sediment transport from the Himalayas to the proximal NE Bengal Fan during the last glacial-interglacial cycle. 2016 , 148, 1-16	45
689	Subduction-related Late Cretaceous high-K volcanism in the Central Pontides orogenic belt: constraints on geodynamic implications. 2016 , 28, 379-411	12
688	Evidence against an ancient non-chondritic mantle source for North Atlantic Igneous Province lavas. 2016 , 440, 91-100	9
687	Unraveling North-African riverine and eolian contributions to central Mediterranean sediments during Holocene sapropel S1 formation. 2016 , 152, 31-48	18
686	Detrital zircon and provenance analysis of Eocene®ligocene strata in the South Sistan suture zone, southeast Iran: Implications for the tectonic setting. 2016 , 8, 615-632	8
685	Neodymium isotope constraints on provenance, dispersal, and climate-driven supply of Zambezi sediments along the Mozambique Margin during the past ~45,000 years. 2016 , 17, 181-198	24
684	Neodymium isotope analyses after combined extraction of actinide and lanthanide elements from seawater and deep-sea coral aragonite. 2016 , 17, 232-240	7
683	Hawaiian imprint on dissolved Nd and Ra isotopes and rare earth elements in the central North Pacific: Local survey and seasonal variability. 2016 , 189, 110-131	33
682	Archean TTGs and sanukitoids from the Jiaobei terrain, North China craton: Insights into crustal growth and mantle metasomatism. 2016 , 281, 656-672	47
681	Petrogenesis of a late-Variscan rhyodacite at the Ossa Morena-Central Iberian zones boundary, Iberian Massif, Central Portugal: Evidence for the involvement of lithospheric mantle and meta-igneous lower crust. 2016 , 76, 429-439	3
680	Geochemical and Nd isotopic constraints on provenance and depositional setting of the Shihuiding Formation in the Shilu Fetottu ore district, Hainan Province, South China. 2016 , 119, 100-117	15
679	Climate change and response in bottom water circulation and sediment provenance in the Central Arctic Ocean since the Last Glacial. 2016 , 427, 98-108	10
678	Accretion timescale and impact history of Mars deduced from the isotopic systematics of martian meteorites. 2016 , 175, 150-167	51
677	Age and characteristics of the Loma del Aire unit (SW Iberia): Implications for the regional correlation of the Ossa-Morena Zone. 2016 , 681, 58-72	15
676	Primary Magmas in Continental Arcs and their Differentiated Products: Petrology of a Post-plutonic Dyke Suite in the Tertiary Adamello Batholith (Alps). 2016 , 57, 495-534	21
675	Petrogenesis and Sr-Nd isotope data of the Chadegan metabasites, Sanandaj-Sirjan Zone, Iran. 2016 , 279, 311-322	
674	Geochronology and petrogenesis of Middle Permian S-type granitoid in southeastern Guangxi Province, South China: Implications for closure of the eastern Paleo-Tethys. 2016 , 682, 1-16	19
673	Geochronology and geochemical constraints on petrogenesis of Early Paleozoic granites from the Laojunshan district in Yunnan Province of South China. 2016 , 29, 248-263	18

(2016-2016)

672	Geochemistry, geochronology and SrMdPbHf isotopic compositions of Middle to Late Jurassic syenitegranodiorites@acite in South China: Petrogenesis and tectonic implications. 2016 , 35, 217-237	21
671	Geochemical and SrNd isotopic variations in palaeoflood deposits at mainstemEributary junction, western India: Implications on late Holocene flood events. 2016 , 139, 32-43	4
670	Neodymium isotopic composition and concentration in the western North Atlantic Ocean: Results from the GEOTRACES GA02 section. 2016 , 177, 1-29	93
669	Geochronology and geochemistry of Eocene potassic felsic intrusions in the Nangqian basin, eastern Tibet: Tectonic and metallogenic implications. 2016 , 246-247, 212-227	17
668	Gradual changes in upwelled seawater conditions (redox, pH) from the late Cretaceous through early Paleogene at the northwest coast of Africa: Negative Ce anomaly trend recorded in fossil bio-apatite. 2016 , 421, 44-54	26
667	U₱b zircon geochronology and anomalous SrषdĦf isotope systematics of late orogenic andesites: Pieniny Klippen Belt, Western Carpathians, South Poland. 2016 , 427, 1-16	8
666	Late Triassic U-bearing and barren granites in the Miao'ershan batholith, South China: Petrogenetic discrimination and exploration significance. 2016 , 77, 260-278	23
665	The Anita Peridotite, New Zealand: Ultra-depletion and Subtle Enrichment in Sub-arc Mantle. 2016 , 57, 717-750	25
664	Provenance weathering and erosion records in southern Okinawa Trough sediments since 28 ka: Geochemical and SrNdPb isotopic evidences. 2016 , 425, 93-109	53
663	Olivine and melt inclusion chemical constraints on the source of intracontinental basalts from the eastern North China Craton: Discrimination of contributions from the subducted Pacific slab. 2016 , 178, 1-19	53
662	Identification of a late Quaternary alluvial Beolian sedimentary sequence in the Sichuan Basin, China. 2016 , 85, 279-289	3
661	Isotopes in cosmochemistry: recipe for a Solar System. 2016 , 31, 841-862	12
660	UPB zircon chronology and petrogenesis of Carboniferous plutons in the northern part of the Eastern Pontides, NE Turkey: Constraints for Paleozoic magmatism and geodynamic evolution. 2016 , 39, 327-346	43
659	Lithophile and siderophile element systematics of Earth mantle at the Archean Proterozoic boundary: Evidence from 2.4 Ga komatiites. 2016 , 180, 227-255	58
658	Detrital zircon in a supercontinental setting: locally derived and far-transported components in the Ordovician Natal Group, South Africa. 2016 , 173, 203-215	27
657	Geochronology and geochemistry of late Carboniferous volcanic rocks from northern Inner Mongolia, North China: Petrogenesis and tectonic implications. 2016 , 36, 545-560	43
656	Radiogenic Isotopes. 2016 , 53-66	
655	NdBr isotopic constraint to the formation of metatexite and diatexite migmatites, Higo metamorphic terrane, central Kyushu, Japan. 2016 , 58, 405-423	5

654	Permo-Carboniferous and early Miocene geological evolution of the internal zones of the Maghrebides lNew insights on the western Mediterranean evolution. 2016 , 96, 146-173		10
653	Geochronology, geochemistry and tectonic significance of the late Mesozoic volcanic sequences in the northern Wuyi Mountain volcanic belt of South China. 2016 , 37, 362-383		18
652	Source-to-sink transport processes of fluvial sediments in the South China Sea. 2016 , 153, 238-273		227
651	The Late Cretaceous igneous rocks of Romania (Apuseni Mountains and Banat): the possible role of amphibole versus plagioclase deep fractionation in two different crustal terranes. 2016 , 105, 819-847		1
650	ReDs and SrNdPb isotope constraints on source of fluids in the Zhifang Mo deposit, Qinling Orogen, China. 2016 , 30, 132-143		36
649	Nd isotope composition of conodonts: An accurate proxy of sea-level fluctuations. 2016 , 34, 284-295		23
648	Zircon UPb dating and SrNdPbHf isotopes of the ore-associated porphyry at the giant Donggebi Mo deposit, Eastern Tianshan, NW China. 2017 , 81, 794-807		53
647	Geochronology and geochemistry of the Tianmugou Mo deposit, Dabie Shan, eastern China: Implications for ore genesis and tectonic setting. 2017 , 81, 484-503		17
646	Petrogenesis and tectonic setting of the Devonian Xiqin A-type granite in the northeastern Cathaysia Block, SE China. 2017 , 141, 43-58		13
645	Controls on erosion patterns and sediment transport in a monsoonal, tectonically quiescent drainage, Song Gianh, central Vietnam. 2017 , 29, 659-683		18
644	Reconstruction of east west deep water exchange in the low latitude Atlantic Ocean over the past 25,000 years. <i>Earth and Planetary Science Letters</i> , 2017 , 458, 327-336	5.3	10
643	Authigenic Nd isotope record of North Pacific Intermediate Water formation and boundary exchange on the Bering Slope. 2017 , 156, 150-163		13
642	Neodymium isotopes and concentrations in aragonitic scleractinian cold-water coral skeletons - Modern calibration and evaluation of palaeo-applications. 2017 , 453, 146-168		13
641	An early Paleozoic monzonoritegranite suite in the South China block: implications for the intracontinental felsic magmatism. 2017 , 111, 709-728		11
640	Geochronology and geochemistry of Permian bimodal volcanic rocks from central Inner Mongolia, China: Implications for the late Palaeozoic tectonic evolution of the south-eastern Central Asian Orogenic Belt. 2017 , 135, 370-389		51
639	Palaeoproterozoic continental arc magmatism, and Neoproterozoic metamorphism in the Aravalli-Delhi orogenic belt, NW India: New constraints from in situ zircon U-Pb-Hf isotope systematics, monazite dating and whole-rock geochemistry. 2017 , 136, 68-88		28
638	Petrogenesis of the middle Jurassic appinite and coeval granitoids in the Eastern Hebei area of North China Craton. 2017 , 278-281, 331-346		17
637	Tracing an Early Jurassic magmatic arc from South to East China Seas. 2017 , 36, 466-492		57

636	Evidence for voluminous bimodal pyroclastic volcanism during rifting of a Paleoproterozoic arc at Snow Lake, Manitoba. 2017 , 54, 654-676	5
635	The Qiman Tagh Orogen as a window to the crustal evolution in northern Qinghai-Tibet Plateau. 2017 , 167, 103-123	39
634	Mineralogical evidence for crystallization conditions and petrogenesis of ilmenite-series I-type granitoids at the Baogutu reduced porphyry Cu deposit (Western Junggar, NW China): M\bar{B}sbauer spectroscopy, EPM and LA-(MC)-ICPMS analyses. 2017 , 86, 382-403	25
633	K isotopes as a tracer of seafloor hydrothermal alteration. 2017 , 114, 1827-1831	41
632	Glacial reduction of AMOC strength and long-term transition in weathering inputs into the Southern Ocean since the mid-Miocene: Evidence from radiogenic Nd and Hf isotopes. 2017 , 32, 265-283	15
631	Geodynamic implications for zonal and meridional isotopic patterns across the northern Lau and North Fiji Basins. 2017 , 18, 1013-1042	7
630	Fingerprinting Northeast Atlantic water masses using neodymium isotopes. 2017 , 210, 267-288	14
629	Origin of calcium in pedogenic carbonate nodules from silicate watersheds in the Far North Region of Cameroon: Respective contribution of in situ weathering source and dust input. 2017 , 460, 54-69	15
628	Petrology of the shoshonitic amball pluton in NE Turkey and implications for the closure of the Neo-Tethys Ocean: Insights from geochemistry, geochronology and SrNd isotopes. 2017 , 284-285, 477-492	15
627	Petrogenesis of Early Cretaceous adakitic granodiorite: Implication for a crust thickening event within the Cathaysia Block, South China. 2017 , 60, 1237-1255	2
626	Using Nd-Sr isotopes and rare earth elements to study sediment provenance of the modern radial sand ridges in the southwestern Yellow Sea. 2017 , 81, 23-35	8
625	Glacial/interglacial changes of Southern Hemisphere wind circulation from the geochemistry of South American dust. <i>Earth and Planetary Science Letters</i> , 2017 , 469, 98-109	40
624	Climatic and glacial impact on erosion patterns and sediment provenance in the Himalayan rain shadow, Zanskar River, NW India. 2017 , 129, 820-836	15
623	Petrogenetic evolution of Cretaceous Samchampi-Samteran Alkaline Complex, Mikir Hills, Northeastern India: Implications on multiple melting events of heterogeneous plume and metasomatized sub-continental lithospheric mantle. 2017 , 48, 237-256	13
622	OIB signatures in basin-related lithosphere-derived alkaline basalts from the Batain basin (Oman) [Constraints from 40Ar/39Ar ages and NdBrPbHf isotopes. 2017 , 286-287, 109-124	4
621	The onset of flysch sedimentation in the Kaoko Belt (NW Namibia) Implications for the pre-collisional evolution of the KaokoDom FelicianoCariep orogen. 2017 , 298, 220-234	26
620	Glacial erosion of East Antarctica in the Pliocene: A comparative study of multiple marine sediment provenance tracers. 2017 , 466, 199-218	20
619	A Nd- and O-isotope study of the REE-rich peralkaline Strange Lake granite: implications for Mesoproterozoic A-type magmatism in the Core Zone (NE-Canada). 2017 , 172, 1	8

618	Antarctic climate, Southern Ocean circulation patterns, and deep water formation during the Eocene. 2017 , 32, 674-691	29
617	Geochemical characterization (REE, Nd and Pb isotopes) of atmospheric mineral dust deposited in two maritime peat bogs from the St. Lawrence North Shore (eastern Canada). 2017 , 32, 617-627	6
616	Fingerprinting Gondwana versus Baltica provenance: Nd and Sr isotopes in Lower Paleozoic clastic rocks of the Maßpolska and Jsogfy terranes, southern Poland. 2017 , 45, 138-151	15
615	Dust composition changes from Taylor Glacier (East Antarctica) during the last glacial-interglacial transition: A multi-proxy approach. 2017 , 162, 60-71	16
614	The Mongol-Okhotsk Ocean subduction-related Permian peraluminous granites in northeastern Mongolia: Constraints from zircon U-Pb ages, whole-rock elemental and Sr-Nd-Hf isotopic compositions. 2017 , 144, 225-242	23
613	The large-scale evolution of neodymium isotopic composition in the global modern and Holocene ocean revealed from seawater and archive data. 2017 , 457, 131-148	58
612	Geochemistry, petrogenesis and tectonic significance of the late Triassic A-type granite in Fujian, South China. 2017 , 36, 166-180	2
611	Neoproterozoic backarc basin on the southeastern margin of the Yangtze block during Rodinia assembly: New evidence from provenance of detrital zircons and geochemistry of mafic rocks. 2017 , 129, 904-919	16
610	Continental igneous rock composition: A major control of past global chemical weathering. 2017, 3, e160218	3 22
609	Diffusion-zoned pyroxenes in an isotopically heterogeneous mantle lithosphere beneath the Dunedin Volcanic Group, New Zealand, and their implications for intraplate alkaline magma sources. 2017 , 9, 463-475	26
608	Investigations of the spatial and temporal variations of Sr and Nd isotopes in sediments from two Indian Rivers: Implications to source identification. 2017 , 18, 1520-1536	4
607	Genesis of the Permian karstic Pingguo bauxite deposit, western Guangxi, China. 2017 , 52, 1031-1048	20
606	Subduction between the Jiamusi and Songliao blocks: Geological, geochronological and geochemical constraints from the Heilongjiang Complex. 2017 , 282-283, 128-144	32
605	Petrogenesis of Ore-Related Granodiorite Porphyry in the Jiande Copper Deposit, SE China: Implications for the Tectonic Setting and Mineralization. 2017 , 67, 117-138	5
604	Increased chemical weathering during the deglacial to mid-Holocene summer monsoon intensification. 2017 , 7, 44310	33
603	Provenance study of the Holocene sediments in the Changjiang (Yangtze River) estuary and inner shelf of the East China sea. 2017 , 441, 147-161	39
602	Chronologic implications for slow cooling of troctolite 76535 and temporal relationships between the Mg-suite and the ferroan anorthosite suite. 2017 , 201, 377-391	20
601	Ocean circulation and freshwater pathways in the Arctic Mediterranean based on a combined Nd isotope, REE and oxygen isotope section across Fram Strait. 2017 , 202, 285-309	26

(2017-2017)

600	Geochemistry, Srindrod isotopes systematics and geochronological constrains on petrogenesis of the Xishan A-type granite and associated Win mineralization in Guangdong Province, South China. 2017 , 88, 739-752	24
599	Increased atmospheric dust deposition during the Neoglacial in a boreal peat bog from north-eastern Canada. 2017 , 469, 34-46	7
598	Evolution of the mantle beneath the eastern North China Craton during the Cenozoic: Linking geochemical and geophysical observations. 2017 , 122, 224-246	17
597	Ages, geochemistry and tectonic implications of the Cambrian igneous rocks in the northern Great Xing and Range, NE China. 2017 , 144, 5-21	23
596	Geochemical and Nd-Sr-Pb isotope characteristics of synorogenic lower crust-derived granodiorites (Central Damara orogen, Namibia). 2017 , 274-275, 397-411	13
595	Enhanced silicate weathering of tropical shelf sediments exposed during glacial lowstands: A sink for atmospheric CO2. 2017 , 200, 123-144	53
594	~2.1 Ga intraoceanic magmatism in the Central India Tectonic Zone: Constraints from the petrogenesis of ferropicrites in the Mahakoshal supracrustal belt. 2017 , 302, 1-17	8
593	Ages and petrogenesis of Jurassic and Cretaceous intrusive rocks in the Matsu Islands: Implications for lower crust modification beneath southeastern China. 2017 , 150, 14-24	11
592	Geochronology, geochemical and SrNdHf-Pb isotopic compositions of the granitoids in the Yemaquan orefield, East Kunlun orogenic belt, northern Qinghai-Tibet Plateau: Implications for magmatic fractional crystallization and sub-solidus hydrothermal alteration. 2017 , 294-295, 339-355	15
591	Mantle geochemistry: Insights from ocean island basalts. 2017 , 60, 1976-2000	8
591 590	Mantle geochemistry: Insights from ocean island basalts. 2017 , 60, 1976-2000 Radiogenic isotopic compositions of low concentration dust and aerosol from the GISP2 ice core. 2017 , 472, 31-43	2
	Radiogenic isotopic compositions of low concentration dust and aerosol from the GISP2 ice core.	
590	Radiogenic isotopic compositions of low concentration dust and aerosol from the GISP2 ice core. 2017 , 472, 31-43 The Ticunzal Formation in central Brazil: Record of Rhyacian sedimentation and metamorphism in	2
590 589	Radiogenic isotopic compositions of low concentration dust and aerosol from the GISP2 ice core. 2017, 472, 31-43 The Ticunzal Formation in central Brazil: Record of Rhyacian sedimentation and metamorphism in the western border of the Sâ Francisco Craton. 2017, 79, 307-325 Geochemical characteristics of the La Rûnion mantle plume source inferred from olivine-hosted melt inclusions from the adventive cones of Piton de la Fournaise volcano (La Rûnion Island). 2017	2
590 589 588	Radiogenic isotopic compositions of low concentration dust and aerosol from the GISP2 ice core. 2017, 472, 31-43 The Ticunzal Formation in central Brazil: Record of Rhyacian sedimentation and metamorphism in the western border of the Sâ Francisco Craton. 2017, 79, 307-325 Geochemical characteristics of the La Rûnion mantle plume source inferred from olivine-hosted melt inclusions from the adventive cones of Piton de la Fournaise volcano (La Rûnion Island). 2017, 172, 1 Provenance of loess in the central Great Plains, U.S.A. based on Nd-Sr isotopic composition, and	2 12 8
590 589 588 587	Radiogenic isotopic compositions of low concentration dust and aerosol from the GISP2 ice core. 2017, 472, 31-43 The Ticunzal Formation in central Brazil: Record of Rhyacian sedimentation and metamorphism in the western border of the Sà Francisco Craton. 2017, 79, 307-325 Geochemical characteristics of the La Rûnion mantle plume source inferred from olivine-hosted melt inclusions from the adventive cones of Piton de la Fournaise volcano (La Rûnion Island). 2017, 172, 1 Provenance of loess in the central Great Plains, U.S.A. based on Nd-Sr isotopic composition, and paleoenvironmental implications. 2017, 173, 114-123 Genesis and evolution of a Paleoproterozoic basement inlier within West Gondwana addressed by	2 12 8
590 589 588 587 586	Radiogenic isotopic compositions of low concentration dust and aerosol from the GISP2 ice core. 2017, 472, 31-43 The Ticunzal Formation in central Brazil: Record of Rhyacian sedimentation and metamorphism in the western border of the Sâ Francisco Craton. 2017, 79, 307-325 Geochemical characteristics of the La Rûnion mantle plume source inferred from olivine-hosted melt inclusions from the adventive cones of Piton de la Fournaise volcano (La Rûnion Island). 2017, 172, 1 Provenance of loess in the central Great Plains, U.S.A. based on Nd-Sr isotopic composition, and paleoenvironmental implications. 2017, 173, 114-123 Genesis and evolution of a Paleoproterozoic basement inlier within West Gondwana addressed by Sm-Nd isotopic geochemistry and Zr saturation thermometry. 2017, 80, 95-106 Petrogenesis of a Mesoproterozoic shoshonitic lamprophyre dyke from the Wajrakarur kimberlite field, eastern Dharwar craton, southern India: Geochemical and Sr-Nd isotopic evidence for a	2 12 8 9

582	Coherent Response of Antarctic Intermediate Water and Atlantic Meridional Overturning Circulation During the Last Deglaciation: Reconciling Contrasting Neodymium Isotope Reconstructions From the Tropical Atlantic. 2017 , 32, 1036-1053	16
581	Foraminiferal M d in the deep north-western subtropical Pacific Ocean: Tracing changes in weathering input over the last 30,000 years. 2017 , 470, 55-66	4
580	Transport and transformation of riverine neodymium isotope and rare earth element signatures in high latitude estuaries: A case study from the Laptev Sea. <i>Earth and Planetary Science Letters</i> , 2017 , 477, 205-217	19
579	The peraluminous Aurumina Granite Suite in central Brazil: An example of mantle-continental crust interaction in a Paleoproterozoic cordilleran hinterland setting?. 2017 , 299, 75-100	23
578	The early differentiation of Mars inferred from HfW chronometry. Earth and Planetary Science Letters, 2017, 474, 345-354	48
577	Link between Indian monsoon rainfall and physical erosion in the Himalayan system during the Holocene. 2017 , 18, 3452-3469	14
576	Distinct control mechanism of fine-grained sediments from Yellow River and Kyushu supply in the northern Okinawa Trough since the last glacial. 2017 , 18, 2949-2969	23
575	Hafnium and neodymium isotopes and REY distribution in the truly dissolved, nanoparticulate/colloidal and suspended loads of rivers in the Amazon Basin, Brazil. 2017 , 213, 383-399	23
574	Controls on modern erosion and the development of the Pearl River drainage in the late Paleogene. 2017 , 394, 52-68	34
573	Isotope geochronology, geochemistry, and mineral chemistry of the U-bearing and barren granites from the Zhuguangshan complex, South China: Implications for petrogenesis and uranium mineralization. 2017 , 91, 1040-1065	20
572	Short-term variability of dissolved rare earth elements and neodymium isotopes in the entire water column of the Panama Basin. <i>Earth and Planetary Science Letters</i> , 2017 , 475, 242-253	22
571	Impact of glacial activity on the weathering of Hf isotopes @bservations from Southwest Greenland. 2017 , 215, 295-316	11
570	Baddeleyite UPb age and geochemical data of the mafic dykes from South Qinling: Constraints on the lithospheric extension. 2017 , 52, 272-285	4
569	Global patterns of dust and bedrock nutrient supply to montane ecosystems. 2017 , 3, eaao1588	29
568	Reconstructing the Evolution of the Submarine Monterey Canyon System From Os, Nd, and Pb Isotopes in Hydrogenetic Fe-Mn Crusts. 2017 , 18, 3946-3963	4
567	TIMS analysis of neodymium isotopes in human tooth enamel using 1013 hamplifiers. 2017, 32, 2391-2400	8
566	Elemental and Sr-Nd isotopic geochemistry of Cretaceous to Early Paleogene granites and volcanic rocks in the Sikhote-Alin Orogenic Belt (Russian Far East): implications for the regional tectonic evolution. 2017 , 146, 383-401	26
565	Geochemical characteristics and petrogenesis of adakites in the Sikhote-Alin area, Russian Far East. 2017 , 145, 512-529	27

564	Crustal contamination versus an enriched mantle source for intracontinental mafic rocks: Insights from early Paleozoic mafic rocks of the South China Block. 2017 , 286-287, 388-395	18
563	Late Eocene E arly Oligocene two-mica granites in NW Turkey (the UludalMassif): Water-fluxed melting products of a mafic metagreywacke. 2017 , 268-271, 334-350	10
562	Geochemical and geochronological constraints on distinct Early-Neoproterozoic and Cambrian accretionary events along southern margin of the Baydrag Continent in western Mongolia. 2017 , 47, 200-227	44
561	Long-lasting Cadomian magmatic activity along an active northern Gondwana margin: UPb zircon and SrNd isotopic evidence from the Brunovistulian Domain, eastern Bohemian Massif. 2017, 106, 2109-2129	21
560	Isotopic and geochemical constraints on lead and fluid sources of the PbZnAg mineralization in the polymetallic Tighza-Jbel Aouam district (central Morocco), and relationships with the geodynamic context. 2017 , 127, 194-210	9
559	Alkaline-rich quartz syenite intrusions of the Western Karelia subprovince. 2017 , 449, 61-88	3
558	Origin of reverse compositional and textural zoning in granite plutons by localized thermal overturn of stratified magma chambers. 2017 , 277, 315-336	5
557	Calcium isotopic compositions of chondrites. 2017 , 201, 364-376	37
556	Age, geochemistry, and SrNdHfPb isotopes of the Caosiyao porphyry Mo deposit in Inner Mongolia, China. 2017 , 81, 706-727	31
555	The tectonomagmatic significance of Neoarchaean variably alkali-enriched gabbro and diorite intrusions of the western Karelia Province. 2017 , 449, 39-60	2
554	Glacial erosion dynamics in a small mountainous watershed (Southern French Alps): A source-to-sink approach. <i>Earth and Planetary Science Letters</i> , 2017 , 458, 366-379	11
553	Water mass circulation and weathering inputs in the Labrador Sea based on coupled HfMd isotope compositions and rare earth element distributions. 2017 , 199, 164-184	17
552	Early to late Yanshanian I-type granites in Fujian Province, SE China: Implications for the tectonic setting and Mo mineralization. 2017 , 137, 194-219	15
551	Genesis and Uranium Sources of Leucogranite-hosted Uranium Deposits in the Gaudeanmus Area, Central Damara Belt, Namibia: Study of Element and Nd Isotope Geochemistry. 2017 , 91, 2126-2137	3
550	Geochemical Constraints Provided by the Freetown Layered Complex (Sierra Leone) on the Origin of High-Ti Tholeiitic CAMP Magmas. 2017 , 58, 1811-1840	32
549	RbBr and 147SmB43Nd systematics of gabbro and dolerites from fragments of ophiolite complexes of the Middle Urals. 2017 , 477, 1270-1276	
548	Clay mineralogy, strontium and neodymium isotope ratios in the sediments of two High Arctic catchments (Svalbard). 2017 ,	
547	The Impact of Benthic Processes on Rare Earth Element and Neodymium Isotope Distributions in the Oceans. 2017 , 4,	39

Neodymium isotopes in the ocean model of the Community Earth System Model (CESM1.3). **2017**,

545	Hydrological variations of the intermediate water masses of the western Mediterranean Sea during the past 20 ka inferred from neodymium isotopic composition in foraminifera and cold-water corals. 2017 , 13, 17-37		20
544	Isotopic characterization and petrogenetic modeling of Early Cretaceous mafic diking Lithospheric extension in the North China craton, eastern Asia. 2017 , 129, 1379-1407		99
543	Geochemistry, geochronology, and SrNd isotopic compositions of Permian volcanic rocks in the northern margin of the North China Block: implications for the tectonic setting of the southeastern Central Asian Orogenic Belt. 2018 , 107, 2143-2161		8
542	Breakup of last glacial deep stratification in the South Pacific. 2018, 359, 900-904		43
541	Geochronology and geochemistry of the Carboniferous Ulann Tolgoi granite complex from northern Inner Mongolia, China: Petrogenesis and tectonic implications for the Uliastai continental margin. 2018 , 53, 2690-2709		4
540	The Kalkarindji Large Igneous Province, Australia: Petrogenesis of the Oldest and Most Compositionally Homogenous Province of the Phanerozoic. 2018 , 59, 635-665		3
539	Continental-scale transport of sediments by the Baltic Ice Stream elucidated by coupled grain size and Nd provenance analyses. <i>Earth and Planetary Science Letters</i> , 2018 , 490, 143-150	5.3	5
538	Formation of Late Archean High-180 Diorites through Partial Melting of Hydrated Metabasalts. 2018 , 59, 419-446		11
537	Riverine supply to the eastern Mediterranean during last interglacial sapropel S5 formation: A basin-wide perspective. 2018 , 485, 74-89		14
536	Petrogenesis of the late Early Cretaceous granodiorite Quartz diorite from eastern Guangdong, SE China: Implications for tectonothagmatic evolution and porphyry CuAuMo mineralization. 2018 , 304-307, 388-411		9
535	Did the circum-Rodinia subduction trigger the Neoproterozoic rifting along the CongoRalahari Craton margin?. 2018 , 107, 1859-1894		36
534	The Sm-Nd Method. 67-98		
533	No Change in Southern Ocean Circulation in the Indian Ocean From the Eocene Through Late Oligocene. 2018 , 33, 152-167		11
532	Circulation Changes in the Eastern Mediterranean Sea Over the Past 23,000 Years Inferred From Authigenic Nd Isotopic Ratios. 2018 , 33, 264-280		19
531	Isotopic systematics of He, Ar, S, Cu, Ni, Re, Os, Pb, U, Sm, Nd, Rb, Sr, Lu, and Hf in the rocks and ores of the Norilsk deposits. 2018 , 56, 46-64		5
530	Tracking Hadean processes in modern basalts with 142-Neodymium. <i>Earth and Planetary Science Letters</i> , 2018 , 484, 184-191	5.3	28
529	Linking Barbados Mineral Dust Aerosols to North African Sources Using Elemental Composition and Radiogenic Sr, Nd, and Pb Isotope Signatures. 2018 , 123, 1384-1400		23

528	SrNd isotopic geochemistry of Holocene sediments from the South Yellow Sea: Implications for provenance and monsoon variability. 2018 , 479, 102-112		16	
527	Geochemical fingerprints of glacially eroded bedrock from West Antarctica: Detrital thermochronology, radiogenic isotope systematics and trace element geochemistry in Late Holocene glacial-marine sediments. 2018 , 182, 204-232		21	
526	Petrogenesis and tectonic setting of Early Cretaceous granodioritic porphyry from the giant Rongna porphyry Cu deposit, central Tibet. 2018 , 161, 74-92		14	
525	Petrogenesis of Early Cretaceous intermediate-felsic dikes in the Jiaodong Peninsula, south-eastern North China Craton: Constraints from geochronology, geochemistry and Sr-Nd-Pb-Hf isotopes. 2018 , 60, 69-93		24	
524	Generation of syntectonic calc-alkaline, magnesian granites through remelting of pre-tectonic igneous sources IJ-Pb zircon ages and Sr, Nd and Pb isotope data from the Donkerhoek granite (southern Damara orogen, Namibia). 2018 , 310-311, 314-331		8	
523	Geochronology, Geochemistry and Sr-Nd-Pb-Hf Isotopes of No. I Complex from the Shitoukengde Niūu Sulfide Deposit in the Eastern Kunlun Orogen, Western China: Implications for the Magmatic Source, Geodynamic Setting and Genesis. 2018 , 92, 106-126		17	
522	182W and HSE constraints from 2.7 Ga komatiites on the heterogeneous nature of the Archean mantle. 2018 , 228, 1-26		30	
521	Early Jurassic mafic dykes from the Aigao uranium ore deposit in South China: Geochronology, petrogenesis and relationship with uranium mineralization. 2018 , 308-309, 118-133		11	
520	Field occurrences and Nd isotopic characteristics of the meta-mafic-ultramafic rocks from the Caozhuang Complex, eastern Hebei: Implications for early Archean crustal evolution of the North China Craton. 2018 , 310, 425-442		10	
519	UBb Age and HfNdBr Isotopic Systematics of Vein Rocks of the Volkovsky Massif, Middle Urals, Russia. 2018 , 56, 199-210		1	
518	Similar mid-depth Atlantic water mass provenance during the Last Glacial Maximum and Heinrich Stadial 1. <i>Earth and Planetary Science Letters</i> , 2018 , 490, 51-61	5.3	12	
517	Late Cretaceous arc igneous activity: the Efikar Monzogranite example. 2018 , 60, 382-400		17	
516	Geochronology, geochemistry and tectonic significance of the ore-associated granites at the Kaladawan FeMo ore field (Altyn), NW China. 2018 , 100, 457-470		8	
515	Geochronology, geochemistry, and tectonic significance of Permian intrusive rocks from the Shaolanghe region, northern margin of the North China Craton. 2018 , 53, 1061-1078		4	
514	Geochronology, geochemistry and Sr-Nd-Pb-Hf isotopes of the Early Jurassic granodiorite from the Sankuanggou intrusion, Heilongjiang Province, Northeastern China: Petrogenesis and geodynamic implications. 2018 , 296-299, 113-128		12	
513	Diverse lamprophyres origins corresponding to lithospheric thinning: a case study in the Jiurui district of Middle-Lower Yangtze River Belt, South China Craton. 2018 , 54, 62-80		11	
512	Characterization and origin of granites from the Luoyang Fe deposit, southwestern Fujian Province, South China. 2018 , 184, 119-135		9	
511	Origin of the Bashierxi monzogranite, Qiman Tagh, East Kunlun Orogen, NW China: A magmatic response to the evolution of the Proto-Tethys Ocean. 2018 , 296-299, 181-194		21	

510	Compositional characteristics and geodynamic significance of late Miocene volcanic rocks associated with the Chah Zard epithermal goldBilver deposit, southwest Yazd, Iran. 2018 , 27, e12223	5
509	Cambrian Drdovician magmatism of the Ikh-Mongol Arc System exemplified by the Khantaishir Magmatic Complex (Lake Zone, south Dentral Mongolia). 2018 , 54, 122-149	42
508	Failed Silurian continental rifting at the NW margin of Gondwana: evidence from basaltic volcanism of the Prague Basin (Tepl B arrandian Unit, Bohemian Massif). 2018 , 107, 1231-1266	12
507	Tectonic transition from a compressional to extensional metallogenic environment at ~120 Ma revealed in the Hushan gold deposit, Jiaodong, North China Craton. 2018 , 160, 408-425	26
506	Prehistoric heavy metal pollution on the continental shelf off Hainan Island, South China Sea: From natural to anthropogenic impacts around 4.0 kyr BP. 2018 , 28, 455-463	17
505	Neoarchean magmatism and implications for crustal growth and evolution of the Kuluketage region, northeastern Tarim Craton. 2018 , 304, 156-170	18
504	Lu-Hf ratios of crustal rocks and their bearing on zircon Hf isotope model ages: The effects of accessories. 2018 , 484, 179-190	23
503	Geochemistry of the Serifos calc-alkaline granodiorite pluton, Greece: constraining the crust and mantle contributions to I-type granitoids. 2018 , 107, 1657-1688	6
502	Bathyal records of enhanced silicate erosion and weathering on the exposed Luzon shelf during glacial lowstands and their significance for atmospheric CO2 sink. 2018 , 476, 302-315	17
501	Provenance and depositional environments of Quaternary sediments in the southern Kalahari Basin. 2018 , 476, 352-369	15
500	Geochronological and geochemical constraints on the genesis of the Huanren skarn Cu Z n deposit, northeast China. 2018 , 92, 366-378	5
499	Petrogenesis of Cretaceous volcanic-intrusive complex from the giant Yanbei tin deposit, South China: Implication for multiple magma sources, tin mineralization, and geodynamic setting. 2018 , 296-299, 163-180	17
498	Geochronology, geochemistry, and petrogenesis of the late Mesozoic Luoyang volcanics: Implications for the geodynamic evolution of the Zhejiang Eujian region, SE China. 2018 , 53, 1635-1655	1
497	Late Triassic intra-oceanic arc system within Neotethys: Evidence from cumulate appinite in the Gangdese belt, southern Tibet. 2018 , 10, 545-565	40
496	Utility of Nd isotope ratio as a tracer of marine animals: regional variation in coastal seas and causal factors. 2018 , 9, e02365	3
495	Major intensification of Atlantic overturning circulation at the onset of Paleogene greenhouse warmth. 2018 , 9, 4954	15
494	Nd and Sr Isotope Composition in the Tooth Enamel from FelMn Nodules of the Cape Basin (Atlantic Ocean): Age and Sources. 2018 , 56, 1209-1219	2
493	Multiproxy Isotopic and Geochemical Analysis of the Siwalik Sediments in NW India: Implication for the Late Cenozoic Tectonic Evolution of the Himalaya. 2018 , 38, 120	7

492	Continuous Holocene input of river sediment to the Indus Submarine Canyon. 2018, 406, 159-176	21
491	The Neodymium Isotope Fingerprint of Adlie Coast Bottom Water. 2018 , 45, 11,247	8
490	Role of dust fluxes in stimulating Ethmodiscus rex giant diatom blooms in the northwestern tropical Pacific during the Last Glacial Maximum. 2018 , 511, 319-331	4
489	High-resolution reconstruction of historical flood events in the Changjiang River catchment based on geochemical and biomarker records. 2018 , 499, 58-70	7
488	Rapid precipitation changes in the tropical West Pacific linked to North Atlantic climate forcing during the last deglaciation. 2018 , 197, 288-306	13
487	Petrogenesis of Mid-Eocene granites in South Sakhalin, Russian Far East: Juvenile crustal growth and comparison with granitic magmatism in Hokkaido and Sikhote-Alin. 2018 , 167, 103-129	9
486	Cretaceous-early Paleocene drainage shift of Amazonian rivers driven by Equatorial Atlantic Ocean opening and Andean uplift as deduced from the provenance of northern Peruvian sedimentary rocks (Huallaga basin). 2018 , 63, 152-168	20
485	Clay mineralogy, strontium and neodymium isotope ratios in the sediments of two High Arctic catchments (Svalbard). 2018 , 6, 141-161	2
484	New constraints on elemental and Pb and Nd isotope compositions of South American and Southern African aerosol sources to the South Atlantic Ocean. 2018 , 78, 372-384	10
483	Petrology and geochemistry of the Mesoproterozoic Vattikod lamproites, Eastern Dharwar Craton, southern India: evidence for multiple enrichment of sub-continental lithospheric mantle and links with amalgamation and break-up of the Columbia supercontinent. 2018 , 173, 1	16
482	Diagenetic overprint on authigenic Nd isotope records: A case study of the Bering Slope. <i>Earth and Planetary Science Letters</i> , 2018 , 498, 247-256	, 1
481	Middlellate Triassic bimodal intrusive rocks from the Tethyan Himalaya in South Tibet: Geochronology, petrogenesis and tectonic implications. 2018 , 318-319, 78-90	14
480	Caldera Life-Cycles of the Yellowstone Hotspot Track: Death and Rebirth of the Heise Caldera. 2018 , 59, 1643-1670	5
479	The Influence of Basaltic Islands on the Oceanic REE Distribution: A Case Study From the Tropical South Pacific. 2018 , 5,	18
478	TAG Plume: Revisiting the Hydrothermal Neodymium Contribution to Seawater. 2018, 5,	9
477	Rare Earth Elements Geochemistry and Nd Isotopes in the Mississippi River and Gulf of Mexico Mixing Zone. 2018 , 5,	14
476	Neoarchean convergent margin Ni-Cu mineralization? Axis Lake and Nickel King Ni-Cu deposits in the south Rae craton of the Canadian Shield. 2018 , 316, 305-323	3
475	First Evidence of the Archean Age of Orogenic Gold of the Russian Part of the Karelian Craton (Fennoscandian Shield): SmNd Mineral Isochron for Gold-Bearing Metasomatites of the Novye Peski Deposit. 2018 , 480, 804-809	

474	Tracing the provenance of aeolian loess in the Yangtze River Delta through zircon UPb age and geochemical investigations. 2018 , 15, 708-721	6
473	Geochemical provenance of sediments from the northern East China Sea document a gradual migration of the Asian Monsoon belt over the past 400,000 years. 2018 , 190, 161-175	9
472	Radiogenic isotope (Nd, Pb, Sr) signatures of surface and sea ice-transported sediments from the Arctic Ocean under the present interglacial conditions. 2018 , 37, 1442982	14
471	Precipitation and subsequent preservation of hydrothermal Fe-Mn oxides in distal plume sediments on Juan de Fuca Ridge. 2018 , 187, 128-140	6
470	Geochronology, geochemistry and Nd⊞f isotopes of the Xiaokouzi granite from the Helanshan complex: Constraints on the Paleoproterozoic evolution of the Khondalite Belt, North China Craton. 2018 , 317, 57-76	11
469	Antarctic Intermediate Water penetration into the Northern Indian Ocean during the last deglaciation. <i>Earth and Planetary Science Letters</i> , 2018 , 500, 67-75	15
468	Geochemical Evidence for Large-Scale Drainage Reorganization in Northwest Africa During the Cretaceous. 2018 , 19, 1690-1712	8
467	The vanadium isotopic composition of L ordinary chondrites. 2018 , 37, 501-508	6
466	Petrogenetic evolution of the Eocene granitoids in eastern part of the Tavant—Zone in northwestern Anatolia, Turkey. 2018 , 314-315, 236-259	3
465	Responses of the East Asian Summer Monsoon in the Low-Latitude South China Sea to High-Latitude Millennial-Scale Climatic Changes During the Last Glaciation: Evidence From a High-Resolution Clay Mineralogical Record. 2018 , 33, 745-765	22
464	Geochemistry and geochronology of Mississippian volcanic rocks from SW Mongolia: Implications for terrane subdivision and magmatic arc activity in the Trans-Altai Zone. 2018 , 164, 322-343	5
463	Extensional tectonics during Late Cretaceous evolution of the Southern Central Andes: Evidence from the Chilean main range at ~35°S. 2018 , 744, 93-117	19
462	Multiple sources of Cretaceous granitoids in northeastern Fujian, coastal area of southeastern China. 2019 , 182, 103939	8
461	Arc-Related Pyroxenites Derived from a Long-Lived Neoarchean Subduction System at the Southwestern Margin of the Cuddapah Basin: Geodynamic Implications for the Evolution of the Eastern Dharwar Craton, Southern India. 2019 , 127, 567-591	3
460	Hydrothermal Alteration of Eudialyte-Hosted Critical Metal Deposits: Fluid Source and Implications for Deposit Grade. 2019 , 9, 422	7
459	Changes in Indian Summer Monsoon Using Neodymium (Nd) Isotopes in the Andaman Sea During the Last 24,000 years. 2019 , 3, 241-253	7
458	Geochemistry, in-situ Sr-Nd-Hf-O isotopes, and mineralogical constraints on origin and magmatic-hydrothermal evolution of the Yulong porphyry Cu Mo deposit, Eastern Tibet. 2019 , 76, 98-114	13
457	Late Eocene onset of the Proto-Antarctic Circumpolar Current. 2019 , 9, 10125	13

456	Enhanced surface melting of the Fennoscandian Ice Sheet during periods of North Atlantic cooling. 2019 , 47, 664-668	17
455	Tectonic evolution of the southwestern margin of Pangea and its global implications: Evidence from the mid Permian riassic magmatism along the Chilean-Argentine border. 2019 , 76, 303-321	14
454	In situ trace element and Sm-Nd isotope analysis of accessory minerals in an Eoarchean tonalitic gneiss from Greenland: Implications for Hf and Nd isotope decoupling in Earth's ancient rocks. 2019 , 524, 394-405	32
453	Petrogenesis and metallogenic implications of volcanic rocks from the Lawu basin, eastern Tibet: Insights into the intracontinental Eocene-Oligocene porphyry copper systems. 2019 , 111, 103001	7
452	Evolution of Antarctic Intermediate Water during the Plio-Pleistocene and implications for global climate: Evidence from the South Atlantic. 2019 , 223, 105945	2
45 ¹	Diversity of igneous rocks from the Isachsen Dome, Ellef Ringnes Island, Canadian High Arctic. 2019 , 5, 71-87	
450	Competing droughts affect dust delivery to Sierra Nevada. 2019 , 41, 100545	9
449	A geochemical approach to reconstruct modern dust fluxes and sources to the South Pacific. 2019 , 264, 205-223	12
448	A new view on the genesis of the Chiweigou gold deposit, Jilin, China: A carbonatite-type deposit. 2019 , 113, 103086	1
447	Characteristics and provenances of rare earth elements in the atmospheric particles of a coastal city with large-scale optoelectronic industries. 2019 , 214, 116836	5
446	Luenha picrites, Central Mozambique lMessengers from a mantle plume source of Karoo continental flood basalts?. 2019 , 346-347, 105152	4
445	Depositional History and Indian Summer Monsoon Controls on the Silicate Weathering of Sediment Transported to the Eastern Arabian Sea: Geochemical Records From IODP Site U1456 Since 3.8 Ma. 2019 , 20, 4336-4353	8
444	New insights into Paleoproterozoic tectonics of the Yangtze Block in the context of early Nuna assembly: Possible collisional granitic magmatism in the Zhongxiang Complex, South China. 2019 , 334, 105452	9
443	Miocene restriction of the Pacific-North Atlantic throughflow strengthened Atlantic overturning circulation. 2019 , 10, 4025	12
442	The Early Eocene Ekmek[]granodiorite porphyry in the Karacabey region(Sakarya Zone, NW Turkey). 2019 , 28, 589-602	1
441	Interaction between oceanic slab and metasomatized mantle wedge: Constraints from sodic lavas from the Qilian Orogen, NW China. 2019 , 348-349, 105182	3
440	Long-term evolution of terrestrial inputs from the Ediacaran to early Cambrian: Clues from Nd isotopes in shallow-marine carbonates, South China. 2019 , 535, 109367	15
439	Source-to-sink processes of fluvial sediments in the northern South China Sea: Constraints from river sediments in the coastal region of South China. 2019 , 185, 104020	10

The History, Relevance, and Applications of the Periodic System in Geochemistry. **2019**, 111

437	Origin and significance of Early Miocene high-potassium I-type granite plutonism in the East Anatolian plateau (the TalFay intrusion). 2019 , 348-349, 105210	5
436	A 16-kyr Record of Ocean Circulation and Monsoon Intensification From the Central Bay of Bengal. 2019 , 20, 872-882	5
435	Neodymium concentration and isotopic composition distributions in the southwestern Indian Ocean and the Indian sector of the Southern Ocean. 2019 , 511, 190-203	12
434	Variations in trace metal concentrations and Sr, Nd isotopic compositions in sediments from two contrasting settings in the Eastern Arabian Shelf: Implications for provenance and paleoclimate reconstruction. 2019 , 509, 134-151	3
433	Chemical weathering of mafic rocks in boreal subarctic environment (northwest Russia) under influence of glacial moraine deposits. 2019 , 509, 115-133	3
432	Platinum-Group Element Geochemistry of the Escondida Igneous Suites, Northern Chile: Implications for Ore Formation. 2019 , 60, 487-514	16
431	Protoliths and tectonic implications of the newly discovered Triassic Baqing eclogites, central Tibet: Evidence from geochemistry, Sr Nd isotopes and geochronology. 2019 , 69, 144-162	7
430	Contrasting isotopic sources (Sm-Nd) of Late Ediacaran series in the Iberian Massif: Implications for the Central Iberian-Ossa Morena boundary. 2019 , 324, 194-207	13
429	Evaluation of neodymium isotope analysis of human dental enamel as a provenance indicator using 10 hmplifiers (TIMS). 2019 , 59, 322-331	4
428	REEs and Sr-Nd isotope variations in a 20 ky-sediment core from the middle Okinawa Trough, East China Sea: An in-depth provenance analysis of siliciclastic components. 2019 , 415, 105970	9
427	Early Paleozoic magmatism and metallogeny related to Proto-Tethys subduction: Insights from volcanic rocks in the northeastern Altyn Mountains, NW China. 2019 , 75, 134-153	9
426	Holocene Changes in Deep Water Circulation Inferred From Authigenic Nd and Hf Isotopes in Sediment Records From the Chukchi-Alaskan and Canadian Beaufort Margins. 2019 , 34, 1038-1056	6
425	Mineralogical and isotopic evidence for the sediment provenance of the western South Yellow Sea since MIS 3 and implications for paleoenvironmental evolution. 2019 , 414, 103-117	6
424	Middle Miocene magmatic activity in the Sophia Basin, Arctic Ocean@vidence from dredged basalt at the flanks of Mosby Seamount. 2019 , 5, 31-48	1
423	Petrogenesis and tectonic implications of Early Cretaceous shoshonitic syenites in the northern Wuyi Mt Range, Southeast China. 2019 , 180, 103877	6
422	Geodynamic transition from subduction to extension: evidence from the geochronology and geochemistry of granitoids in the Sangsang area, southern Lhasa Terrane, Tibet. 2019 , 108, 1663-1681	4
421	History of Yellow River and Yangtze River delivering sediment to the Yellow Sea since 3.5 Ma: Tectonic or climate forcing?. 2019 , 216, 74-88	25

420	Relict subduction initiation along a passive margin in the northwest Indian Ocean. 2019 , 10, 2248	17
419	Provenance of the Neogene sediments from the Solimps Formation (Solimps and Acre Basins), Brazil. 2019 , 93, 232-241	8
418	Controls on the geochemistry of suspended sediments from large tropical South American rivers (Amazon, Orinoco and Maroni). 2019 , 522, 38-54	19
417	Strontium and Neodymium Isotopes. 2019 , 89-132	
416	Modeling Neodymium Isotopes in the Ocean Component of the Community Earth System Model (CESM1). 2019 , 11, 624-640	9
415	Records of Holocene climatic fluctuations and anthropogenic lead input in elemental distribution and radiogenic isotopes (Nd and Pb) in sediments of the Gulf of Lions (Southern France). 2019 , 29, 1292-1304	1
414	Staged fine-grained sediment supply from the Himalayas to the Bengal Fan in response to climate change over the past 50,000 years. 2019 , 212, 164-177	14
413	Heterogeneous lithospheric mantle beneath the southeastern Tibetan Plateau: Evidence from Cenozoic high-Mg potassic volcanic rocks in the JinshajiangAilaoshan Cenozoic magmatic belt. 2019 , 180, 103849	9
412	Twenty million years of post-orogenic fluid production and hydrothermal mineralization across the external Araliaôorogen and adjacent Sâ Francisco craton, SE Brazil. 2019 , 342-343, 557-572	16
411	Determination of the geographical origin of marine mussels (Mytilus spp.) using Nd/Nd ratios. 2019 , 148, 12-18	8
410	Holocene shifts in sub-surface water circulation of the North-East Atlantic inferred from Nd isotopic composition in cold-water corals. 2019 , 410, 135-145	4
409	REE distribution and Nd isotope composition of estuarine waters and bulk sediment leachates tracing lithogenic inputs in eastern Canada. 2019 , 211, 117-130	17
408	Genesis of the Singhbhum Craton, eastern India; implications for Archean crust-mantle evolution of the Earth. 2019 , 512, 85-106	59
407	The evolution and control of detrital sediment provenance in the middle and northern Okinawa Trough since the last deglaciation: Evidence from Sr and Nd isotopes. 2019 , 522, 1-11	3
406	Ice-sheet driven weathering input and water mass mixing in the Nordic Seas during the last 25,000 years. <i>Earth and Planetary Science Letters</i> , 2019 , 514, 108-118	6
405	Recognizing metasedimentary sequences potentially hosting concealed massive sulfide accumulations in the Iberian Pyrite Belt using geochemical fingerprints. 2019 , 107, 973-998	5
404	New evidence on the provenance of Red Lustrous Wheel-made Ware (RLW): Petrographic, elemental and Sr-Nd isotope analysis. 2019 , 24, 412-433	4
403	Natural Titanite Reference Materials for In Situ U-Pb and Sm-Nd Isotopic Measurements by LA-(MC)-ICP-MS. 2019 , 43, 355-384	19

402	Deep Atlantic Ocean carbon storage and the rise of 100,000-year glacial cycles. 2019 , 12, 355-360	31
401	Generation of Archaean TTG Gneisses Through Amphibole-Dominated Fractionation. 2019 , 124, 3605-3619	24
400	Millennial-scale variations of the Holocene North Atlantic mid-depth gyre inferred from radiocarbon and neodymium isotopes in cold water corals. 2019 , 211, 93-106	5
399	Pre-concentration of thorium and neodymium isotopes using Nobias chelating resin: Method development and application to chromatographic separation. 2019 , 202, 600-609	7
398	Geochemical and isotope evidence for mantle-derived source rock of high-K calc-alkaline I-type granites, PernambucoAlagoas Domain, northeastern Brazil. 2019 , 108, 1095-1120	7
397	The rise of the Brunovistulicum: age, geological, petrological and geochemical character of the Neoproterozoic magmatic rocks of the Central Basic Belt of the Brno Massif. 2019 , 108, 1165-1199	17
396	Sources and petrogenesis of Late Triassic Zhiduo volcanics in the northeast Tibet: Implications for tectonic evolution of the western Jinsha Paleo-Tethys Ocean. 2019 , 336-337, 169-182	6
395	The Effect of Melt Infiltration on Metagranitic Rocks: the Snieznik Dome, Bohemian Massif. 2019 , 60, 591-618	10
394	Simulating the Occurrence of the Last Sapropel Event (S1): Mediterranean Basin Ocean Dynamics Simulations Using Nd Isotopic Composition Modeling. 2019 , 34, 237-251	16
393	The Qiman Tagh Orogen as a Window to the Crustal Evolution in Northern Qinghai-Tibet Plateau. 2019 , 1-41	
392	Divergent Mediterranean seawater circulation during Holocene sapropel formation Reconstructed using Nd isotopes in fish debris and foraminifera. Earth and Planetary Science Letters , 2019, 511, 141-153	12
392 391	Divergent Mediterranean seawater circulation during Holocene sapropel formation Reconstructed using Nd isotopes in fish debris and foraminifera. Earth and Planetary Science Letters 5.3	12
	Divergent Mediterranean seawater circulation during Holocene sapropel formation Reconstructed using Nd isotopes in fish debris and foraminifera. Earth and Planetary Science Letters , 2019, 511, 141-153 Glacial-interglacial Nd isotope variability of North Atlantic Deep Water modulated by North	
391	Divergent Mediterranean seawater circulation during Holocene sapropel formation Reconstructed using Nd isotopes in fish debris and foraminifera. Earth and Planetary Science Letters, 2019, 511, 141-153 Glacial-interglacial Nd isotope variability of North Atlantic Deep Water modulated by North American ice sheet. 2019, 10, 5773 Origin of Pumice in Sediments from the Middle Okinawa Trough: Constraints from Whole-Rock	24
391 390	Divergent Mediterranean seawater circulation during Holocene sapropel formation [1] Reconstructed using Nd isotopes in fish debris and foraminifera. Earth and Planetary Science Letters , 2019, 511, 141-153 Glacial-interglacial Nd isotope variability of North Atlantic Deep Water modulated by North American ice sheet. 2019, 10, 5773 Origin of Pumice in Sediments from the Middle Okinawa Trough: Constraints from Whole-Rock Geochemical Compositions and Sr-Nd-Pb Isotopes. 2019, 7, 462 Late Pliocene and Early Pleistocene Variability of the REE and Nd Isotope Composition of Caribbean Bottom Water: A Record of Changes in Sea Level and Terrestrial Inputs During the Final	1
391 390 389	Divergent Mediterranean seawater circulation during Holocene sapropel formation [] Reconstructed using Nd isotopes in fish debris and foraminifera. Earth and Planetary Science Letters , 2019, 511, 141-153 Glacial-interglacial Nd isotope variability of North Atlantic Deep Water modulated by North American ice sheet. 2019, 10, 5773 Origin of Pumice in Sediments from the Middle Okinawa Trough: Constraints from Whole-Rock Geochemical Compositions and Sr-Nd-Pb Isotopes. 2019, 7, 462 Late Pliocene and Early Pleistocene Variability of the REE and Nd Isotope Composition of Caribbean Bottom Water: A Record of Changes in Sea Level and Terrestrial Inputs During the Final Stages of Central American Seaway Closure. 2019, 34, 2067-2079 Distribution and provenance implication of rare earth elements and Sr-Nd isotopes in surface	24
391 390 389 388	Divergent Mediterranean seawater circulation during Holocene sapropel formation II Reconstructed using Nd isotopes in fish debris and foraminifera. Earth and Planetary Science Letters , 2019, 511, 141-153 Glacial-interglacial Nd isotope variability of North Atlantic Deep Water modulated by North American ice sheet. 2019, 10, 5773 Origin of Pumice in Sediments from the Middle Okinawa Trough: Constraints from Whole-Rock Geochemical Compositions and Sr-Nd-Pb Isotopes. 2019, 7, 462 Late Pliocene and Early Pleistocene Variability of the REE and Nd Isotope Composition of Caribbean Bottom Water: A Record of Changes in Sea Level and Terrestrial Inputs During the Final Stages of Central American Seaway Closure. 2019, 34, 2067-2079 Distribution and provenance implication of rare earth elements and Sr-Nd isotopes in surface sediments of Jiulong River, Southeast China. 2019, 19, 1499-1510 Geochronology, geochemistry, and SrNdHif isotopic compositions of maficilltramafic intrusions in the Niubiziliang Ni(Cu) sulfide deposit, North Qaidam Orogenic Belt, NW China: Implications for	24 1 2 3

384	Limited influence of basalt weathering inputs on the seawater neodymium isotope composition of the northern Iceland Basin. 2019 , 511, 358-370	3
383	Heterogeneous Oceanic Arc Volcanic Rocks in the South Qilian Accretionary Belt (Qilian Orogen, NW China). 2019 , 60, 85-116	24
382	The Neoproterozoic B lood Falls[in Tarim Craton and Their Possible Connection With Snowball Earth. 2019 , 124, 229-244	4
381	U-Pb geochronology, bulk-rock geochemistry and petrology of Late Cretaceous syenitic plutons in the Glky (Ordu) area (NE Turkey): Implications for magma generation in a continental arc extension triggered by slab roll-back. 2019 , 171, 305-320	9
380	Evaluating the effect of leaching on trace element and Nd-Pb isotopic systematics in continental basalts. 2019 , 4, 1-11	O
379	Nd isotope composition of seep carbonates: Towards a new approach for constraining subseafloor fluid circulation at hydrocarbon seeps. 2019 , 503, 40-51	12
378	Geochronology and geochemistry of the Dasuji Mo deposit in the northern margin of the North China Block: Implications for ore genesis and tectonic setting. 2019 , 104, 101-113	5
377	Dating agpaitic rocks: A multi-system (U/Pb, Sm/Nd, Rb/Sr and 40Ar/39Ar) isotopic study of layered nepheline syenites from the Ilmaussaq complex, Greenland. 2019 , 324-325, 74-88	10
376	Reassessing the origin and chronology of the unique achondrite Asuka 881394: Implications for distribution of 26Al in the early Solar System. 2019 , 244, 478-501	9
375	Water mass transformation in the Barents Sea inferred from radiogenic neodymium isotopes, rare earth elements and stable oxygen isotopes. 2019 , 511, 416-430	12
374	Quaternary sedimentary record in the northern Okinawa Trough indicates the tectonic control on depositional environment change. 2019 , 516, 126-138	5
373	The distribution of neodymium isotopes and concentrations in the eastern tropical North Atlantic. 2019 , 511, 265-278	9
372	The Thickness of the Mantle Lithosphere and Collision-Related Volcanism in the Lesser Caucasus. 2019 , 60, 199-230	13
371	Late Eocene granites in the Central Sakhalin Island (Russian Far East) and its implication for evolution of the Sakhalin-Hokkaido orogenic belt. 2019 , 324-325, 684-698	5
370	Petrogenesis and Tectonic Implications of the Yuhuashan A-Type Volcanic-Intrusive Complex and Mafic Microgranular Enclaves in the Gan-Hang Volcanic Belt, Southeast China. 2019 , 127, 37-59	3
369	Evolution of ca. 2.5 Ga Dongargarh volcano-sedimentary Supergroup, Bastar craton, Central India: Constraints from zircon U-Pb geochronology, bulk-rock geochemistry and Hf-Nd isotope systematics. 2019 , 190, 273-309	18
368	Intraplate extension of the Indochina plate deduced from 26 to 24 Ma A-type granites and tectonic implications. 2019 , 61, 1691-1705	3
367	Geochemistry of metamorphosed volcanic rocks in the Neoarchean Qingyuan greenstone belt, North China Craton: Implications for geodynamic evolution and VMS mineralization. 2019 , 326, 196-221	11

366	Detrital SrNd isotopes, sediment provenances and depositional processes in the Laxmi Basin of the Arabian Sea during the last 800 ka. 2020 , 157, 895-907	9
365	A new report of the early Palaeozoic hornblendite in South China and its tectonic significance. 2020 , 55, 210-222	О
364	First data on U-Pb age of mafic dyke in the Mirny Station area (Pravdy Coast, East Antarctica). 2020 , 80, 125480	1
363	Eocene tonalitegranodiorite from the Havza (Samsun) area, northern Turkey: adakite-like melts of lithospheric mantle and crust generated in a post-collisional setting. 2020 , 62, 1131-1158	6
362	Crustal thickening prior to 43 Ma in the Himalaya: Evidence from lower crust-derived adakitic magmatism in Dala, eastern Tethyan Himalaya, Tibet. 2020 , 55, 4021-4046	5
361	The multiple depleted mantle components in the Hawaiian-Emperor chain. 2020 , 532, 119324	7
360	Late Jurassic to Early Cretaceous magmatism in the XiongBrshan gold district, central China: implications for gold mineralization and geodynamics. 2020 , 157, 435-457	4
359	Silicic volcanism triggered by increased denudation rates in the Quaternary Andean arc of central Chile between 33°50?-34°30?S. 2020 , 354-355, 105242	1
358	Late Cambrian Œarly Ordovician magmatism in the Sierra de Pie de Palo, Sierras Pampeanas (Argentina): implications for the early evolution of the proto-Andean margin of Gondwana. 2020 , 157, 321-339	1
357	Petrogenesis and tectonic implications of 2.45 Ga potassic A-type granite in the Daqingshan area, Yinshan Block, North China Craton. 2020 , 336, 105435	10
356	The application of Neodymium isotope as a chronostratigraphic tool in North Pacific sediments. 2020 , 157, 768-776	2
355	Atmospheric contribution to cations cycling in highly weathered catchment, Guadeloupe (Lesser Antilles). 2020 , 531, 119354	3
354	Balancing Rare Earth Element distributions in the Northwestern Mediterranean Sea. 2020 , 532, 119372	10
353	Neodymium isotopes track sources of rare earth elements in acidic mine waters. 2020 , 269, 465-483	8
352	Tectonomagmatic evolution of the Sveconorwegian orogen recorded in the chemical and isotopic compositions of 1070 M20 Ma granitoids. 2020 , 340, 105527	8
351	Eocene arc petrogenesis in Central Chile (c. 33.6° S) and implications for the Late Cretaceous Miocene Andean setting: tracking the evolving tectonic regime. 2020 , 177, 258-275	1
350	The changing Patagonian landscape: Erosion and westward sediment transfer paths in northern Patagonia during the Middle and Late Pleistocene. 2020 , 32, 1035-1053	3
349	Fluid and ore sources of the tungsten mineralisation in the Yangbishan ironEungsten deposit, Heilongjiang Province, North-eastern China: Constraints from fluid inclusions, sulphide SPb isotopes and scheelite CHDBmNd isotopes. 2020 , 55, 3957-3976	O

348	Uranium isotopic constraints on the nature of the prehistoric flood at the Lajia site, China. 2020, 48, 15-18	3
347	The effects of mafic-felsic magma interaction on magma diversity: insights from an early Paleozoic hornblendite-quartz monzonite suite in the South China block. 2020 , 114, 71-90	2
346	Development of a protocol to obtain the composition of terrigenous detritus in marine sediments -a pilot study from International Ocean Discovery Program Expedition 361. 2020 , 535, 119449	3
345	Linking Danube River activity to Alpine Ice-Sheet fluctuations during the last glacial (ca. 33¶7 ka BP): Insights into the continental signature of Heinrich Stadials. 2020 , 229, 106136	17
344	Geochronology, geochemistry, and SrNdHfD isotopes of the Zhongqiuyang rhyolitic tuff in eastern Guangdong, SE China: Constraints on petrogenesis and tectonic setting. 2020 , 55, 5082-5100	6
343	Geochemical and isotopic (Sm Nd) provenance of Ediacaran-Cambrian metasedimentary series from the Iberian Massif. Paleoreconstruction of the North Gondwana margin. 2020 , 201, 103079	12
342	Tracing subduction zone fluids with distinct Mg isotope compositions: Insights from high-pressure metasomatic rocks (leucophyllites) from the Eastern Alps. 2020 , 271, 154-178	8
341	Geochemistry of the Middle Jurassic sediments in Gfhflane, north-eastern Turkey: Implications for weathering and provenance. 2020 , 55, 4954-4976	6
340	Control of seasonal and inter-annual rainfall distribution on the Strontium-Neodymium isotopic compositions of suspended particulate matter and implications for tracing ENSO events in the Pacific coast (Tumbes basin, Peru). 2020 , 185, 103080	3
339	In situ U-Pb geochronology, Lu-Hf and Sm-Nd isotope systematics of the Hoidas Lake REE deposit, northern Saskatchewan, Canada. 2020 , 339, 105591	Ο
338	Controls on the provenance of late Eocene to Quaternary Mozambique Channel shales (DSDP 25 Site 242). 2020 , 421, 106090	2
337	Modern-style tectonic cycle in earliest Proterozoic time: Petrogenesis of dioritic-granitic rocks from the Daqingshan Wulashan Terrane, southern Yinshan Block, North China Craton. 2020 , 352-353, 105322	2
336	The tectonic evolution of the East Kunlun Orogen, northern Tibetan Plateau: A critical review with an integrated geodynamic model. 2020 , 191, 104168	18
335	Tracing water mass mixing and continental inputs in the southeastern Atlantic Ocean with dissolved neodymium isotopes. <i>Earth and Planetary Science Letters</i> , 2020 , 530, 115944	13
334	Characteristics and provenance implications of rare earth elements and SrNd isotopes in PM2.5 aerosols and PM2.5 fugitive dusts from an inland city of southeastern China. 2020 , 220, 117069	7
333	Provenance of loess deposits and stepwise expansion of the desert environment in NE China since ~1.2 Ma: Evidence from Nd-Sr isotopic composition and grain-size record. 2020 , 185, 103087	5
332	Cretaceous granitic magmatism and mineralization in the Shanhu W-Sn ore deposit in the Nanling Range in South China. 2020 , 126, 103758	6
331	Crust-mantle interaction during syn-collisional magmatism Œvidence from the Oamikaub diorite and Neikhoes metagabbro (Damara orogen, Namibia). 2020 , 351, 105955	4

330	Petrogenesis of early syn-tectonic monzonite-granodiorite complexes ©rustal reprocessing versus crustal growth. 2020 , 351, 105957	2
329	Isotopic mapping reveals the location of crustal fragments along a long-lived convergent plate boundary. 2020 , 372-373, 105687	1
328	ParticleBeawater Interaction of Neodymium in the North Atlantic. 2020, 4, 1700-1717	6
327	'Alexandrian' glass confirmed by hafnium isotopes. 2020 , 10, 11322	14
326	The Flux and Provenance of Dust Delivered to the SW Pacific During the Last Glacial Maximum. 2020 , 35, e2020PA003869	3
325	A circumpolar dust conveyor in the glacial Southern Ocean. 2020 , 11, 5655	9
324	Influence of Elevated Nd Fluxes on the Northern Nd Isotope End Member of the Atlantic During the Early Holocene. 2020 , 35, e2020PA003973	6
323	From subduction initiation to arcpolarity reversal: Life cycle of an Archean subduction zone from the Zunhua ophiolitic mlange, North China Craton. 2020 , 350, 105868	12
322	Late Neoproterozoic (Lambrian magmatism in Dronning Maud Land (East Antarctica): UPb zircon geochronology, isotope geochemistry and implications for Gondwana assembly. 2020 , 350, 105880	4
321	ca. 2.1 Ga Mahakoshal Supracrustal Belt: An allochthonous terrain in Central India Tectonic Zone. 2020 , 374-375, 105705	4
320	Ultra-depleted 2.05 Ga komatiites of Finnish Lapland: Products of grainy late accretion or core-mantle interaction?. 2020 , 554, 119801	13
319	Provenance of northwestern Patagonian river sediments (44월8°S): A critical evaluation of mineralogical, geochemical and isotopic tracers. 2020 , 408, 105744	2
318	Increasing terrigenous sediment supply from Taiwan to the southern Okinawa Trough over the last 3000 years evidenced by SrNd isotopes and geochemistry. 2020 , 406, 105725	4
317	Clay minerals, Sr-Nd isotopes and provenance of sediments in the northwestern South China Sea. 2020 , 202, 104531	1
316	New geochemical and Sr-Nd-Pb isotope evidence for FOZO and Azores plume components in the sources of DSDP Holes 559 and 561 MORBs. 2020 , 557, 119858	2
315	Multiphase Late Devonian to Carboniferous volcanic events in the west of Oyu Tolgoi, southeastern Mongolia: New geochronological, geochemical, and isotopic constraints on tectonic history. 2020 , 88, 169-184	2
314	The role of melting on the geochemical evolution and isotopic variability of an anatectic complex in the Iberian Variscides. 2020 , 378-379, 105769	2
313	SrNd isotopes indicating the provenance of siliciclastic sediments and paleoenvironmental changes in the middle Okinawa Trough during the last deglaciation. 2020 , 210, 104277	1

(2020-2020)

312	Fluid expulsion system and tectonic architecture of the incipient Cascadia convergent margin as revealed by Nd, Sr and stable isotope composition of mid-Eocene methane seep carbonates. 2020 , 558, 119872	7	7
311	Intermediate and deep ocean current circulation in the Mozambique Channel: New insights from ferromanganese crust Nd isotopes. 2020 , 430, 106356	3	3
310	Variations in eastern Mediterranean hydrology during the last climatic cycle as inferred from neodymium isotopes in foraminifera. 2020 , 237, 106306	5	5
309	Late Mio-Pliocene landscape evolution around the Chaka Basin in the NE Tibetan Plateau: Insights from geochemical perspectives. 2020 , 552, 109778	2	2
308	Genesis of the graphite orbicules in the Huangyangshan graphite deposit, Xinjiang, China: Evidence from geochemical, isotopic and fluid inclusion data. 2020 , 122, 103505	2	2
307	Neodymium isotope constraints on chemical weathering and past glacial activity in Svalbard. <i>Earth and Planetary Science Letters</i> , 2020 , 542, 116319	; 8	3
306	Primary or secondary? A dichotomy of the strontium isotope anomalies in the Ediacaran carbonates of Saudi Arabia. 2020 , 343, 105720	1	14
305	Ultrapotassic magmatism in the heyday of the Variscan Orogeny: the story of the TBbPluton, the largest durbachitic body in the Bohemian Massif. 2020 , 109, 1767-1810	1	15
304	Climate-Driven Weathering Shifts Between Highlands and Floodplains. 2020 , 21, e2020GC008936	7	7
303	Water mass mixing versus local weathering inputs along the Bay of Biscay: Evidence from dissolved hafnium and neodymium isotopes. 2020 , 224, 103844	1	[
302	Rare earth elements and Nd isotopes as tracers of modern ocean circulation in the central Mediterranean Sea. 2020 , 185, 102340	3	3
301	Imprints of ancient recycled oceanic lithosphere in heterogeneous Indian Ocean mantle: Evidence from petrogenesis of Carlsberg ridge basalts from Northwest Indian Ocean. 2020 , 86, 60-82	ϵ	5
300	Geochronology, petrogenesis and oxidation state of the Wenyu igneous suite in the Xiaoqinling district, North China Craton: Implications for lithospheric thinning and magma fertility. 2020 , 370-371, 105646	2	2
299	Early Cretaceous Wulong intermediate-mafic dike swarms in the Liaodong Peninsula: Implications for rapid lithospheric delamination of the North China Craton. 2020 , 362-363, 105473	Ş)
298	Significant 🛮 4/40Ca variations between carbonate- and clay-rich marine sediments from the Lesser Antilles forearc and implications for mantle heterogeneity. 2020 , 276, 239-257	ϵ	ś
297	Evolution of the Global Overturning Circulation since the Last Glacial Maximum based on marine authigenic neodymium isotopes. 2020 , 241, 106396	2	20
296	Oxygen-Hafnium-Neodymium Isotope Constraints on the Origin of the Talnakh Ultramafic-Mafic Intrusion (Norilsk Province, Russia). 2020 , 115, 1195-1212	4	1
295	The nature of subduction system in the Neoarchean: Magmatic records from the northern Yangtze Craton, South China. 2020 , 347, 105834	7	7

294	Geochemical and Nd isotopic signature of felsic volcanic rocks as a proxy of volcanic-hosted massive sulphide deposits in the Iberian Pyrite Belt (SW, Spain): The Paymogo Volcano-Sedimentary Alignment. 2020 , 120, 103408	5
293	Mineralogy and geochemistry of the Morro dos Seis Lagos siderite carbonatite, Amazonas, Brazil. 2020 , 360-361, 105433	4
292	The Sources and Transport Dynamics of Eolian Sediments in the NE Tibetan Plateau Since 6.7 Ma. 2020 , 21, e2019GC008682	0
291	Climate swings in the northern Red Sea over the last 150,000 years from Nd and Mg/Ca of marine sediments. 2020 , 231, 106205	4
29 0	Crustmantle interaction during subduction zone processes: Insight from late Mesozoic I-type granites in eastern Guangdong, SE China. 2020 , 192, 104284	7
289	Sr and Nd isotopes of cold seep carbonates from the northern South China sea as proxies for fluid sources. 2020 , 115, 104284	5
288	Generation of a potassic to ultrapotassic alkaline complex in a syn-collisional setting through flat subduction: Constraints on magma sources and processes (Otjimbingwe alkaline complex, Damara orogen, Namibia). 2020 , 82, 267-287	8
287	The Permian Sn metallogenic event and its geodynamic setting in East Kunlun, NW China: Evidence from zircon and cassiterite geochronology, geochemistry, and Sr即d田f isotopes of the Xiaowolong skarn Sn deposit. 2020 , 118, 103370	5
286	Climate-Dependent Sediment Composition and Transport of Mountainous Rivers in Tectonically Stable, Subtropical East Asia. 2020 , 47, e2019GL086150	8
285	Holocene dynamics of the southern westerly winds over the Indian Ocean inferred from a peat dust deposition record. 2020 , 231, 106169	5
284	Re-Os Geochronology, Whole-Rock and Radiogenic Isotope Geochemistry of the Wulandele Porphyry Molybdenum Deposit in Inner Mongolia, China, and Their Geological Significance. 2020 , 10, 374	0
283	Monte Santo suite, an example of Ediacaran-Cambrian deformed alkaline rocks in the Araguaia Belt, Central Brazil. Implications for Western Gondwana evolution. 2020 , 366-367, 105552	3
282	Intraplate adakite-like rocks formed by differentiation of mantle-derived mafic magmas: A case study of Eocene intermediate-felsic porphyries in the Machangqing porphyry Cu-Au mining district, SE Tibetan plateau. 2020 , 196, 104364	1
281	Petrogenesis of Paleogene lamprophyres in the Ailaoshan tectonic belt, western Yangtze Craton: Implications for the mantle source of orogenic gold deposits. 2020 , 122, 103507	4
2 80	Volcanic reconstruction and geochemistry of the Powderhouse formation in the Paleoproterozoic VMS-hosting Chisel sequence, Snow Lake, Manitoba, Canada. 2021 , 58, 247-267	
279	Early Mesozoic subduction of the Mongol-Okhotsk Ocean and its effect on the central Great Xing'an Range: Insights from the monzodiorite in the Erdaohe deposit. 2021 , 56, 1604-1624	4
278	Episodic ferruginous conditions associated with submarine volcanism led to the deposition of a Late Carboniferous iron formation. 2021 , 292, 1-23	7
277	The Tapes Complex (Nico Prez Terrane, Uruguay): Constraining the Mesoproterozoic evolution of the Rô de la Plata Craton. 2021 , 105, 102906	3

276	Provenance and Weathering of Clays Delivered to the Bay of Bengal During the Middle Miocene: Linkages to Tectonics and Monsoonal Climate. 2021 , 36, e2020PA003917		7
275	New Zealand as a source of mineral dust to the atmosphere and ocean. 2021 , 251, 106659		8
274	Paleoenvironmental implications of Sr and Nd isotopes variability over the past 48 ka from the southern Sea of Japan. 2021 , 432, 106393		1
273	Distinguishing Glacial AMOC and Interglacial Non-AMOC Nd Isotopic Signals in the Deep Western Atlantic Over the Last 1 Myr. 2021 , 36,		2
272	Late Eifelian Kaß Episode in the epeiric Belarusian Basin: Role of terrestrial-marine teleconnections. 2021 , 562, 110106		2
271	Dissolved neodymium and hafnium isotopes and rare earth elements in the Congo River Plume: Tracing and quantifying continental inputs into the southeast Atlantic. 2021 , 294, 192-214		5
270	Neodymium isotope composition of Palaeoproterozoic Birimian shales from the Wa-Lawra Belt, north-west Ghana: Constraints on provenance. 2021 , 56, 2072-2081		
269	Petrogenesis of mafic microgranular enclaves (MMEs) in the oligocene-miocene granitoid plutons from northwest Anatolia, Turkey. 2021 , 81, 125713		O
268	Distribution Coefficients of the REEs, Sr, Y, Ba, Th, and U between ⊞-HIBA and AG50W-X8 Resin. 2021 , 5, 55-65		5
267	Variations in deep water masses along the western margin of South Africa, spanning the last two glacial terminations. 2021 , 562, 110148		3
266	Lithogenic Particle Transport Trajectories on the Northwest Atlantic Margin. 2021, 126,		3
265	Petrogenesis of a low-87Sr/86Sr, two-mica, garnet-bearing leucogranite (Donkerhoek batholith, Damara orogen, Namibia). 2021 , 174, 104055		2
264	Petrogenesis of the Quanzigou porphyry Mo deposit at the northern margin of the North China Craton: Constrains from geochronology, geochemistry, and SrNdHf isotopes characteristics. 2021 , 231, 106681		2
263	Three North African dust source areas and their geochemical fingerprint. <i>Earth and Planetary Science Letters</i> , 2021 , 554, 116645	5.3	6
262	Geochemistry and zircon ages of the Yushigou diabase in the Longshoushan area, Alxa Block: implications for crustthantle interaction and tectonic evolution. 2021 , 158, 685-700		1
261	Nd isotope record of ocean closure archived in limestones of the Devonian arboniferous carbonate platform, Greater Karatau, southern Kazakhstan. 2021 , 178, jgs2020-077		4
260	Petrogenesis and tectonic significance of the Early Devonian lamprophyres and diorites in the Alxa Block, NW China. 2021 , 81, 125685		0
259	Landscape responses to intraplate deformation in the Kalahari constrained by sediment provenance and chronology in the Okavango Basin. 2021 , 33, 1170-1193		1

258	Geochemistry and SmNd isotopic sources of Late Ediacaran siliciclastic series in the OssaMorena Complex: IberianBohemian correlations. 2021 , 110, 467-485	5
257	Whole-rock and SmNd isotopic geochemistry of Triassic SW Iberia sandstones: implications for provenance. 2021 , 47, 189-207	
256	Tectonic setting and isotopic sources (SmNd) of the SW Iberian Autochthon (Variscan Orogen). 2021 , 47, 121-150	4
255	Routine high-precision Nd isotope analyses: an optimized chromatographic purification scheme. 2021 , 36, 1946-1959	O
254	Drivers of river reactivation in North Africa during the last glacial cycle. 2021 , 14, 97-103	9
253	A genetic link between albitic magmas and IOCG mineralization in the Ossa Morena Zone (SW Iberia). 2021 , 47, 85-119	1
252	Permian lamprophyres from the Western Carpathians: a review. SP513-2020-237	1
251	Geochemistry and detrital zircon geochronology of metasedimentary rocks in the Sierra Madre Terrane, Mexico: Implications of deposition along the western margin of Pangea. 2021 , 56, 3342-3377	1
250	Geochemical and Isotopic Evidence for Provenance of the Western Sea of Japan Over the Last 30000 Years. 2021 , 9,	0
249	Mineralogy, alteration, geochemistry, and fluid inclusion studies of the Balazard Cu-Au prospect, southwest of Nehbandan. 2021 , 29, 179-196	
248	Geochronology, Petrogenesis and Oxidation State of the Northparkes Igneous Suite, New South Wales, Australia: Implications for Magma Fertility.	4
247	Neodymium isotopic constraints on Cenozoic Asian dust provenance changes linked to the exhumation history of the northern Tibetan Plateau and the Central Asian Orogenic Belt. 2021 , 296, 38-55	5
246	Persistent Provenance of South Asian Monsoon-Induced Silicate Weathering Over the Past 27 Million Years. 2021 , 36, e2020PA003909	10
245	Impact of Climate Change on Past Indian Monsoon and Circulation: A Perspective Based on Radiogenic and Trace Metal Geochemistry. 2021 , 12, 330	O
244	Influence of Hydraulic Connectivity on Carbon Burial Efficiency in Mackenzie Delta Lake Sediments. 2021 , 126, e2020JG006054	1
243	The role of magmatism in hydrocarbon generation in sedimented rifts: A Nd isotope perspective from mid-Cretaceous methane-seep deposits of the Basque-Cantabrian Basin, Spain. 2021 , 303, 223-223	5
242	Petrogenesis of a late-stage calc-alkaline granite in a giant S-type batholith: geochronology and SrNdPb isotopes from the Nomatsaus granite (Donkerhoek batholith), Namibia. 2021 , 110, 1453-1476	0
241	Magmatic-hydrothermal processes and controls on rare-metal enrichment of the Baerzhe peralkaline granitic pluton, inner Mongolia, northeastern China. 2021 , 131, 103984	3

(2021-2021)

240	Provenance constraints on the Cretaceous-Paleocene erosional history of the Guiana Shield as determined from the geochemistry of clay-size fraction of sediments from the Arapaima-1 well (Guyana-Suriname basin). 2021 , 434, 106433	1
239	Neodymium Isotopes in Glauconite for Palaeoceanographic Reconstructions at Continental Margins: A Preliminary Investigation From Demerara Rise. 2021 , 9,	2
238	Lithogeochemical, isotopic, and UPb (zircon) age constraints on arc to rift magmatism, northwestern and central Avalon Terrane, Newfoundland, Canada: implications for local lithostratigraphy. 2021 , 58, 332-354	2
237	Changes in the Intermediate Water Masses of the Mediterranean Sea During the Last Climatic CycleNew Constraints From Neodymium Isotopes in Foraminifera. 2021 , 36, e2020PA004153	O
236	Late Pleistocene Emergence of Crystalline Canadian Shield Sources in Sediments of the Northern Gulf of Mexico. 2021 , 36, e2020PA004082	
235	Global continental and marine detrital [Id: An updated compilation for use in understanding marine Nd cycling. 2021 , 567, 120119	7
234	A Preliminary Framework for Magmatism in Modern Continental Back-Arc Basins and Its Application to the Triassic-Jurassic Tectonic Evolution of the Caucasus. 2021 , 22, e2020GC009490	0
233	Age, origin and tectonic implications of Late Carboniferous-Early Permian felsic magmatic rocks from central Inner Mongolia, south-eastern Central Asian Orogenic Belt. 1-22	
232	Deep-ocean circulation in the North Atlantic during the Plio-Pleistocene intensification of Northern Hemisphere Glaciation (~2.65\overline{\mathbb{Q}}.4'\text{Ma}). 2021 , 165, 101998	
231	Texture, geochemistry and geochronology of titanite and pyrite: Fingerprint of magmatic-hydrothermal fertile fluids in the Jiaodong Au province. 2021 ,	2
230	Loess accumulation in Harbin with implications for late Quaternary aridification in the Songnen Plain, Northeast China. 2021 , 570, 110365	1
229	Origin, petrogenesis and geodynamic implications of the early Eocene Alt—np—nar adakitic andesites in the eastern Sakarya Zone, northeastern Turkey. 2021 , 81, 125766	2
228	Experimental investigation into the disturbance of the Sm-Nd isotopic system during metasomatic alteration of apatite. 2021 ,	3
227	Paleogene Sedimentary Records of the Paleo-Jinshajiang (Upper Yangtze) in the Jianchuan Basin, Yunnan, SW China. 2021 , 22, e2020GC009500	1
226	Two billion years of episodic and simultaneous websteritic and eclogitic diamond formation beneath the Orapa kimberlite cluster, Botswana. 2021 , 176, 1	O
225	Glacial and environmental changes in northern Svalbard over the last 16.3 ka inferred from neodymium isotopes. 2021 , 201, 103483	O
224	Leaf Wax and Sr-Nd Isotope Evidence for High-Latitude Dust Input to the Central South China Sea and Its Implication for Fertilization. 2021 , 48, e2020GL091853	1
223	The imprint of windblown dust from the North American Southwest on the California Channel Islands and Pacific Ocean sediments. 2021 , 261, 106934	4

222	~2.5 Ga asthenospheric-melt impregnated continental crust: Implications for sporadically eroded lithosphere beneath the Dharwar craton, India. 2021 , 358, 106184	1
221	Early Permian continental arc magmatism in the Zhaojinggou area of the northern North China Craton: Implications for crust-mantle interactions during southward Paleo-Asian plate subduction. 2021 , 390-391, 106110	O
220	Petrogenesis and tectonic implications of the late Paleoproterozoic (ca. 1.7 Ga) post-collisional magmatism in the southwestern Gyeonggi Massif at Garorim Bay, South Korea. 2021 , 5, 100050	O
219	Magmatic processes recorded in plagioclase and the geodynamic implications in the giant Shimensi WIIuMo deposit, Dahutang ore field, South China. 2021 , 212, 104734	1
218	Seawater-Particle Interactions of Rare Earth Elements and Neodymium Isotopes in the Deep Central Arctic Ocean. 2021 , 126, e2021JC017423	О
217	The effects of Antarctic alteration and sample heterogeneity on Sm-Nd and Lu-Hf systematics in H chondrites. 2021 , 305, 106-129	O
216	Origin of ore-forming fluids of Tokuzbay gold deposit in the South Altai, northwest China: Constraints from SrNdPb isotopes. 2021 , 134, 104165	3
215	Constraints on the source of reactive phases in sediment from a major Arctic river using neodymium isotopes. <i>Earth and Planetary Science Letters</i> , 2021 , 565, 116933	2
214	Bitumen Sm-Nd, pyrite Rb-Sr and zircon U-Pb isotopes constrain timing of ore formation and hydrocarbon deposition in the Erdaokan Ag-Pb-Zn deposit, NE China. 2021 , 134, 104161	1
213	Hydrous juvenile lower crust at the western Yangtze Craton margin as the main source of the Beiya porphyry-skarn Au deposit.	1
212	Detrital neodymium and (radio)carbon as complementary sedimentary bedfellows? The Western Arctic Ocean as a testbed. 2021 , 315, 101-101	О
211	Stable Atlantic Deep Water Mass Sourcing on Glacial-Interglacial Timescales. 2021 , 48, e2021GL092722	2
21 0	The nature and origin of upper mantle heterogeneity beneath the Mid-Atlantic Ridge 33B5°N: A Sr-Nd-Hf isotopic perspective. 2021 , 307, 72-85	3
209	A major change in magma sources in late Mesozoic active margin of the circum-Sea of Japan domain: Geochemical constraints from late Paleozoic to Paleogene mafic dykes in the Sergeevka belt, southern Primorye, Russia. 2021 , 30, e12426	2
208	Quantitative evaluation of human and climate forcing on erosion in the alpine Critical Zone over the last 2000 years. 2021 , 268, 107127	3
207	Stratigraphy and Provenance of the Paleogene Syn-Rift Sediments in Central-Southern Palawan: Paleogeographic Significance for the South China Margin. 2021 , 40, e2021TC006753	3
206	Determination of Nd isotopic composition in seawater using newly developed solid phase extraction and MC-ICP-MS. 2021 , 232, 122435	5
205	Geochemically Defined Mean Position of the Intertropical Convergence Zone in the Central Pacific. 2021 , 48, e2021GL094432	O

204	Neodymium Isotope Records From the Northwestern Pacific: Implication for Deepwater Ventilation at Heinrich Stadial 1. 2021 , 36, e2021PA004312	1
203	Control of oceanic circulation on sediment distribution in the southwestern Atlantic margin (23 to 55° S). 2021 , 17, 1213-1229	Ο
202	Sediment Routing and Anthropogenic Impact in the Huanghe River Catchment, China: An Investigation Using Nd Isotopes of River Sediments. 2021 , 57, e2020WR028444	0
201	Enhanced Late Miocene Chemical Weathering and Altered Precipitation Patterns in the Watersheds of the Bay of Bengal Recorded by Detrital Clay Radiogenic Isotopes. 2021 , 36, e2021PA004252	2
200	Genesis and Nd Isotope Composition of Ferromanganese Deposits of the Sea of Okhotsk and the Kuril Island Arc. 2021 , 62, 1074-1087	1
199	Neodymium isotopes in modern human dental enamel: An exploratory dataset for human provenancing. 2021 , 38, 107375	
198	Sandstone petrographic and mudstone REE and Nd-isotopic evidence for Middle Pennsylvanian arrival of Gondwana sediments in the Fort Worth Basin. 2021 , 579, 110590	2
197	Using Sr-Nd-Pb isotope systems to trace sources of sediment and trace metals to the Weser River system (Germany) and assessment of input to the North Sea. 2021 , 791, 148127	1
196	Disentangle the sediment mixing from geochemical proxies and detrital zircon geochronology. 2021 , 440, 106572	2
195	North Atlantic Deep Water during Pleistocene interglacials and glacials. 2021 , 269, 107146	3
194	Geochemistry and mineralogy of the sediments in the New Britain shelf-trench continuum, offshore Papua New Guinea: Insights into sediment provenance and burial in hadal trenches. 2021 , 177, 103621	1
193	UNRAVELING MINERALIZATION AND MULTISTAGE HYDROTHERMAL OVERPRINTING HISTORIES BY INTEGRATED IN SITU U-Pb AND Sm-Nd ISOTOPES IN A PALEOPROTEROZOIC BRECCIA-HOSTED IOCG DEPOSIT, SW CHINA. 2021 , 116, 1687-1710	6
192	Evaluation of origin-depended nitrogen input through atmospheric deposition and its effect on primary production in coastal areas of western Kyusyu, Japan. 2021 , 291, 118034	0
191	Crustal vs. mantle contributions in the Erzgebirge/Kru n 'hory Mts. magmatism: Implications for generation of zoned, A-type silicic rocks in the late-Variscan Altenberg-Teplice Caldera, Central Europe. 2021 , 404-405, 106429	O
190	Provenance of the Middle Jurassic-Cretaceous sedimentary rocks of the Arequipa Basin (South Peru) and implications for the geodynamic evolution of the Central Andes. 2022 , 101, 59-76	2
189	New loading method for high precision Sm isotope analysis of nuclear materials using thermal ionization mass spectrometry. 2021 , 327, 317-327	3
188	Lithopetrographic and geochemical features of the Saalian tills in the Szczerc outcrop (Poland) in various deformation settings. 2021 , 13, 001-015	
187	Geochemical Characteristics of Archaean Ultramafic and Mafic Volcanic Rocks: Implications for Mantle Composition and Evolution. 1984 , 25-46	10

186	Lu-Hf garnet geochronology of eclogites from the Balma Unit (Pennine Alps): implications for Alpine paleotectonic reconstructions. 2008 , S173-S189	2
185	Encyclopedia of Scientific Dating Methods. 2015 , 379-390	6
184	Neodymium Isotope Evidence for the Age and Origin of the Proterozoic of Telemark, South Norway. 1985 , 435-448	10
183	The Southern Part of the Fongen-Hyllingen Layered Mafic Complex, Norway: Emplacement and Crystallization of Compositionally Stratified Magma. 1987 , 145-184	11
182	Geochronology, geochemistry, and SrNdPbHf isotopes of the Zhunsujihua granitoid intrusions associated with the molybdenum deposit, northern Inner Mongolia, China: implications for petrogenesis and tectonic setting. 2018 , 107, 687-710	7
181	Early magmatic phase in the Oslo Rift and its related stress regime. 1992 , 37-54	2
180	Metallogeny of the large-scale Carboniferous karstic bauxite in the Sanmenxia area, southern part of the North China Craton, China. 2020 , 556, 119851	7
179	Late Oligocene-Miocene proto-Antarctic Circumpolar Current dynamics off the Wilkes Land margin, East Antarctica. 2020 , 191, 103221	11
178	Diabase-hosted copper mineralization in the Qunjsai deposit, West Tianshan, NW China: Geological, geochemical and geochronological characteristics and mineralization mechanism. 2018 , 92, 430-448	5
177	Early Neoproterozoic assembly of the Yangtze Block decoded from metasedimentary rocks of the Miaowan Complex. 2020 , 346, 105787	4
176	Isotopic and Trace Element Geochemistry of the Kiglapait Intrusion, Labrador: Deciphering the Mantle Source, Crustal Contributions and Processes Preserved in Mafic Layered Intrusions. 2019 , 60, 553-590	7
175	Early Cretaceous magmatism and post-Early Cretaceous deformation on Ellef Ringnes Island, Canadian High Arctic, related to the formation of the Arctic Ocean. 2019 , 303-323	2
174	Controls on erosion in the western Tarim Basin: Implications for the uplift of northwest Tibet and the Pamir. 2017 , 13, 1747-1765	14
173	The Inishkea Division of northwest Mayo: Dalradian cover rather than pre-Caledonian basement. 1992 , 149, 167-170	12
172	Asynchronous changes in vegetation, runoff and erosion in the nile river watershed during the holocene. 2014 , 9, e115958	30
171	Hafnium isotope variations in Bure volcanic rocks from the northwestern Ethiopian volcanic province: a new insight for mantle source diversity. 2010 , 105, 101-111	14
170	SrNdPbHf isotopic constraints on the diversity of magma sources beneath the Aden Ridge (central Gulf of Aden) and plumeEdge interaction. 2015 , 110, 97-110	5
169	Ancient versus modern mineral dust transported to high-altitude Alpine glaciers evidences Saharan sources and atmospheric circulation changes.	2

168	Ancient versus modern mineral dust transported to high-altitude alpine glaciers evidences saharan sources and atmospheric circulation changes.	8
167	High-resolution neodymium characterization along the Mediterranean margins and modelling of <i></i>_{Nd} distribution in the Mediterranean basins. 2016 , 13, 5259-5276	17
166	Reconstructing the Nd oceanic cycle using a coupled dynamical Diogeochemical model.	20
165	Influence of the Atlantic thermohaline circulation on neodymium isotopic composition at the Last Glacial Maximum & modelling sensitivity study.	1
164	Holocene climate variability in the winter rainfall zone of South Africa.	2
163	Holocene climate variability in the Winter Rainfall Zone of South Africa.	5
162	A major change in North Atlantic deep water circulation during the Early Pleistocene transition 1.6 million years ago.	1
161	A database of marine and terrestrial radiogenic Nd and Sr isotopes for tracing earth-surface processes. 2019 , 11, 741-759	11
160	Modeling the Nd isotopic composition in the North Atlantic basin using an eddy-permitting model.	1
159	REE and Sr-Nd Isotopic Composition of the Shelf Sediments around Jeju Island, Korea. 2012 , 33, 481-496	2
158	Reconstruction of Ocean Circulation Based on Neodymium Isotopic Composition: Potential Limitations and Application to the Mid-Pleistocene Transition. 2020 , 33,	1
157	Authigenic Neodymium Isotope Record of Past Ocean Circulation. 2014 , 23, 249-259	2
156	Little Change in Ice Age Water Mass Structure From Cape Basin Benthic Neodymium and Carbon Isotopes. 2021 , 36, e2021PA004281	1
155	Isotopic fingerprints of recycled eclogite facies sediments in the generation of the Huanglongpu carbonatite, central China. 2021 , 139, 104534	2
154	Timing and genesis of the Tudiling trachyte Nb-Ta-Zr-REE deposit in the South Qinling (Central China): Implications for rare metal enrichment in extrusive peralkaline magmatic systems. 2021 , 139, 104535	2
153	An ancient continental crustal source for Mo mineralisation in the eastern Central Asian Orogen: A case study of the Bilugangan Mo deposit. 2021 , 139, 104513	
152	Archean to Paleoproterozoic evolution of the Crixâgreenstone belt, Central Brazil: Insights from two contrasting assemblies of metaigneous rocks. 2021 , 404-405, 106493	1
151	Rare earth element and neodymium isotopes of the eastern US GEOTRACES Equatorial Pacific Zonal Transect (GP16). <i>Earth and Planetary Science Letters</i> , 2021 , 576, 117233	O

150 Metabazyty pasma Novĥo M\(\text{Sta} \) ta. **2013**,

149	Composition and Structure of the Earth Interior. 2014 , 375-427	
148	Cosmo- and Geochemical Cycles and Balance For the Contents of Yttrium and/or Rare Earth Elements. 1987 , 137-205	
147	Encyclopedia of Scientific Dating Methods. 2015 , 768-780	О
146	RB-SR- 日-47SM-143ND- 	
145	PEEge Metamorfitlerindeki Amfibolit Fasiyesi Granatlar̃n Petrokimyas̃ ve Sm-Nd °zotop Jeokimyas̃.	O
144	Zircon U-Pb age, geochemistry and Sr-Nd isotope characteristics of the Duolong SSZ-type ophiolites in Geize County, Tibet: Evidence for intra-oceanic subduction of the Bangonghu-Nujiang Ocean during the Late Permian. 2019 , 35, 505-522	2
143	Petrogenesis and tectonic setting of the quartz porphyry in Mazhuangshan gold deposit, Eastern Tianshan Orogen: Evidence from geochemistry, zircon U-Pb geochronology and Sr-Nd-Hf isotopes. 2019 , 35, 1503-1518	2
142	Multi-stage melting of enriched mantle components along the eastern Gakkel Ridge. 2021 , 586, 120594	1
141	Geochemical and geochronological constraints on the genesis of Pliocene post-collisional granite porphyry and shoshonite in Quanshuigou, western Kunlun Mountains, NW Qinghai ibet Plateau. 1-22	O
140	Discovery of 102Ma gabbro in the Tianshuihai area of Karakoram terrane, and its constraints on regional Mesozoic tectonic evolution. 2020 , 36, 1041-1058	1
139	Geochemical characteristics and petrogenesis of Late Cretaceous hypersthene-bearing intrusive rocks in the Gangdese batholith, southern Tibet. 2020 , 36, 2667-2700	2
138	Evidence for a Northern Hemispheric trigger of the 100,000-y glacial cyclicity. 2021 , 118,	4
137	Encyclopedia of Geochemistry. 1999 , 18-19	
136	Encyclopedia of Geochemistry. 1999 , 23-25	
135	Deep-Water Circulation over the Last Two Glacial Cycles Reconstructed from Authigenic Neodymium Isotopes in the Equatorial Indian Ocean (Core HI1808-GPC04). 1	
134	Widespread lithogenic control of marine authigenic neodymium isotope records? Implications for paleoceanographic reconstructions. 2021 , 319, 318-318	O
133	Provenance of Baker River sediments (Chile, 48°S): Implications for the identification of flood deposits in fjord sediments.	O

132	Neodymium Isotope Geochemistry of a Subterranean Estuary. 2021, 3,	O
131	Elemental and SrNd isotopic compositions of surface clay-size sediments in the front end of major ice shelves around Antarctica and indications for provenance. 2021 , 195, 105011	
130	Early global mantle chemical and isotope heterogeneity revealed by the komatiite-basalt record: The Western Australia connection. 2021 , 320, 238-238	3
129	Late Holocene dust provenance at Siple Dome, Antarctica. 2021 , 274, 107271	1
128	Absence of a strong, deep-reaching Antarctic circumpolar current zonal flow across the Tasmanian gateway during the oligocene to early miocene. 2021 , 103718	1
127	Petrogenesis and geodynamic significances of the early Late Cretaceous intrusion in the Langxian Complex, eastern Gangdese batholith of southern Tibet. 2021 , 37, 3348-3376	
126	Protolith and tectonic implications of the No. IV pluton in Xiarihamu area, East Kunlun, Qinghai Province. 2021 , 37, 3118-3130	O
125	Early Cretaceous magmatism of the Langxian complex in the eastern Gangdese batholith, southern Tibet: Neo-Tethys ocean subduction re-initiation. 2021 , 37, 2995-3034	1
124	Mineralization and Its Controls. 2022 , 765-842	
123	Ediacaran iron formations from the North Qilian Orogenic Belt, China: Age, geochemistry, Sm N d isotopes and link with submarine volcanism. 2022 , 368, 106498	O
122	PorphyryBkarn Mo Systems. 2022 , 363-516	
121	Dynamic response of East Antarctic ice sheet to Late Pleistocene glacial[hterglacial climatic forcing. 2022 , 277, 107299	
120	Chemical isolation and isotopic analysis of terrigenous sediments with emphasis on effective removal of contaminating marine phases including barite. 2022 , 589, 120673	О
119	Source compositions and peritectic assemblage entrainment as the main compositional driver in the granitoids: A case study of the Ningshan granitic plutons in South Qinling. 2021 , 37, 3815-3848	
118	Magmatic-Hydrothermal Vein Systems. 2022 , 517-624	
117	Origin of the Holocene Sediments in the Ninetyeast Ridge of the Equatorial Indian Ocean. 1	O
116	Metamorphic Hydrothermal (Orogenic-Type) Systems. 2022 , 625-764	
115	Natural Allanite Reference Materials for In Situ U-Th-Pb and Sm-Nd Isotopic Measurements by LA-(MC)-ICP-MS.	1

114	Dissolved neodymium isotopes in the Mediterranean Sea. 2022 ,	O
113	Discovery of late Early Cretaceous diorite porphyrite from the Shamuluo Formation in the Gaize area, Tibet: Response to the northward subduction plate rollback event of Bangongco-Nujiang Tethys Ocean. 2022 , 38, 185-208	
112	The role of crustal contamination in magma evolution of Neoproterozoic metaigneous rocks from Southwest Svalbard. 2022 , 370, 106521	1
111	Neodymium isotopes as a paleo-water mass tracer: A model-data reassessment. 2022 , 279, 107404	1
110	Composition, Age, and Origin of Ordovician-Devonian Tanjianshan granitoids in the North Qaidam Orogenic Belt of northern Tibet: Implications for Tectonic Evolution. 1-28	
109	Radioisotopes as Chronometers. 2022 , 192-237	
108	Zircon UPb dating and geochemistry of intrusive rocks in the Shangdan suture zone of the Qinling Orogenic Belt: petrogenesis and tectonic implications. jgs2021-157	
107	New Perspectives on the 143 Nd/ 144 Nd Palaeoceanographic Tracer on Foraminifera: The State-of-the-Art Frontiers of Analytical Methods. 2022 , 23,	O
106	Nd and Sr Isotopes and REE Investigation in Tropical Weathering Profiles of Amazon Region. 2022 , 10,	
105	Source of the aeolian sediments in the Yarlung Tsangpo valley and its potential dust contribution to adjacent oceans.	O
104	The komatiite testimony to ancient mantle heterogeneity. 2022 , 594, 120776	1
103	Episodic emplacement of the Lingshan Granitic Complex and related two-stage molybdenum mineralization in the Dabie orogenic belt. 2022 , 144, 104820	O
102	Generation of crystal-rich rhyodacites by fluid-induced crystal-mush rejuvenation: Perspective from the Late Triassic Nageng (sub-)volcanic complex of the East Kunlun Orogen, NW China. 2022 , 599, 120833	2
101	Modelling the Formation of Linear Geochemical Trends Using the Magma Chamber Simulator: A Case Study of the Jindabyne Granitoids, Lachlan Fold Belt, Australia. 2022 , 63,	1
100	A large West Antarctic Ice Sheet explains early Neogene sea-level amplitude 2021, 600, 450-455	2
99	Neoproterozoic I-type granites in the Central Tianshan Block (NW China): geochronology, geochemistry, and tectonic implications. 2022 , 14, 82-101	O
98	Boundary processes and neodymium cycling along the Pacific margin of West Antarctica. 2022,	0
97	Refining the contribution of riverine particulate release to the global marine Nd budget. 2022 , 9,	Ο

96 GEOCHRONOLOGYGeochronology. **1984**, 215-222

95	Image1.PDF. 2017 ,	
94	Enhanced weathering triggered the transient oxygenation event at ~1.57 Ga.	
93	Clay Mineralogical Records in the North Bohai Coast of China in the Last Century: Sediment Provenance and Morphological Implications. 2022 , 10,	O
92	Interannual variability in the source location of North African dust transported to the Amazon.	O
91	Reconstruction of Chemical Weathering Intensity and Asian Summer Monsoon Evolution in the Red River basin over the Past 36 kyr.	O
90	Terrigenous and volcanogenic contribution to the deep basin of the South China Sea: Evidence from trace elements and Sr-Nd isotopes. 2022 , 448, 106811	0
89	Geometry of the Meridional Overturning Circulation at the Last Glacial Maximum. 2022, 1-56	
88	Rift-related multistage evolution of the Mangalwar Complex, Aravalli Craton (NW India): Evidence from elemental and SrNd isotopic features of Proterozoic amphibolites.	0
87	Geochronology, geochemistry, and isotopic composition of the early Neoproterozoic granitoids in the Bikou Terrane along the northwestern margin of the Yangtze Block, South China: Petrogenesis and tectonic implications. 2022 , 377, 106724	O
86	In-situ monazite Nd and pyrite S isotopes as fingerprints for the source of ore-forming fluids in the Jiaodong gold province. 2022 , 104965	1
85	GNOM v1.0: an optimized steady-state model of the modern marine neodymium cycle. 2022 , 15, 4625-4656	O
84	Apatites Record Sedimentary Provenance Change 4B Myrs Before Clay in the Oligocene/Miocene Alpine Molasse. 10,	
83	Age and Chemostratigraphy of the Finlayson Lake District, Yukon: Implications for Volcanogenic Massive Sulfide (VMS) Mineralization and Tectonics along the Western Laurentian Continental Margin. 2022 , 2022,	
82	Transient mobilization of subcrustal carbon coincident with Palaeocene Hocene Thermal Maximum.	1
81	On the unusual presence of a Quaternary peralkaline volcanic center, rear-arc region of the Trans-Mexican Volcanic Belt eastern sector: geochemical and isotopic characterization of the Las Navajas⊞idalgo stratovolcano.	1
80	An Intertropical Convergence Zone shift controlled the terrestrial material supply on the Ninetyeast Ridge. 2022 , 18, 1369-1384	0
79	Slab break-off-related magnesian andesites and dacites with adakitic affinity from the early Quaternary Keßboyduran stratovolcano, Cappadocia province, central Turkey: evidence for slab/sediment melthantle interaction and magma mixing. 2022, 177,	

78	Landscape Topography and Regional Drought Alters Dust Microbiomes in the Sierra Nevada of California. 13,	
77	A deep Tasman outflow of Pacific waters during the last glacial period. 2022 , 13,	
76	The effect of crystal fractionation on the geochemical composition of syn-exhumation magmas: Implication for the formation of high B6Fe granites in collisional orogens. 2022 ,	О
75	Geochronology of Diamonds. 2022 , 88, 567-636	2
74	Reconstruction of Kuroshio intrusion into the south China sea over the last 40 kyr. 2022 , 290, 107622	1
73	Climate and sea level forcing of terrigenous sediments input to the eastern Arabian Sea since the last glacial period. 2022 , 450, 106860	
7 ²	A shift of mantle sources for the post-collisional lavas and tectonic links with synchronous deformation in the SE Tibetan Plateau. 2022 , 607, 121009	
71	Astronomically controlled aridity in the Sahara since at least 11 million years ago.	1
70	Chemical Weathering of the Mekong River Basin With Implication for East Asian Monsoon Evolution During the Late Quaternary: Marine Sediment Records in the Southern South China Sea. 10,	0
69	Petrogenesis of the Early Cretaceous Zhouguan Granodiorite in Jiaodong Peninsula: Evidence from Mineralogy, Geochemistry, Geochronology, and Sr-Nd Isotopes. 2022 , 12, 962	
68	Ocean-forced instability of the West Antarctic Ice Sheet since the mid-Pleistocene.	
67	Enhanced Weathering Triggered the Transient Oxygenation Event at ~1.57 Ga. 2022 , 49,	1
66	Evolution of the northern part of the Lesser Antilles arc ©eochemical constraints from St. Barthlemy Island lavas.	
65	The deposition and significance of an Ediacaran non-glacial iron formation.	
64	Mineral and isotopic (Nd, Sr) signature of fine-grained deglacial and Holocene sediments from the Mackenzie Trough, Arctic Canada. 2022 , 54, 346-367	1
63	Characterization of water masses around the southern Ryukyu Islands based on isotopic compositions. 2022 , 9,	
62	In-situ silt generation in the Taklimakan Desert evidenced by uranium isotopes.	0
61	Unraveling late Quaternary atmospheric circulation in the Southern Hemisphere through the provenance of Pampean loess. 2022 , 232, 104143	Ο

60	Geochronology and geochemistry of the Miocene volcanics from the Ktahya area: Constraints for post-collisional magmatism in western Anatolia, Turkey. 2022 , 195, 104679	1
59	Evolution of rare earth element and Ad compositions of Gulf of Mexico seawater during interaction with Mississippi River sediment. 2022 , 335, 231-242	O
58	Dust sources in Westernmost Asia have a different geochemical fingerprint to those in the Sahara. 2022 , 294, 107717	О
57	Tectonic switch of the north Yangtze Craton at ca. 2.0 Ga: Implications for its position in Columbia supercontinent. 2022 , 381, 106842	O
56	Coeval minimum south American and maximum Antarctic last glacial maximum dust deposition: A causal link?. 2022 , 295, 107768	O
55	In situ measurement of SmNd isotopic ratios in geological materials with Nd < 100 🗓 g1 by LA-MC-ICP-MS. 2022 , 37, 1776-1786	O
54	Peraluminous granite related to tin mineralization formed by magmatic differentiation and fluid exsolution of metaluminous melt: a case study from the Bozhushan batholith, South China Block. 2022 , 105148	O
53	Tectonic and climatic controls on sediment transport to the Southeast Indian Ocean during the Eocene: New insights from IODP Site U1514. 2022 , 217, 103956	O
52	Origin of highly variable and unusually low ILi in mineral separates from ultramafic intrusive rocks in a convergent tectonic setting in the Tibetan plateau. 2022 , 611, 121133	О
51	Continental growth during migrating arc magmatism and terrane accretion at Sikhote-Alin (Russian Far East) and adjacent northeast Asia. 2022 , 432-433, 106891	1
50	Aeolian Dust Preserved in the Guliya Ice Cap (Northwestern Tibet): A Promising Paleo-Environmental Messenger. 2022 , 12, 366	О
49	Active Nordic Seas deep-water formation during the last glacial maximum.	O
48	Xenoliths of High-Alumina Pyroxenites in the Basalts of the Sigurd Volcano, Spitsbergen Island (Svalbard Archipelago), as Indicators of the Paleozoic Geodynamics of the Regional Lithosphere. 2022 , 63, 1093-1110	О
47	Genesis of the recently discovered Daxiyingzi Rb B e deposit on the northern margin of the North China Craton: Evidence from 40Ar/39Ar ages and geochemical data. 2022 , 150, 105152	O
46	Eurasian Ice Sheet derived meltwater pulses and their role in driving atmospheric dust activity: Late Quaternary loess sources in SE England. 2022 , 296, 107804	О
45	Enhanced continental weathering (I' Li, Nd) during the rise of East African complex polities: an early large-scale anthropogenic forcing?. 2022 , 354, 319-337	O
44	Assessing neodymium isotopes as an ocean circulation tracer in the Southwest Atlantic. 2022, 599, 117846	O
43	Birth of the Pearl River at 30 Ma: Evidence from sedimentary records in the northern South China Sea. 2022 , 600, 117872	1

42	A large-scale Sr and Nd isotope baseline for archaeological provenance in Silk Road regions and its application to plant-ash glass. 2023 , 149, 105695	0
41	Carboniferous mafic-ultramafic intrusions in the Eastern Pontides (Pulur complex): Implications for the source of coeval voluminous granites. 2022 , 106946	2
40	Geochemical Indicators in Provenance Estimation. 2022 , 95-121	О
39	A 1.8 million year history of Amazon vegetation. 2023 , 299, 107867	Ο
38	Non-traditional stable isotopic analysis for source tracing of atmospheric particulate matter. 2023 , 158, 116866	O
37	Identifying the clay-size sediment provenance of the radial sand ridges in the southwestern Yellow Sea using geochemical and Sr Nd isotopic tracers. 2023 , 455, 106957	O
36	Mantle contribution to the generation of the giant Jinduicheng porphyry Mo deposit, Central China: New insights from combined in-situ element and isotope compositions of zircon and apatite. 2023 , 616, 121238	0
35	Osmium isotopes record a complex magmatic history during the early stages of formation of the North American Midcontinent Rift Implications for rift initiation. 2023 , 436-437, 106966	O
34	Dissipation of Tungsten-182 Anomalies in the Archean Upper Mantle: Evidence from the Black Hills, South Dakota, USA. 2023 , 617, 121255	0
33	Petrogenesis of Meso-Neoarchean granitoids from the Chitradurga Greenstone Belt: Implications on crustal growth and reworking of the Dharwar Craton, southern India. 2023 , 242, 105494	O
32	Mesozoic slab-derived magmas from mid-eastern China: Responses to a ridge-transform fault-ridge subduction system. 2023 , 617, 121259	Ο
31	??????-???????????????????????????????	O
30	A 500 ka Record of Volcanism and Paleoenvironment in the northern Garibaldi Volcanic Belt, British Columbia	0
29	Modern-like deep water circulation in Indian Ocean caused by Central American Seaway closure. 2022 , 13,	O
28	A database of radiogenic SrNd isotopes at the Ehree poles 12022, 14, 5349-5365	0
27	Golpayegan Metamorphic Complex (SanandajBirjan Zone, Iran) as Evidence for Cadomian Back-Arc Magmatism: Structure, Geochemistry and Isotopic Data.	O
26	Sr, Nd, and Pb isotope provenance of surface sediments on the East Siberian Arctic Shelf and implications for transport pathways. 2022 , 121277	О
25	Mineralogy and geochemistry of modern Red River sediments (North Vietnam): Provenance and weathering implications. 2022 , 92, 1169-1185	O

24	Fast-eroding Taiwan and transfer of orogenic sediment to forearc basins and trenches in the Philippine and South China seas. 2022 , 104291	0
23	The early-mid Miocene abyssal brown/green claystone from IODP Site U1503A in the northern South China Sea: Implications for paleoclimate and paleoceanography. 2022 ,	О
22	Increased discharge of Yellow River sediments into the western Bohai Sea since 0.71 Ma. 1-9	О
21	A new A-type granitoid occurrence in southernmost Fennoscandia: geochemistry, age and origin of rapakivi-type quartz monzonite from the Pietkowo IG1 borehole, NE Poland.	o
20	Unradiogenic reactive phase controls the Nd of authigenic phosphates in East Antarctic margin sediment. 2023 ,	1
19	Authigenic and detrital carbonate Nd isotope records reflect pulses of detrital material input to the Labrador Sea during the Heinrich Stadials.	О
18	Enhanced weathering input from South Asia to the Indian Ocean since the late Eocene. 2023,	0
17	The late Cenozoic evolution of the Humboldt Current System in coastal Peru: Insights from neodymium isotopes. 2023 , 116, 104-112	1
16	Tectonic and magmatic evolution of NE Cathaysia Block controls sediment geochemical heterogeneity of rivers in SE China. 2023 , 223, 106910	O
15	High-K andesites as witnesses of a continental arc system in the Western Alps, Italy: constraints from HFSE and HfNdBrPbD isotope systematics. 2023 , 178,	o
14	Neodymium isotopes in peat reveal past local environmental disturbances. 2023 , 871, 161859	O
13	Survival of whole-rock SmNd isotope system from REE redistribution and mineral-scale isotopic resetting amid hydrothermal alteration in REE-rich Fe-Cu deposit. 2023 , 348, 9-26	o
12	Slab-failure or Slab-success? Examining the contributions of crust and mantle to post-subduction magmatism in the Ratagain Complex, NW Scotland. 2023 , 448-449, 107139	0
11	Geochemical and geochronological constraints on the tectonic and magmatic evolution of the southwestern Mariana subduction zone. 2023 , 197, 104039	0
10	Sr-Nd isotopic fingerprints of Red River sediments and its implication for provenance discrimination in the South China Sea. 2023 , 457, 106997	0
9	Weakening of the South Asian summer monsoon linked to interhemispheric ice-sheet growth since 12 Ma. 2023 , 14,	0
8	Constraints on the Nd-isotopic composition and nature of the last major influx of magma into the Bushveld Complex. 2023 , 178,	0
7	Equatorial Pacific dust fertilization and source weathering influences on Eocene to Miocene global CO2 decline. 2023 , 4,	O

6	Simulating marine neodymium isotope distributions using Nd v1.0 coupled to the ocean component of the FAMOUSMOSES1 climate model: sensitivities to reversible scavenging efficiency and benthic source distributions. 2023 , 16, 1231-1264	О
5	Exploring Icehouse Cyclicity Pattern and Seawater Dynamics on an Ancient Carbonate Platform With Nd Isotopes (Carboniferous, Southern Kazakhstan). 2023 , 38,	O
4	Farming stimulated stronger chemical weathering in South China since 3.0 ka BP. 2023, 307, 108065	O
3	Ferroan A-type metagranites from the PernambucoAlagoas Domain, northeastern Brazil attest Tonian crustal extension. 2023 , 126, 104321	O
2	Chronology and paleoclimatic implications of the upper Ganga catchment floods since Marine Isotopic Stage-2. 2023 , 620, 111566	О
1	Isotopic (SmNd) and Geochemical (Nb/Y@r/Y) Systematics of the Sikhote-Alin Basic-Hyperbasic Complexes. 2023 , 61, 324-347	O